Development of diagnostic assays for emergent RNA viruses

Ge Wu

Thesis submitted to the University of Nottingham for the degree of Doctor of Philosophy, September 2019.

Primary supervisors: Dr Janet Daly

Secondary Supervisor: Dr Stephen Dunham

Abstract

This study aims to develop novel diagnostic assays for zika virus (ZIKV) and equine influenza viruses (EIV) by

- Generating pseudotyped ZIKV as a surrogate for wild-type virus in the virus neutralisation (VN) test
- Producing plant-expressed ZIKV non-structural (NS) 1 protein as a surrogate for wild-type virus in the ELISA
- Identifying lineage-specific antibodies against EIV using Next Generation Phage Display (NGPD) to replace antibodies produced by immunizing animals for use in ELISA.

Co-circulation and cross-reaction among flaviviruses have become the major obstacle for an accurate diagnosis. Antigenic drift and shift of influenza viruses underline the importance of close monitoring and surveillance for precise diagnosis and vaccine production. This study aimed to develop novel diagnostic assays for emergent/re-emergent viruses, namely, Zika virus (ZIKV) and equine influenza virus (EIV) using various techniques including pseudotyping, plant expression and next-generation phage display (NGPD) to improve their current diagnostic assays.

Vesicular stomatitis virus (VSV) backboned pseudotype virus (PV) was generated by co-transfecting producer cells with commercially available VSV plasmids. ZIKV envelope protein (ZIKV E) was used to replace the VSV glycoproteins to generate VSV-backboned ZIKV PV, which showed no infectivity. However, VSV backboned Chikungunya virus (CHIKV) PV used as a control exhibited similar luciferase activity as the VSV PV ($\sim 1\times10^7$ RLU/ml), indicating successful production of VSV-backboned CHIKV PV. The virus budding site of ZIKV is different from CHIKV and VSV, which was identified as one of the possible reasons for the failure of infectivity of ZIKV PV. Future work would be to mutate the ER-retention signals in the transmembranes of ZIKV prME for its translocation to the plasma

membrane and to incorporate furin proteases during pseudotyping for the ZIKV E to achieve a mature and infectious form.

Next, a ZIKV non-structural protein 1 (NS1) ELISA was developed using ZIKV NS1 proteins expressed in plants. Unlike envelope proteins, NS1 does not elicits flavivirus cross-reactive neutralisation antibodies but induces a non-neutralising yet virus-specific antibody response. NS1 gene was codon-optimised, synthesised and inserted into a plant expression vector pEAQ-HT to obtain expressed protein. Preliminary results using the resultant ELISA showed around 95% sensitivity and 95% specificity using 20 ZIKV positive human serum samples and 19 Dengue-only positive samples. For future work, a bigger sample size should be tested for the proper validation of this plant produced NS1 ELISA.

Finally, antibody peptide sequences that specifically recognise a strain of EIV from clade 2 and not the strain from clade 1 were identified using NGPD and data analysis. It is important to be able to distinguish different clades to keep current equine vaccine effective for the circulating strain. Future work would include the recovery of the peptide sequences using inverse PCRs and testing their specificities against other EIV strains in the two clades. Identified antibody peptides could be used to replace ferret antisera in the haemagglutination test for characterising circulating EIVs.

Acknowledgement

I would like to express my deepest sense of thanks and gratitude to Dr Janet Daly, for whom without her unchanging patience, guidance and motivation, I would not have made this far. It has been my privilege to have worked in her lab. I also owe a deep sense of gratitude to Dr Steve Dunham and Dr Kevin Gough for their timely and scholarly advice.

I would like to thank the Unversity of Nottingham for giving me the un-imaginable opportunity to completely my study here, I will not forget all the help I received from the staff members Dr Belinda Wang, Dr Barney King, Dr Jon Owen, Dr Alison Gray, and Dr Toshana Foster, and my fellow postgrads Dr Sanjeeva Kumar, Dr Laymaa Al Dalawi, Sadie Cotterill and Anitha Varghese.

I also would like to thank Professor Lomonossoff and Dr Keith Saunders from the John Innes Centre for their hospitality during my short visit and help with the plant expression work.

Finally, last but not least, I am extremely thankful for my family, especially my parents and grandma for always being the solid rock for me, my friends Yangyi Chen and Lu Ban for their continuous moral support.

Table of Contents

Chapter 1 Introduction 15
1.1 Re-emergent viruses — why and how? 15
1.2 Flaviviruses 16
1.2.1 Yellow fever virus (YFV) 17
1.2.2 West Nile virus (WNV) 17
1.2.3 Dengue virus (DENV) 18
1.2.4 Replication and assembly 18
1.2.5 Diagnostic challenges 22
1.3 Influenza viruses 22
1.3.1 Human (seasonal) influenza 23
1.3.2 Avian influenza (H5, H7 and H9) 23
1.3.3 Swine influenza 24
1.3.4 Vaccine 24
1.3.5 Surveillance 25
1.4 Traditional serological assays 25
1.4.1 The plaque reduction neutralisation test (PRNT) 25
1.4.2 The haemagglutination inhibition (HI) test 27
1.4.3 The virus neutralisation (VN) test 27
1.4.4 Complement fixation (CF) 28
1.4.5 Western blot (WB) 28
1.4.6 Enzyme-linked immunosorbent assay (ELISA) 30
1.5 Aims 34
Chapter 2 General materials and methods 35
2.1 Cell culture methods 35
2.1.1 Cell lines 35
2.1.2 Sub-culturing adherent cells 35
2.1.3 Counting cells 35
2.1.4 Freezing cells 36
2.1.5 Recovery of cells from liquid nitrogen 36
2.2 Molecular cloning methods 37
2.2.1 Preparation of Luria Bertani (LB) agar plates 37
2.2.2 Transformation of standard chemically competent DH5-α *E. coli* cells 37
2.2.3 Inoculating a starter bacterial culture 37
2.2.4 Making a larger bacterial culture 38
2.2.5 Making glycerol stocks 38
2.2.6 Plasmid purification using EndoFree plasmid Maxi kit 38
2.2.7 Plasmid purification using Plasmid Mini kit 38
2.2.8 Plasmid purification using lysozyme and chemical solutions 39
2.2.9 Restriction digestion of plasmid DNA 40

2.2.10 Agarose gel electrophoresis 40
2.2.11 Ligation 41
2.3 Virology methods 41
2.3.1 Propagation of Zika Virus (ZIKV) 41
2.3.2 Infection of Vero cells with ZIKV 41
Chapter 3 Generation of pseudotyped Zika Virus (ZIKV) 43
3.1 Introduction 43
3.1.1 Background 43
3.1.2 Pseudotyped viruses (PV) 44
3.2 Aim 47
3.3 Materials and methods 47
3.3.1 Plasmids, virus and cell lines 47
3.3.2 Transfection of pI.18ZIKV-E in 293T cells 49
3.3.3 Detection of Zika envelope (E) protein using Western Blot 50
3.3.4 Propagation of Fowlpox-T7 helper virus (FPV-T7) 51
3.3.5 Primary virus rescue of VSV PV from plasmids using FPV-T7 52
3.3.6 Plaque purification of VSV PV 53
3.3.7 Amplification of VSV PV plaque isolates and generation of VSV PV working stocks 54
3.3.8 Pseudotyping ΔG-VSV with heterologous envelope proteins 54
3.3.9 Cell surface expression assay using a flow cytometer 55
3.4 Results 56
3.4.1 Restriction Digestion 56
3.4.2 Western blot 59
3.4.3 Propagation of FPV-T7 59
3.4.4 Primary recovery of VSV PV 60
3.4.5 Cell surface expression using a flow cytometer 65
3.5 Discussion 67
3.5.1 Virus budding sites 67
3.5.2 ER retention signal 69
3.5.3 Cell lines 72
Chapter 4 Development of a ZIKV NS1-based enzyme-linked immunosorbent assay (ELISA) using plant expressed NS1 protein 73
4.1 Introduction 73
4.1.1 ZIKV diagnosis 73
4.1.2 ZIKV-NS1 75
4.1.3 Plant expression system 76
4.2 Aim 78
4.3 Materials and methods 78
4.3.1 General materials 78
4.3.2 PCR cloning of pEAQ-HT-ZIKV-NS1-His by conventional PCR cloning 79

4.3.3 Second attempt—Gibson Assembly® Cloning of pEAQ-HT-ZIKV-NS1-His 83
4.3.4 PCR colony screening to confirm successful ligation 84
4.3.5 Third attempt—ZIKV NS1 expression vector construction by gene synthesis . 85
4.3.6 Transient Expression of ZIKV NS1 proteins in *N.benthamiana* 86
4.3.7 Testing ZIKV-NS1 based ELISA in detecting antibodies against Zika and Dengue 87
4.4 Results 88
4.4.1 PCR cloning of pEAQ-HT-ZIKV-NS1-His 88
4.4.2 Gibson Assembly cloning of pEAQ-HT-ZIKV-NS1-His 92
4.4.3 ZIKV NS1 expression by gene synthesis 95
4.4.4 ZIKV NS1-based ELISA performance 97
4.5 Discussion 98
4.5.1 First and second attempt 98
4.5.2 Third attempt 99
4.5.3 Validation of an ELISA assay 101
Chapter 5 Identification of clade-specific antibodies against Equine Influenza Virus (EIV) using Next Generation Phage Display (NGPD) 102
5.1 Introduction 102
5.1.1 Equine Influenza Virus (EIV) 102
5.1.2 Phage display 105
5.1.3 Next-generation phage display 111
5.2 Aim 112
5.3 Experiment design and panning strategy 112
5.4 Materials and methods 114
5.4.1 General materials 114
5.4.2 Protein assay 116
5.4.3 Helper phage (Ex-phage) production 117
5.4.4 Helper phage (Ex-phage) titration 117
5.4.5 TG1 stock production 118
5.4.6 Experiment 1A and 1B: 118
5.4.7 Experiment 2 123
5.4.8 Round 3 and round 5 screening 125
5.4.15 NGS sample preparation— PCR amplification of CDRs 126
5.4.16 NGS data analysis 128
5.5 Results 130
5.5.1 Experiment 1A — targeting Devon, no subtraction 130
5.5.2 Experiment 1B — targeting Kentucky, no subtraction 134
5.5.3 Experiment 2 — targeting Devon, with subtraction 135
5.6 Discussion 135
5.6.1 Replacement of animal use 136
5.6.3 Phage ELISA 136

5.6.5 Future work 138
Chapter 6 Conclusions 140
Appendix 1 144
Appendix 2 152
References 154

Figure 1. 1 Flavivirus genome structure (Adapted from (Lindenbach, 2007)). 18
Figure 1. 2 Flavivirus replication cycle (Adapted from (Heinz and Stiasny, 2017)). 20
Figure 1. 3 Diagrams of the dengue 2 and Zika virus E protein dimers in their side and top views, respectively. TM, transmembrane. The three E protein domains are displayed in red (DI), yellow (DII), and blue (DIII), and the DI-DIII as well as DIII-stem linkers are shown in purple. The fusion loop at the tip of domain II is shown in orange. (Adapted from (Heinz and Stiasny, 2017)). 21
Figure 1. 4 Indirect or Sandwich ELISA (Adapted from (Wade, 1989)). 31
Figure 1. 5 Competitive indirect ELISA for antigen detection (Adapted from (Wade, 1989)). 33
Figure 1. 6 Competitive antigen capture ELISA (Adapted from (Wade, 1989)).....34

Figure 3. 1 Schematic representation of the production of ZIKV PVs (Adapted from (Tani, 2014)). 45
Figure 3. 2 The plasmid map of VSV P as an example of plasmids encoding VSV structural proteins (adapted from https://www.kerafast.com/product/701/pbs-p-t-plasmid).....48
Figure 3. 3 Sequence designed for ZIKV-E synthesis in pI18 plasmid. Prediction of Zika signal sequence was done by Dr Simon Scott based on various prediction programs. 48
Figure 3. 4 Construction of C2 by replacing of the WNV E transmembrane domains (TM) with the TM and c-tail of VSV G, which contains the export signal sequence. (Figure is drawn by Dr Barney King (University of Nottingham)) 49
Figure 3. 5 'Sandwich' method for protein transfer.....50
Figure 3. 6 Six well plate layout for dilution factors of VSV PV original stock for plaque purification. 54
Figure 3. 7 Twelve-well plate layout for transfecting the cells with different plasmids. 56
Figure 3. 8 Restriction Digestion of pBS-P-ΦT and pBS-N-ΦT to confirm their identity. 57
Figure 3. 9 Restriction Digestion of pBS-G-ΦT. From left to right: 1kb DNA ladder (NEB); undigested pBS-G-ΦT; pBS-G-ΦT digested with ApaI; pBS-G-ΦT digested with BamHI; pBS-G-ΦT digested with both ApaI and BamHI. Gel electrophoresis confirms the plasmid is pBS-G-ΦT. 58
Figure 3. 10 Restriction Digestion result of pI18-ZIKV-E. From left to right: 1kb DNA ladder (NEB); undigested pI18-ZIKV-E; pI18-ZIKV-E digested with BamHI; pI18-ZIKV-E digested with both BamHI and XhoI; pI18-ZIKV-E digested with both BamHI and EcoRI. Gel electrophoresis confirms the plasmid is pI18-ZIKV-E. .58
Figure 3. 11 Western blot result shows the ZIKV-E was expressed by 293T cells and the size was correct. Full range rainbow molecular weight marker (Fisher Scientific) was used. Strong bands were observed in the first three lanes which were loaded with samples produced by transfecting 293T cells with plasmid pI18-ZIKV-E, whereas no bands were shown in the negative control lanes where the samples were untransfected 293T cells. 59
Figure 3. 12 Observations of cytopathic effect (CPE) in chicken embryonic fibroblast (CEF) cells infected with Fowlpox T7 helper (FPV-T7) virus. 60
Figure 3. 13 Luciferase activities in producer cells transfected with the same amount of plasmids, FPV-T7 helper virus and helper plasmid ratio but using different volumes of Lipofectamine. A large difference in luciferase activity was observed between Lipofectamine. This experiment was not performed in replicates; therefore, no error bars were presented. 61
Figure 3. 14 Luciferase activities in target cells infected with recovered VSV PV supernatant. Only target cells in the '15µl' well showed luciferase activity. This experiment was not performed in replicates; therefore, no error bars were presented.....61
Figure 3. 15 Image of producer cells transiently transfected with C2 and infected with VSV PV taken 16H P.I.. The red arrow shows possible aggregations of dead cells, which were not observed in negative control cells which were untransfected producer cells and infected with VSV PVs (B). 63

Figure 3. 16 Images of producer cells A. transiently transfected with CHIKV-E and infected with VSV PV taken 16 hours post-infection. B. negative control cells. C. producer cells transiently transfected with ZIKV-E. D. producer cells transiently transfected with VSV-G. 63
Figure 3. 17 A producer cell luciferase activity when attempting to generate ΔG-VSV PVs with foreign glycoproteins, no error bars were presented because data was collected from single well; B target cell luciferase activity after they were infected with ΔG-VSV PVs formed with foreign glycoproteins. 64
Figure 3. 18 Cell surface expression of ZIKV envelope proteins on BHK-21 cells. 65
Figure 3. 19 Cell surface expression of influenza HA envelope proteins on BHK-21 cells. 66
Figure 3. 20 Topology of yellow fever virus (YFV) envelope proteins (Adapted from (Ciczora et al., 2010)). .. 71
Figure 3. 21 Schematic diagrams of a recommended chimeric protein construct for pseudotyping ZIKV by the author. 72

Figure 4. 1 The significant laboratory diagnostic markers in (1) primary ZIKV infections and (2) secondary flavivirus infections with ZIKV. Titer course of anti-ZIKV IgM and IgG in (3) a traveller from the non-endemic area after primary infection with ZIKV, and (4) a resident from the endemic region of multiple flaviviruses who contracted ZIKV as secondary flavivirus infection (Adapted from (Ohst et al., 2018)). . 74
Figure 4. 2 pEAQ vector with a GFP insert. 77
Figure 4. 3 Plasmid map of pEAQ-HT. The insert region is flanked by two 6×His tags and two AgeI restriction sites. 78
Figure 4. 4 PCR amplification of ZIKV NS1. Restriction site AgeI and a start codon were added to ZIKV NS1 N-terminus by a forward primer. Also, restriction site XhoI, a stop codon and a 6-Histidine tag were added to C-terminus of ZIKV NS1 by two reverse primers in two separate PCR reactions. 80
Figure 4. 5 (a) estimated Round 2 PCR products, features including an upstream AgeI restriction site and a downstream XhoI restriction site, ZIKV NS1 sequence followed by a hexa his-tag. (b) Theoretical PCR cloning end product. 82
Figure 4. 6 ZIKV NS1 amplified using primers designed for Gibson Assembly® Cloning. It is different from ZIKV NS1 amplified for PCR cloning in two main areas: 1, there are two AgeI restriction sites flanking ZIKV NS1, whereas only one AgeI site was kept in the first attempt; 2, there are two consecutive 6His-tags after ZIKV NS1, whereas there is only one 6 His tag attached to ZIKV NS1 in the previous attempt. 84
Figure 4. 7 Codon optimised and synthesised ZIKV NS1. N-terminal features include AgeI site, Kozak sequence and PR1a signal peptide. C-terminal features include a 6×His tag SEKDEL sequence and XhoI restriction site. 85
Figure 4. 8 ELISA plate layout. 88
Figure 4. 9 Gradient PCR using ZIKV NS1 forward primer and 'His tag Rev 1' reverse primer for adding the first four histidine tags to C-terminus of ZIKV NS1 sequence 89
Figure 4. 10 Gradient PCR using ZIKV NS1 forward primer and 'His tag Rev 2' reverse primer for adding the remaining two histidine tags, a stop codon and restriction site XhoI to the C-terminus of ZIKV NS1 sequence. Templates used in this gradient PCR were PCR products from previous gradient PCR. 90
Figure 4. 11 Colony PCR using two sets of primers both confirmed the successful ligation of the vector pEAQ-HT and the insert ZIKV NS1. 91
Figure 4. 12 SDS gel electrophoresis confirmed that there were no ZIKV NS1 expressed by the plants N.benthamiana. 91
Figure 4. 13 Gradient PCR for amplification of ZIKV NS1 for Gibson Assembly cloning using specifically design ed primers 'MyInsert F1' and 'MyInsert R1'. 92
Figure 4. 14 Colony PCR for confirmation of Gibson Assembly. Various brightnesses of the bands may be due to different sizes of the colony when picking, and they were subsequently amplified in different degrees. 93
Figure 4. 15 Insert check. A. Sanger sequencing results were translated using ExPASy. B. sequences from pEAQ-HT were in Bold. ZIKV NS1 sequence was underlined. Restriction sites AgeI and XhoI were in italic. 93
Figure 4. 16 SDS gel electrophoresis performed to check ZIKV NS1 and SBV N proteins expression by plants. A clear band just below 28 KDa was observed in SBV N elution samples after extraction and purification; however, no strong band around the expected size was observed in ZIKV NS1 elution samples. 94
Figure 4. 17 A. Protein translation of synthesised and optimised ZIKV NS1 sequence. B. Protein translation of Sanger sequencing results of pEAQ-HT-ZIKV-NS1-C-His using primers BK79 and BK80. 95

Figure 4. 18 SDS gel electrophoresis performed to check ZIKV NS1 proteins expression by plants. SBV N protein expression was used as positive control. A band just below 28 kDa was seen in the SBV N extraction gel. And a band between 39—51 kDa was seen in the ZIKV NS1 extraction gel. 96
Figure 4. 19 Comparisons of ZIKV NS1 plant expression between second and third attempt. The bands between 39—51 kDa were not seen in the first two attempts. 96
Figure 4. 20 Average absorbance reading at 30 min post substrate addition. Green: ZIKV samples; Blue: Dengue samples; pink: negative controls. Sensitivity (95%) and specificity (95%) of this ELISA were calculated based on a cut-off value of 0.9. 97

Figure 5. 1 Structure of influenza A virus (Adapted from (Clancy, 2008)). Influenza A virus has 8 RNA segments: PB2, PB1, PA, HA, NP, NA, M and NS. 103
Figure 5. 2 Molecular Phylogenetic analysis by Maximum Likelihood method. The analysis involved 43 nucleotide sequences. Evolutionary analyses were conducted in MEGA7. Kentucky/1/14 is used as a representative of Florida lineage clade 1 EIV in this study, Devon/1/11 represents Florida lineage clade 2 EIV and Richmond/1/07 is used as the backbone of the recombinant EIVs (see Figure 5. 11)..... 104
Figure 5. 3 Ff phage structure (Adapted from (Sidhu and Geyer, 2015)). 106
Figure 5. 4 pIII domain structure and initiation of Ff phage infection (Adapted from (Sidhu and Geyer, 2015)). pIII has three domains and infection initiates from the binding of D2 to the tip of F pilus, followed by the release of D1 and interaction of D1 with co-receptor TolA. 108
Figure 5. 5 Different formats of phage display (Adapted from (Wang and Yu, 2004)). The '3' system uses a phage vector that has a modified pIII which is fused to the peptide of interest, i.e. antibody. The '33' system uses a phage vector that has both a wild type pIII and a fusion pIII. The '3+3' system uses a phagemid vector in combination with a helper phage. The pIII gene is from two sources. The '3' system can only express one type of pIII; however, the '33' and '3+3' system produce mosaics. 109
Figure 5. 6 A typical IgG antibody and a VHH (Doshi et al., 2014). 110
Figure 5. 7 Experiment 1A procedure. The VHH library was directedly incubated with Devon, after four rounds of panning, the eluted phage pool is subjected to polyclonal phage ELISA, monoclonal phage ELISA and next-generation sequencing..... 113
Figure 5. 8 Experiment 1B procedure, same as experiment 1A but phage ELISAs were omitted. And experiment 1B was conducted at the same time as experiment 1A 113
Figure 5. 9 Experiment 2 procedure. A subtraction step was included where phage library was incubated with Kentucky to subtract potential binders before panning against Devon. Subsequently, eluted phage pool was sent for NGS sequencing. 114
Figure 5. 10 Phagemid construct –pSD3-VHH generated by Dr Alison Gray, not published. 115
Figure 5. 11 Equine influenza virus reassortants. One stock of virus contains all gene segments from A/equine/Richmond/1/07 except for segment 4, which is from A/equine/Kentucky/1/14. The other stock contains all gene segments from A/equine/Richmond/1/07 but segment 4, which is from A/equine/ Devon/1/11. 116
Figure 5. 12 Plate A was coated with Kentucky and plate B was coated with Devon. From D2-D11, 10 wells per plate were pre-coated with 100 µl of each antigen at 20 µg/ml, diluted in sodium carbonate buffer. 118
Figure 5. 13 Maxisorb 96 well plate layout for polyclonal ELISA. 121
Figure 5. 14 Illustration of round 2 panning against Devon HA with subtraction. 124
Figure 5. 15 Maxisorb 96 well plate layout for round 3 and 5 screening. 125
Figure 5. 16 Ninety-five phage samples from two different panning experiments were selected for next-generation sequencing. 126
Figure 5. 17 Amplification of CDR3 of VHH library for NGS in two rounds of PCR. 127
Figure 5. 18 Step by step flowchart of NGS data analysis using Ubuntu, a Linux operating system. Scripts used to analyse the data were written by Dr Jon Owen. Each step and its function was included in Appendix 2. 129
Figure 5. 19 Polyclonal ELISAs for first panning experiment. Results from the first attempt (left figure) show overall signals were very low and not increased throughout panning rounds. In the second polyclonal ELISA, although signals have been increased, indicating successful enrichment, the enriched phage could not differentiate the two targets. 130
Figure 5. 20 Round 1 PCR results as an example of NGS sample preparation. All 95 samples were amplified successfully and negative control was not contaminated. 131

Figure 5. 21 Monoclonal ELISA. 1-30 colonies are from round 2, 31-60 colonies are from round 3, 61-90 colonies are from round 4, 91-120 colonies are from round 5 screening. Earlier rounds had less binders but more diversity; later rounds had more binders but less diversity , as same binder being amplified throughout multiple rounds. 132

Abbreviations

BHK	Baby hamster kidney
BME	Beta-mercaptoethanol
CO_2	Carbon dioxide
cDNA	Complementary deoxyribonucleic acid
CNS	Central nervous system
CHIKV	Chikungunya virus
CHO	Chinese hamster ovary
CPMV	Cowpea mosaic virus
CPE	Cytopathic effect
CCHFV	Crimean-Congo haemorrhagic fever virus
CF	Complement fixation
CEF	Chicken embryonic fibroblast
CaMV	Cauliflower mosaic virus
CDR	Complementarity-determining region
DNA	Deoxyribonucleic acid
DENV	Dengue virus
DHF	Dengue haemorrhagic fever
DSS	Dengue shock syndrome
DMSO	Dimethyl sulfoxide
DMEM	Dulbecco's Modified Eagle Media
E	Envelope
ER	Endoplasmic reticulum
EIV	Equine influeza virus
ELISA	Enzyme-linked immunosorbant assay
FFRNT	Fluorescent focus reduction neutralisation test
FBS	Fetal bovine serum
FPV	Fowpox virus
FACS	Fluorescence-activated cell sorter

Fab	Antigen-binding fragment
GFP	Green fluorescent protein
GAG	Glycosaminoglycan
HIV	Human immunodeficiency virus
HA	Haemagglutinin
HPAI	High pathogenic avian influenza virus
HRP	Horseradish peroxidase
HCV	Heptitis C virus
HI	Haemagglutination inhibition
ISP	Ion sphere particles
IG	Intergenic region
JEV	Japanese encephalitis virus
LPAI	Low pathogenic avian influenza virus
LB	Lysogeny broth
MDCK	Madin-Darby canine kidney
MVEV	Murray Valley encephalitis virus
mRNA	messenger RNA
MLV or MuLV	Murine leukemia virus
NS	Non-structural
Nos	Nopaline synthase
NA	Neuraminidase
NGPD	Next-generation phage display
NGS	Next-generation sequencing
ORF	Open reading frame
OIE	World Organisation for Animal Health
prM	pre-membrane
PCR	Polymerase chain reaction
PRNT	Plaque reduction neutralisation test
PFU/CFU	plaque/colony forming unit

PPRNT	Pseudo-plaque reduction neutralisation test
PVDF	Polyvinylidene difluoride
PVNT	Pseudotyped virus neutralisation test
PV	Pseudotyped virus
PEG	Polyethylene glycol
RNA	Ribonucleic acid
RT-PCR	Reverse transcription-polymerase chain reaction
rRT-PCR	real-time reverse transcription-polymerase chain reaction
RLU	Relative luminescence unit
RF	Replicative form
RNP	Ribonucleoprotein
SDS	Sodium dodecyl sulfate
SLEV	Saint Louis encephalitis virus
SEKDEL	Peptide sequence Ser-Glu-Lys-Asp-Glu-Leu
SBV	Schmallenberg virus
SRH	Single radial haemolysis
scFv	Single-chain variable fragment
TM1prM	First transmembrane domain of prM
TM1E	First transmembrane domain of E
TM2E	Second transmembrane domain of E
UV	Ultraviolet
UTR	Untranslated region
VN	Virus neutralisation
VSV	Vesicular stomatitis virus
WNV	West Nile virus
WB	Western blot
YFV	Yellow fever virus
ZIKV	Zika virus

Chapter 1 Introduction

1.1 Re-emergent viruses — why and how?

It was argued that human populations had experienced previously two epidemiological transitions and are now going through the third one (Armelagos et al., 2005). Occurring approximately 10000 years ago, marked by the emergence of infections, the first epidemiological transition was created by the shift from foraging to an agricultural subsistence economy in Neolithic human populations. With the domestication of plants and animals, there was a striking increase in the prevalence of infectious disease. The second epidemiological transition was observed in some populations about a century ago, characterised by declines in infectious disease and a rise in non-infectious, chronic and degenerative diseases. Driving forces for the second epidemiological transition include immunisation programmes, improved nutrition, and advances in medicine. Human populations are currently undergoing the third epidemiological transition, in which there is a re-emergence of infectious diseases, many of which potentially have a great impact on global health and formerly considered 'under control', and the emergence of new diseases (Armelagos et al., 2005).

Many have argued that the emergence or re-emergence of infectious diseases is a consequence of social, demographic and environmental changes in global ecology as well as adaptation and evolution of pathogens (Armelagos et al., 2005). On the one hand, Howard (2012) suggests that the ease of long-distance air travel and human migration facilitates the spread of new infectious agents worldwide. The drastic deforestation in the last 50 years, resulting in a reduced bio-diversity, brings rodents, insects and other potential carriers of infectious disease even closer to human populations. Global warming caused by the increased greenhouse gases such as CO_2 is producing either floods or sustained droughts globally, which greatly affects diseases dependent on mosquito populations and rodent reservoirs. The emergence (re-emergence) of viral or other

diseases, to some extent, is regarded as warning signs of our disturbed ecosystem (Howard, 2012).

On the other hand, RNA viral genomes have much higher mutation rates compared to DNA viruses, due to the lack of proofreading step by host cell enzymes. The RNA virus-infected cells are unable to repair errors during translation of viral RNA into mRNA or errors introduced during genome replication. Consequently, RNA viruses can rapidly adapt to increasing levels of host immunity, changed dynamics in animal reservoir population and vector competence. The adaptability of RNA viruses with segmented genomes is further strengthened, as reassortment can occur between physically separate gene segments when a host cell is infected by two phenotypically different viruses at the same time. A good example is influenza virus where both point mutation (causing antigenic drift) and reassortment (causing antigenic shift) can create new viruses with significant changes in species specificity and pathogenicity (Howard, 2012).

1.2 Flaviviruses

ZIKV is a mosquito-borne flavivirus. Flaviviruses are a group of enveloped positive-sense single-stranded RNA viruses that causes a wide range of zoonotic diseases (Fernandez-Garcia et al., 2009). They belong to the family *Flaviviridae* and genus Flavivirus, which consists of 73 confirmed species. Most of these viruses are mosquito-borne and tick-borne; the rest have no known vectors and are not important human pathogens (Solomon, 2003, Maeda and Maeda, 2013). Some species are extremely pathogenic to humans and cause distinct clinical diseases, viruses such as dengue virus (DENV) and yellow fever virus (YFV) cause vascular leakage and haemorrhage. Other groups of viruses can cause neurological diseases such as Murray Valley encephalitis virus (MVEV), Saint Louis encephalitis virus (SLEV), Japanese encephalitis virus (JEV) and West Nile virus (WNV) (Fernandez-Garcia et al., 2009).

1.2.1 Yellow fever virus (YFV)

Yellow fever virus is a prototype member of the flaviviruses with a successful live attenuated vaccine (17D) developed for human use. It is transmitted by *Aedes* or *Haemagogus* mosquitoes in tropical regions of Africa and the Americas with two transmission cycles: the sylvatic cycle in which humans are infected by epizooties-affected non-human primates, and the urban cycle which is maintained in towns and cities by peri-domestic mosquitoes such as *Aedes* aegypti. Since late 2016, Brazil has suffered the most severe YFV epidemic in decades. Moreover, YFV has rapidly spread to areas where the virus has not been detected for 70 years, and vaccine coverage is close to nil (Bonaldo et al., 2017).

1.2.2 West Nile virus (WNV)

West Nile virus (WNV) was first isolated from the blood of a woman in 1937 in the West Nile district of Uganda but not regarded as a causative agent for meningoencephalitis until 1957. It remained relatively obscure between 1975 to 1993 (Howard, 2012). After that, WNV started to cause several outbreaks in Europe and the Mediterranean area among humans and horses, with the largest outbreaks recorded in Russia, Israel and Romania. WNV was first recognised in the Western hemisphere in 1999 when it caused an outbreak in New York and its suburbs (Huhn et al., 2003). Since then, WNV spread rapidly and steadily westwards across US mainland states and into the Caribbean and Central Americas. The main vectors are mosquitoes and birds, with migrating birds bringing infected mosquitoes being the most likely route of spread. WNV has a broad range of bird hosts. Infected birds have a high and sustained viraemia, which is ideal for increasing the chance of a feeding mosquito acquiring an infectious dose. However, WNV viraemia in humans and other mammals is comparatively short-lived, and titres are also too low to pose a risk of human transmission through an insect bite. Thus humans and other animals are not essential in maintaining the transmission cycle, being incidental or dead-end hosts (Howard, 2012). During the 2002 epidemic, it was the first time that human viremia was

implicated in person-to-person transmission through blood, blood products, and organ transplantation, and possibly through breast milk and intrauterine infection (Huhn et al., 2003).

1.2.3 Dengue virus (DENV)

The four serotypes of Dengue virus are threatening over a third of the human population and the emergence of new clinical profiles including dengue haemorrhagic fever (DHF) and dengue shock syndrome (DSS) has developed over the past 50 years. Furthermore, dengue 2 has evolved rapidly as a virus less dependent on animal reservoirs, with the life cycle maintained predominantly by human-human transmission (Howard, 2012).

1.2.4 Replication and assembly

Flaviviruses all share a similar genomic organisation and replication strategy. The genome encodes for a single polyprotein (see Figure 1. 1) of 3400 amino acids, which is cleaved co- and post-translationally by viral and host proteases to generate three structural proteins: core, pre-membrane (prM), and envelope protein (E), and seven non-structural (NS) proteins: NS1, NS2A, NS2B, NS3, NS4A, NS4B and NS5 (Fernandez-Garcia et al., 2009).

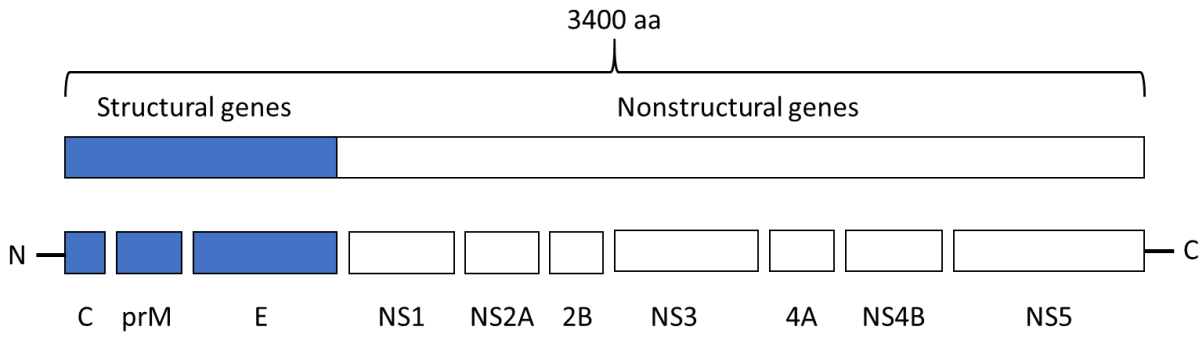


Figure 1. 1 Flavivirus genome structure (Adapted from (Lindenbach, 2007)).

Flavivirus genome encodes a single polyprotein which is co- and post-translationally cleaved by host and viral proteases to generate three structural proteins and seven non-structural proteins.

The virus enters host cells by receptor-mediated endocytosis (see Figure 1. 2). In the endosome, virus envelope proteins undergo a pH-triggered conformational change, which leads to the fusion of the virus and cell membranes and release of the viral genome (Fernandez-Garcia et al., 2009). The flavivirus genome is approximately 11,000 nucleotides in size and encodes a single long open reading frame (ORF). The 5' end of the genome is capped; however, unlike cellular messenger RNA (mRNA), the 3' end is not modified with a polyadenylated tail (Lindenbach, 2007). After translation of the positive-sense RNA, a negative-sense complementary RNA is made which serves as the template for synthesis of new positive-strand RNA. Positive-sense RNA is copied approximately 10-fold more than the negative-sense RNA. Subsequently, the immature virions assemble within the endoplasmic reticulum (ER), where viral RNA forms complexes with C proteins, wrapped by the ER-derived lipid bilayer containing heterodimers of prM and E proteins. Nascent C protein contains a C-terminal hydrophobic anchor that serves as a signal peptide for prM to translocate to the ER. This C-terminal domain is cleaved from mature C by the viral serine protease (Lindenbach, 2007).

The prM plays an important role in preventing premature maturation of E protein. It acts as a 'chaperone' and stops the acid-catalysed rearrangement of E protein to the fusogenic form during transit in the secretory pathway. The virion matures at the end of the secretory pathway when prM is cleaved into pr and M protein by the Golgi-resident protease furin or its related enzyme. After the cleavage, the prM-E heterodimer dissociates, the pr fragment is released, and E proteins form homodimers. The mature virion leaves the host cell by exocytosis (Lindenbach, 2007).

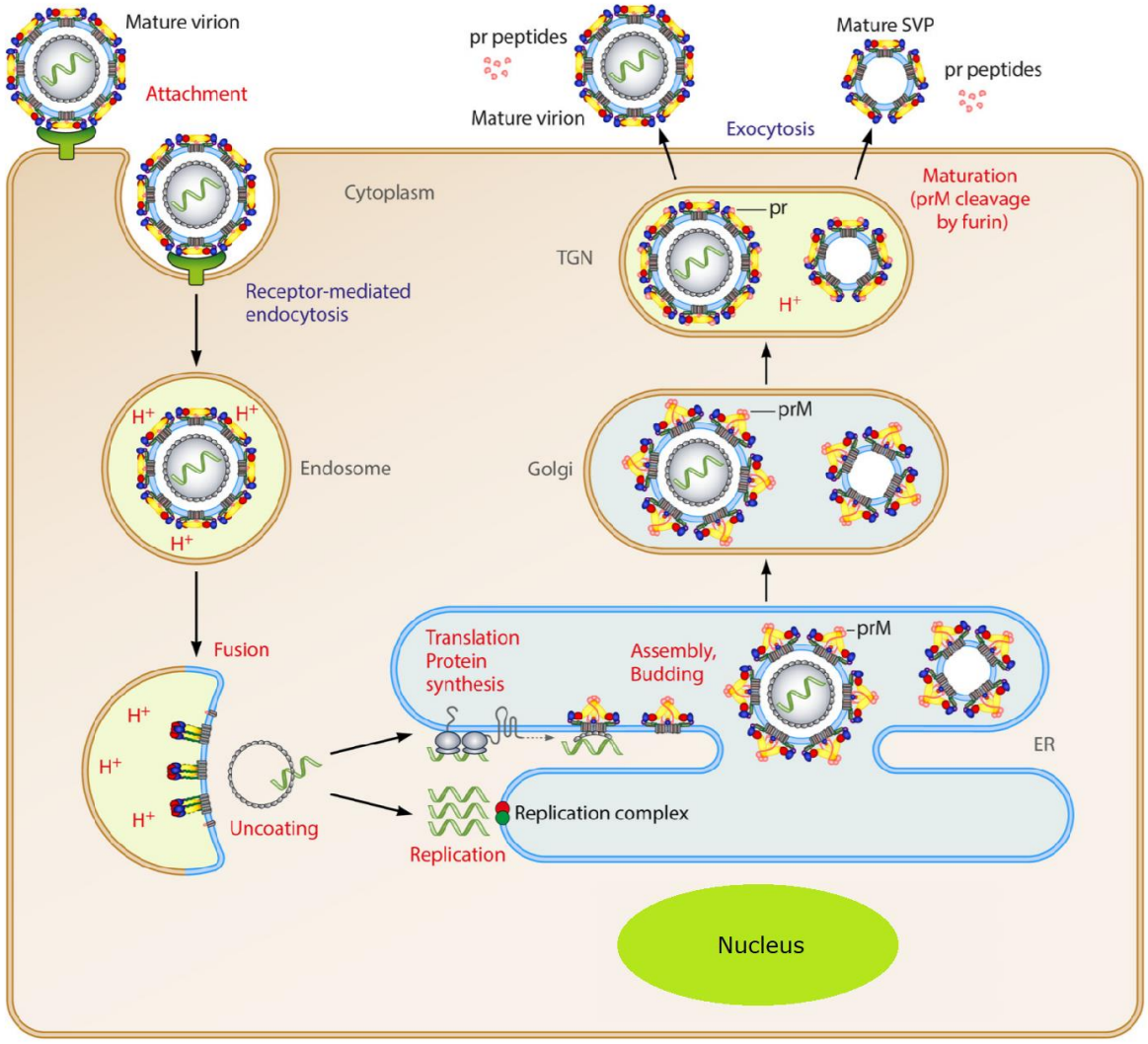


Figure 1. 2 Flavivirus replication cycle (Adapted from (Heinz and Stiasny, 2017)).

The flavivirus replication cycle starts from the receptor-mediated endocytosis. In the endosome, virus envelope proteins undergo a pH-triggered conformational change, which leads to the fusion of the virus and cell membranes and release of the viral genome. Virus assembly and budding occur on the ER membrane. prM is cleaved by protease furin at the end of the secretory pathway. Mature virion exit the host cell by exocytosis.

The E protein is the largest structural protein on the surface of the flavivirus virion. The major functions of E protein include mediating viral attachment via cellular receptors, specific membrane fusion, and eliciting a humoral immune response (Lindenbach, 2007, Daly, 2010). Native E proteins form head-to-tail homodimers lying parallel with the virus envelope, and each subunit contains three domains (See Figure 1. 3). Domain I contains a beta-barrel and functions as a hinge between domains II and III. Domain II is the elongated dimerisation part, and the fusion peptide responsible for insertion into target cell membranes is located at the tip of domain II. Domain III has an immunoglobulin-like fold; it is thought to be the cellular receptor-binding site and is a target of neutralising antibodies (Lindenbach, 2007). Because of E proteins parallel arrangement with the membrane surface, the flaviviruses do not have surface projections compared to many other enveloped viruses such as influenza viruses (Howard, 2012).

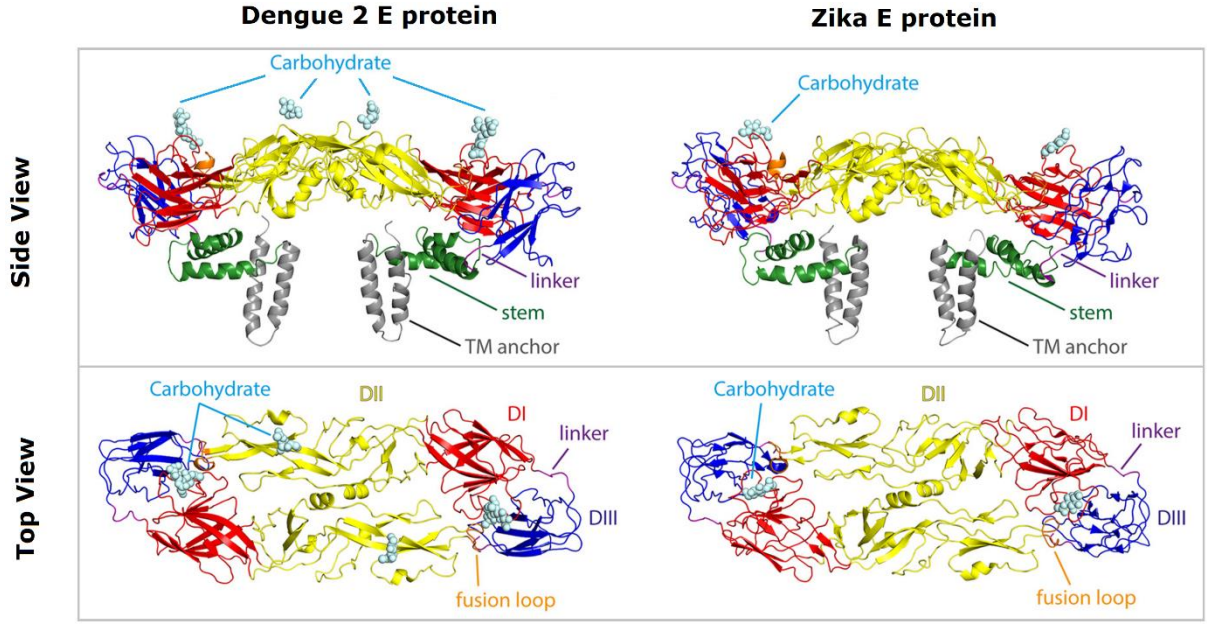


Figure 1. 3 Diagrams of the dengue 2 and Zika virus E protein dimers in their side and top views, respectively. TM, transmembrane. The three E protein domains are displayed in red (DI), yellow (DII), and blue (DIII), and the DI-DIII as well as DIII-stem linkers are shown in purple. The fusion loop at the tip of domain II is shown in orange. (Adapted from (Heinz and Stiasny, 2017)).

1.2.5 Diagnostic challenges

Development of an efficient and accurate diagnosis for flavivirus infection is still facing some challenges. Firstly, serology remains the most common approach to confirm viral infection. However, cross-reactivity of sera raised against one flavivirus recognising another flavivirus has been observed (Calisher et al., 1989). Cross-reactive sites were identified on the envelope glycoproteins of different flavivirus species. Flavivirus cross-reactivity may, therefore, result in false-positive results (Mansfield et al., 2011). Consequently, diagnosis is particularly challenging in persons living in regions with flavivirus co-circulation and people travelling between different flavivirus endemic countries (Lustig et al., 2018).

Secondly, flavivirus viraemia in human and animals tends to be short-lived and low in titre, which obstructs the use of molecular diagnostic methods for detecting viral RNAs such as the polymerase chain reaction (PCR). Lanciotti et al. (2000) showed that the sensitivity for WNV RNA in acute phase central nervous system (CNS) fluid and blood was as low as 57% and 14 % respectively.

1.3 Influenza viruses

Influenza viruses are the main causes of respiratory tract disease in humans and domesticated animals, mostly horses, pigs and poultry. Influenza B and C viruses are mostly restricted to humans and influenza A viruses are avian viruses that evolved to fully adapt to humans, pigs, or horses, which raise the most concerns for public health. Influenza A virus displays extensive genetic and antigenic diversity: 18 serotypes based on the haemagglutinin (H) molecules and 11 serotypes based on neuraminidase (N) molecules. All 16 H subtypes of influenza A viruses occur naturally in aquatic birds, only three subtypes (H1, H2 and H3) have caused widespread infections in humans. H1 and H3 also infect pigs; moreover, H3 also infect horses (Howard, 2012).

1.3.1 Human (seasonal) influenza

Seasonal influenza viruses are transmitted by inhalation of water droplets, contaminated dust and fomites or through contact with contaminated surfaces. Spread between humans is primarily by aerosols generated during coughing and sneezing. H3N2, H1N1 and influenza B viruses used to be the predominant viruses circulating in previous years. However, the severity and circulating strains were rarely the same in any two consecutive years due to the antigenic changes. The constant mutations in the viral genes leads to a gradual loss of antibody reactivity in the sera of immune individuals, which means vaccination against seasonal influenza has to be done annually against the prevalent serotypes circulating in any one year. The unpredictability of the succession strains hinders vaccine production. Point mutation alone usually cannot create a major alteration in antigenicity, which leads to pandemics. It is generally caused by a significant reassortment of genes between two different subtypes or complete transfer of the virus from one species to another. As a result, a new strain can emerge into the human population where there is very little pre-existing herd immunity (Howard, 2012).

1.3.2 Avian influenza (H5, H7 and H9)

Avian influenza viruses are usually classified according to their lethality for chickens. The highly pathogenic avian influenza viruses (HPAI) are defined by the World Organisation for Animal Health (OIE) as having an intravenous pathogenicity index >1.2 in 6-week-old birds and those that kill over 75% of intravenously infected 4 to 8-week old chickens (Machalaba et al., 2015). Transmission of both H7 HPAI and low pathogenic strains (LPAI) from poultry to humans was reported, with infection causing human respiratory disease or conjunctivitis. Some HPAI subtypes can cause severe human disease, which is potentially fatal. The natural reservoir of influenza A virus is aquatic birds. The virus mainly replicates in the intestinal epithelia, and thus transmission is mostly by the faecal-oral route. Nonetheless, the highly pathogenic H5N1 virus emerged in 2002 seems to have evolved to spread from the avian respiratory tract. In 2003, severe outbreaks of H5N1 in

poultry occurred in many countries of Southeast Asia. Wild bird populations were subsequently affected. The death of thousands of migratory birds followed, more than 60 wild bird species have been infected with the HPAI strain of H5N1.

Moreover, by earlier 2005, H5N1 had resulted in 55 confirmed human cases, with a mortality rate of 76%. Phylogenetic analysis showed the circulation of multiple genetically and antigenically different lineages of the H5N1 virus. Clade 1 viruses have been found mostly in Thailand and Vietnam, while clade 2 viruses circulated predominantly in Indonesia and China (Howard, 2012).

1.3.3 Swine influenza

H1N1, H3N2 and H1N2 are three influenza A virus subtypes circulating and causing respiratory diseases in pigs. As pigs are susceptible to human, avian and swine influenza viruses, it has been proposed that domesticated pigs may serve as a mixing vessel for these viruses and reassortment in pigs may give rise to the emergence of new human pandemic strains. Except for the 2009 pandemic of swine-origin H1N1, swine influenza is not considered as a causative agent for serious diseases in humans. In the 2009 pandemic, the swine-origin H1N1 is a triple reassortment virus containing genes from human, avian and swine influenza viruses (Howard, 2012).

1.3.4 Vaccine

Global vaccination production for seasonal influenza is approximately 450 million does per year. The traditional approach for manufacturing influenza vaccine is by producing high growth reassortment viruses in embryonated hen’s eggs through simultaneous infection of eggs with the wild type recommended strain and A/PR/8/34 virus. The goal is to produce reassortments containing the 6 gene segments of A/PR/8/34 coding all but the viral envelope proteins which will be replaced by the 2 gene segments of the wild type virus coding for haemagglutinin and neuraminidase (Howard, 2012).

Vaccines are developed and used to control avian HPAI H5/H7 subtypes in a number of countries including Pakistan, Indonesia, China and Mexico. Vaccines for LPAI are also used to control LPAI H5/H7 in the USA, Italy, Mexico and some Latin American countries. Furthermore, horses are routinely vaccinated with inactivated H7N7 or H3N8 viruses with multiple doses, and racehorses are often re-vaccinated every 3 to 6 months, which has been relatively successful in controlling equine influenza. However, manufacturers do not always match the antigenic formulation to any minor changes caused by antigenic drift in the prevalent virus (Howard, 2012).

1.3.5 Surveillance

Surveillance of susceptible animals and human populations plays an important role in more accurately predicting virulence and transmissibility changes of influenza viruses (Howard, 2012).

1.4 Traditional serological assays

1.4.1 The plaque reduction neutralisation test (PRNT)

Most viruses can cause cytopathic effects (CPE) in host cells in which they are replicating. The infected cell undergoes shape change and many other alterations before it is killed or lysed. Where virus infection is localised this can cause plaque formation. With proper dilution and conditions, a single virus can produce such a plaque, and it is termed a plaque-forming unit (PFU) (Wagner, 1999).

The plaque reduction neutralisation test (PRNT) is used to quantify the neutralising antibody present in patient serum samples to detect the serological immune responses to the specific virus. In a conventional PRNT, patient's serum samples are serially diluted and mixed with a standardised amount of live virus. After incubation, allowing binding of antibodies to viruses, the mixtures are then incubated with a monolayer of permissive cells in culture plates and overlaid with agarose or carboxyl-methylcellulose to keep the

virus from wide diffusion. Those cells treated with serum with higher antibody concentrations will produce fewer and smaller plaques than will those treated with more diluted serums. Then median effective dose (ED50) can be calculated to quantify serum antibody concentration, which is the dilution in which the number of plaques is reduced by 50% or plaques are 50% smaller than untreated controls (Wagner, 1999). In some tests, a 90% reduction in plaques (PRNT90 or EP90) is also used for serum antibody titration (Mansfield et al., 2013, Simoes et al., 2012).

PRNT is considered the 'gold standard' for serodiagnosis as it is quantitative and more sensitive than HI and ELISA. However, there are still some disadvantages of PRNT. It is time-consuming to perform and takes up to 7 days for incubation. It requires a lot of labour for testing a large number of serum samples. It is very difficult to standardise due to the variabilities between laboratories (Cohen et al., 2007). Even with the same sample panel, a wide variation in PRNT titer results could occur in response to varied testing conditions such as cell types, control virus passages and the use of complement (Thomas et al., 2009). Most importantly, PRNT with wild-type flaviviruses can be technically difficult, as many flaviviruses grow slowly and have pinpoint-sized plaque phenotypes (Di Gennaro et al., 2014).

Currently, many modifications of PRNT have been developed for its safer and wider applications, such as pseudo-plaque reduction neutralisation test (PPRNT) and fluorescent focus reduction neutralisation test (FFRNT). They were used to measure neutralising antibodies against Crimean-Congo haemorrhagic fever virus (CCHFV), which is a virus with no or poor CPE in cell culture depending on the strain and can only be worked with in high level biocontainment facilities (Canakoglu et al., 2013).

1.4.2 The haemagglutination inhibition (HI) test

The HI test is used to measure antibody levels in the serum or detect antibodies to viral haemagglutinin in animal and human sera. Antibodies against viral proteins that induce haemagglutination can inhibit the binding ability of such virus to erythrocytes, therefore inhibit the virus-mediated agglutination of red blood cells. In this assay, dilutions of serum samples or antibodies are incubated with a standardised amount of virus for the antibody-antigen complex to form. Erythrocytes are then added. After incubation, agglutination, which is characterised by a diffuse red or salmon-pink solution, will be observed from the serum samples with low antibody concentration. If there is no agglutination, the pellet of cells will be observed as a red dot when using the 'V'-shaped well from 96-well plate. The HI titre is read as the highest dilution of antibody that inhibits haemagglutination. HI assays measure both IgM and IgG antibodies against viruses (Maeda and Maeda, 2013). This test is not accurate but is sensitive, simple, inexpensive and rapid (Wagner, 1999, Flint, 2009).

1.4.3 The virus neutralisation (VN) test

Neutralising antibodies can bind to the surface of the virus and block the viral infectivity by blocking a series of events such as binding to cell surface receptors, endocytosis or viral membrane fusion with the cell membrane, or release of the viral genome into the cell (Wagner, 1999). This reaction between specific antibodies and viruses can stop the virus from initiating infection in a cultured cell, an egg or an animal. Serially-diluted antibodies are mixed with the virus and incubated with test subjects mentioned above. The endpoint is defined as the highest dilution of antibody that inhibits the development of CPE in cells or viral replication in eggs or animals (Flint, 2009).

The VN test can be used to distinguish different serotypes of viruses and is valuable for virus classification. For instance, type 1 poliovirus is only neutralised by antibodies to type 1 virus but not by antibodies to type 2 or type 3, and so on. However, this test cannot be

used for some viruses such as hepatitis B and C, which cannot be readily grown in cell culture (Nathanson, 2007).

1.4.4 Complement fixation (CF)

Complement is a group of serum proteins that bind to an antibody-antigen complex on the surface of a cell, and sequentially undergo a complex maturation process resulting in cell lysis. The ability of complement to bind to antibody-antigen complexes at the Fc region of the antibody is termed fixation because once bound; the complement is no longer free in solution. CF is used to determine if antibodies against a virus are present in the serum. CF titration can be used to measure antibody-antigen reactions.

The standard procedure for CF is described as follows: the serum samples are heated to inactivate endogenous complement and then incubated with the virus and a standardised amount of guinea pig complement. If the antibody of interest is present and antibody-antigen complex forms, the complement will be fixed. Then sheep red blood cells coated with rabbit anti-red blood cell antibodies are added for detection. If complement fixation occurs, the red blood cells remain intact; otherwise, red blood cells are lysed by free complement. CF titre can be measured by the amount of red colour in the solution (Wagner, 1999).

Crude preparations of viral antigens, which include proteins or epitopes shared by viruses from the same family, are often used in this test. Therefore, CF is not highly specific or sensitive. However, it is low-cost, rapid, and often, the first assay used to identify the family to which an infecting virus belongs (Flint, 2009).

1.4.5 Western blot (WB)

In a WB, complex mixtures of proteins are first separated based on their sizes by polyacrylamide gel electrophoresis, where sodium dodecyl sulfate (SDS), an anionic

detergent, is added in the gel and buffers. Protein samples are prepared and heated in SDS before electrophoresis to enable their denaturation and ensure all proteins have roughly the same charge density. The separated proteins are then transferred or blotted onto a membrane, typically nitrocellulose or polyvinylidene difluoride (PVDF). This process can be accomplished by various methods such as electrophoretic transfer, capillary transfer or passive diffusion. The electrophoretic transfer is the most commonly used method because of its speed and transfer efficiency. After that, the membrane is blocked to prevent non-specific binding in the unreacted sites by blocking buffers such as nonfat dried milk, normal serum or highly purified proteins. This step, along with adequate washing, will increase the WB sensitivity and reduce background interference. Subsequently, the transferred proteins can either be stained or probed for detection of the protein of interest. Commonly used stains include amido black, Coomassie blue, which stains proteins irreversibly, or Ponceau S, which is a reversible stain due to its water solubility and can easily be washed away before the blot is probed (Howard and Kaser, 2007).

The specificity between the membrane-bound antigen and its specific probe, the primary antibody, will allow the detection of the presence of either a specific protein in a mixture such as from a tissue extract or a particular group of antibodies among a mixture such as in serum (Howard and Kaser, 2007). For instance, when performing a serodiagnosis using WB, a specific protein fragment from a virus can be used to detect if the antibody against that viral is present in patients serum samples (Yeh et al., 1994). Visual detection of the protein of interest can be achieved in two ways, either directly by the primary antibody which is conjugated to an enzyme that catalyses the colour change of a chromogenic substrate; or indirectly by a secondary antibody which recognize and binds to the primary antibody and also is linked to a signalling molecule, such as horseradish peroxidase (HRP) (Howard and Kaser, 2007).

WB is a highly sensitive and very specific assay that allows the visualisation and identification of the protein of interest after it has been separated from other proteins (Howard and Kaser, 2007). By comparison of protein levels, WB can produce a semi-quantitative result (Mahmood and Yang, 2012).

1.4.6 Enzyme-linked immunosorbent assay (ELISA)

ELISA is extensively used for the detection of both antigens and antibodies in human and veterinary infectious diseases. In an ELISA, the antigen can be used either as a target or a labelled detector and antibody can be used as a capture or a detector. The capture antibody is an antibody that has a high binding capacity for its corresponding antigen. And detector antibody is conjugated with enzymes such as horseradish peroxidase and alkaline phosphatase (Wade, 1989). When their substrates are added, the enzyme conjugated to detector antibody catalyses a colour change of the substrate indicating the presence of the antigen or antibody.

Various types of ELISA have been developed. In a direct ELISA, which is considered as the simplest form of ELISA, the antigen is bound passively by incubation with the microtitre plate. The bottom of the plate is blocked to eliminate non-specific binding by adding proteins such as bovine serum albumin. Then the detector antibody is applied directly to the antigen. Unbound antibody is removed by washing; the bound antigen-antibody complex is detected by the enzyme's substrate. As a result of using the labelled primary antibody, it can be time-consuming and inconvenient to label the primary antibody individually when performing multiple experiments. Moreover, direct ELISA is relatively less sensitive as the signal is less amplified.

Whereas in an indirect ELISA, an unlabelled primary antibody against the antigen is used, and the detection is accomplished by adding the secondary antibody, which is the enzyme-labelled anti-immunoglobulin (see Figure 1. 4). If the secondary antibody is particular for

a type of immunoglobulin, then the class specificity of antibody can be determined. Indirect ELISA is highly sensitive and very flexible because different types of primary antibody can be paired with a single secondary antibody. Nonetheless, this method has limitations when detecting immunoglobulin classes present in low concentration. IgE, usually found in serum, is present in nanogram quantities and the rest of immunoglobulin classes are present in milligram amounts. False-negative results could happen due to competitive inhibition, and false-positive results could occur due to the interference of Ig M anti-immunoglobulin (Wade, 1989).

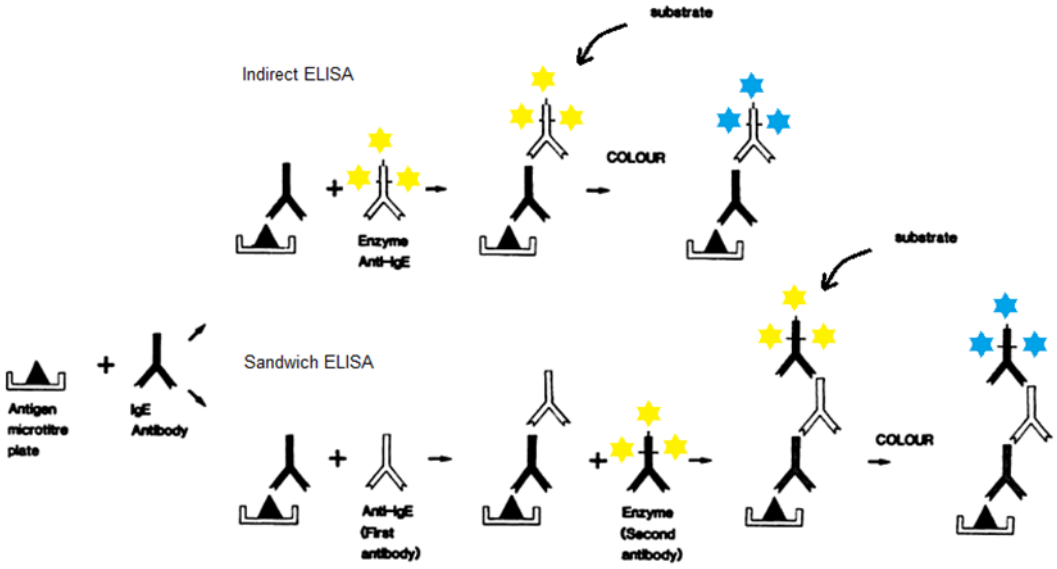


Figure 1. 4 Indirect or Sandwich ELISA (Adapted from (Wade, 1989)).

In an indirect ELISA, the antigen is immobilised to the microtitre plate and the primary antibody, which is unlabelled, is first incubated with the antigen. Next, a labelled secondary antibody is used for detection. In a sandwich ELISA, a second anti-species antibody is used when it is undesirable to label the secondary antibody.

In circumstances where it is impossible or undesirable to label the secondary antibody directly for detection, a second anti-species immunoglobulin conjugated with enzymes can be employed; this is called a sandwich ELISA (see Figure 1. 4). It can increase the sensitivity of the assay but also can increase the possibility of non-specific interactions between the two detector antibodies (Wade, 1989).

A two-site ELISA can be used to determine the concentration of the antigen. The capture antibody, which is used to capture the antigen in the test sample, is first immobilised on a solid phase such as a multiwell microtitre plate. The binding capacity of the capture antibody will have a significant effect on the sensitivity and reproducibility of the assay. Subsequently, the bound antigen is detected by the enzyme labelled detector antibody and its substrate. It is preferable that the two antibodies used are from the same species to reduce the possibility of species cross-interaction (Wade, 1989).

Competitive ELISA can be used to measure the concentration of antibody using an antigen-coated microtitre plate (see Figure 1. 5). When only the detector antibody and its substrates are added to the plate, a colour change will be observed. When the detector antibody and an unknown antibody from a test sample are both added to the plate, there would be a competition for binding to the antigen between the labelled and unlabelled antibody, resulting in a weaker or no colour change observed. Normally, the concentration of the reagent antibody is fixed, and the level of the test antibody is varying. Different concentrations of the unlabelled antigen should be added to the plate sequentially before adding the detector antibody to increase the sensitivity of this assay. Most importantly, the signal of all competitive assays is inversely related to the concentration of test antibody in the sample, which means higher signal indicates the lower concentration of antibody in the sample and vice versa (Wade, 1989).

This assay can also be used to detect antigen, using an antigen-coated micro-titre plate. For instance, to determine the concentration of antigenic determinants recognised by human antibodies, the unknown antigen and detector antibody are both added to the plate. The free test antigen will bind to the detector antibody inhibiting the binding of the bound antigen on the plate to the detector antibody. As a result, when corresponding substrates are added, the colour change would be inhibited. This is called competitive indirect ELISA. It has been applied to test the potency of allergen extracts (Wade, 1989).

In a competitive antigen capture ELISA, the antigen can also be detected using an antibody-coated plate (see Figure 1. 6). The competition lies between the test antigen and the labelled reagent antigen as they both bind to the antibody on the solid phase. This assay is highly specific and sensitive, however, to achieve this, the reagent antigen has to meet high levels of requirements, such as being pure enough to allow efficient labelling and have the same specificity as the test antigen (Wade, 1989).

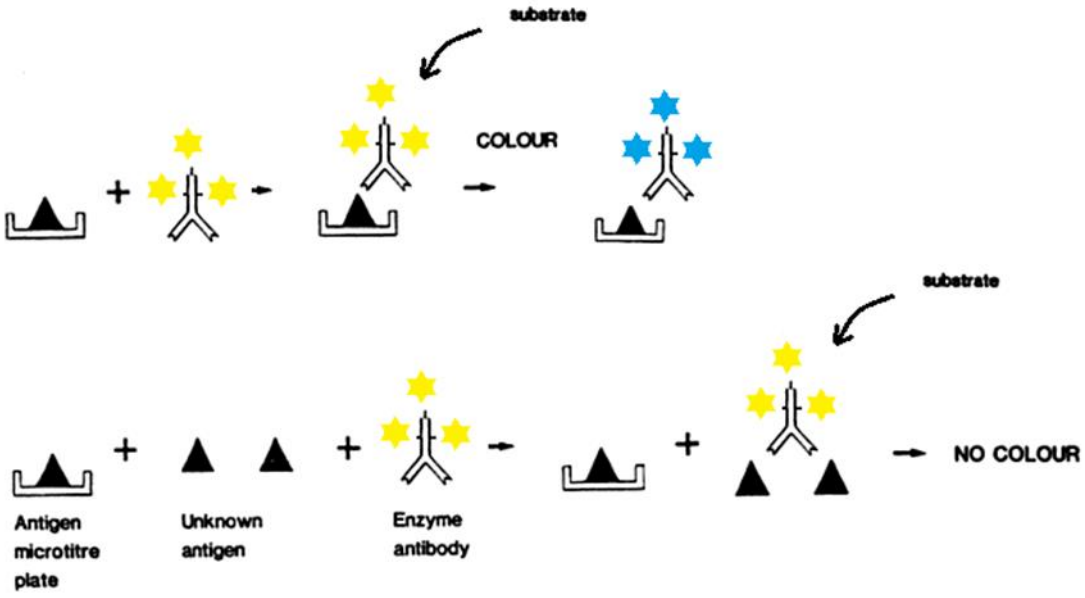


Figure 1. 5 Competitive indirect ELISA for antigen detection (Adapted from (Wade, 1989)).

In a competitive indirect ELISA, the antigen is immobilised, the unknown antigen and detector antibody are both added to the plate. The binding of unknown antigen to the antibody will dampen or inhibit the colour change after adding substrate.

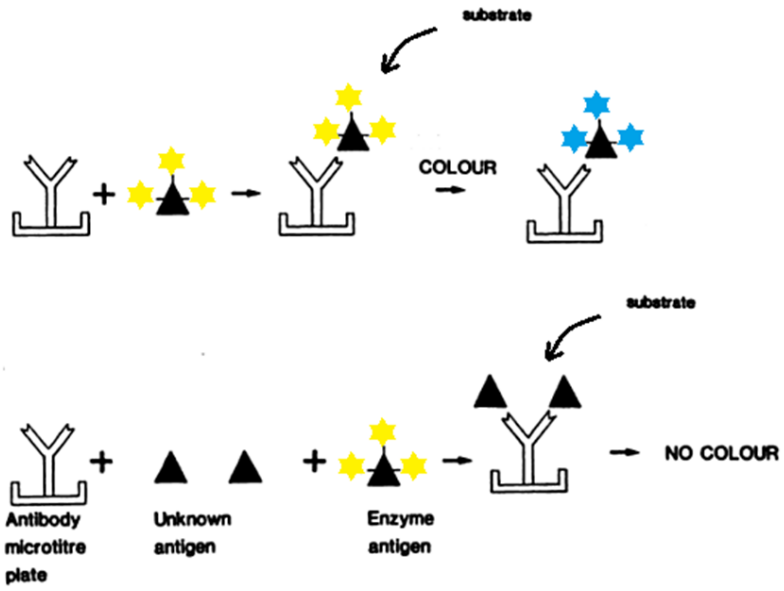


Figure 1. 6 Competitive antigen capture ELISA (Adapted from (Wade, 1989)).

In a competitive antigen capture ELISA, the antibody is immobilised and the unknown antigen and the reagent antigen are both added.

1.5 Aims

Co-circulation and cross-reaction among flaviviruses have become the major obstacle for an accurate diagnosis. Antigenic drift and shift of influenza viruses underline the importance of close monitoring and surveillance for precise diagnosis and vaccine production. This study aims to develop novel diagnostic assays for zika virus (ZIKV) and equine influenza viruses (EIV) by

- Generating pseudotyped ZIKV as a surrogate for wild-type virus in the VN test
- Producing plant-expressed ZIKV NS1 proteins as a surrogate for wild-type virus in the ELISA
- Identifying lineage-specific antibodies against EIV using Next Generation Phage Display (NGPD)

Chapter 2 General materials and methods

2.1 Cell culture methods

2.1.1 Cell lines

Vero E6 cells (ATCC CCL 81) were used for Zika virus (ZIKV) propagation and titration. Baby hamster kidney (BHK) 21 cells (ECACC General Cell Collection: 85011433, BHK 21 (clone 13)) and 293T cells (ATCC® CRL-3216™) were used for transfection. Chicken embryonic fibroblast (CEF) cells (primary cell line) were used for the propagation of FPV-T7 virus.

2.1.2 Sub-culturing adherent cells

Growth medium was discarded, and cells were washed with pre-warmed PBS. An appropriate amount of trypsin was added to cover the cell monolayer and to dissociate cells from the bottom of a flask. Two volumes of complete growth medium (Appendix 1) was added to neutralise the trypsin. The cell suspension was transferred to a Falcon centrifuge tube and centrifuged at 400 *g* for 5 min. The supernatant was discarded, and the cell pellet was re-suspended with complete growth medium. According to a required cell density, 1ml or 2ml of this cell suspension was seeded into a new flask containing an appropriate amount of complete growth medium. The newly sub-cultured cells were placed back into the 37°C incubator containing 5% CO_2. The rest of the cell suspension was mixed with Trigene and discarded into the sink after at least 24 hours.

2.1.3 Counting cells

The cell suspension was prepared the same way as sub-culturing adherent cells. Haemocytometer and coverslip were cleaned with 75% ethanol before use. The coverslip was moistened and affixed to the haemocytometer. Proper adhesion was indicated by the presence of Newton's rings under the coverslip. The cell suspension was gently swirled to

ensure the cells were evenly distributed. Seven microliters of cell suspension were added onto one of the chambers from the side of the coverslip and allowed to be drawn inside by capillary action. Under a light microscope with a 10X objective, the cells were counted using a hand tally counter. When counting, a system was employed whereby only cells on the left-hand and bottom boundary lines as well as within a square were counted. Usually, for seeding a 6-well plate, two sets of 16 corner squares of cells were counted. The two cell counts from the two sets of 16 corner squares were averaged and multiplied by 10^4 to calculate the number of cells/ml in the cell suspension.

2.1.4 Freezing cells

Ten millilitres of the freezing medium, which consists of 10% of DMSO and 90% of FBS was prepared in a universal tube. The cell suspension is prepared the same way as sub-culturing adherent cells except that cell pellet was resuspended in the desired amount of freezing medium. Cells were then counted, aliquoted and stored as 1 ml aliquots in 1.8 ml cryotubes in Mr Frosty cell freezing container in -80°C freezer overnight. Cells are transferred to liquid nitrogen storage the following day.

2.1.5 Recovery of cells from liquid nitrogen

Cells were taken out from liquid nitrogen and put into Mr Frosty cell freezer or a box of dry ice during transfer. Vials of cells were carefully put in a water bath (to prevent contamination) until 10% thawed. The tubes were cleaned with 75% ethanol before opening in a tissue culture hood. The cell suspension was transferred into a 15ml Falcon tube containing 10 ml of prewarmed complete growth medium. Cells then were centrifuged at 800 *g* for 10 min. The supernatant was removed, cells were resuspended with fresh complete growth medium, transferred to an appropriate sterile flask and placed in a 37°C incubator, with 5% CO_2.

2.2 Molecular cloning methods

2.2.1 Preparation of Luria Bertani (LB) agar plates

Luria Bertani (LB) agar solution (Appendix 1) was reheated by microwave under 'mid-low' power setting for 5—8 min until fully dissolved, and allowed to cool down until safe to handle. The desired number of 90 mm Petri dishes were prepared and labelled with name, lab number, date and antibiotic added. A Bunsen burner was turned on, and its air hole was kept fully open as part of the aseptic techniques. Petri dishes and LB agar were brought close to Bunsen burner flame. Ampicillin was added to LB agar and mixed thoroughly to have a final concentration of 100µg/ml. LB agar was poured into the plate until the plate was completely covered. All the plates with LB agar added were allowed to cool and settle for 30 min to 1 hour before packing them for storage at 4°C.

2.2.2 Transformation of standard chemically competent DH5-α *E. coli* cells

Aliquots of chemically competent DH5-α *E. coli* cells were taken out from -80°C freezer and thawed on ice for 5—10 min. Each aliquot contained 25 µl of cells. One to two microliters of plasmid DNA were added to the cells and incubated on ice for 20 min. Cells were then heat-shocked in a 42°C water bath for 40 seconds and returned to ice for 2 min. To each aliquot, 500 µl of LB broth (Appendix 1) was added and mixed with the cells by gently inverting. The cells were incubated in air incubator at 37°C for 1 hour and then centrifuged at 16000 *g* for 2 min. Supernatants were discarded, and cells were re-suspended with 100 µl of fresh LB broth. The transformed cell suspensions were plated onto fully labelled LB agar plates using cell spreaders on the bench under Bunsen burner flame. They were left to settle for 5 min and flipped upside down before placing in a 37°C air incubator overnight.

2.2.3 Inoculating a starter bacterial culture

Close to a Bunsen burner flame, 5 ml of LB broth and 10 µl of ampicillin (50 mg/ml) were both added to a labelled universal tube to reach a final antibiotic concentration of 100

μg/ml. A single colony of the bacteria from the agar plates was picked, and the top of the inoculation loop was inserted into the LB broth and swirled a few times to make sure the bacteria were transferred. The universal tube was then incubated in a shaking incubator at 37°C and 300 rpm overnight.

2.2.4 Making a larger bacterial culture

Close to a Bunsen burner flame, 100 ml of LB broth and 200 μl of ampicillin was added to an autoclaved 1 L conical flask to make sure the working concentration of the antibiotic was 100 μg/ml. Two hundred microlitres bacterial culture from the 5 ml starter culture was added to the flask as well. The flask was covered by a piece of aluminium foil and incubated in a shaking incubator at 37°C and 300 rpm overnight.

2.2.5 Making glycerol stocks

In a 1.5 ml screw-cap microcentrifuge tube, 500 μl of overnight bacterial culture and 500 μl of 50% glycerol were added and mixed by inverting. The tubes were labelled and stored in a -80°C freezer until further use.

2.2.6 Plasmid purification using EndoFree plasmid Maxi kit

Purification of plasmid DNA from *E.coli* DH5-α cell culture suspension was performed using an EndoFree Plasmid Maxi kit following the manufacturer's instructions. The concentrations of purified plasmid DNAs were determined by UV absorption using a NanoDrop 8000 spectrophotometer. Eluted DNA samples were stored at -80°C until further use.

2.2.7 Plasmid purification using Plasmid Mini kit

Purifications of plasmid DNA from DH5-α cell culture suspension were performed using a plasmid mini kit (Qiagen) following the manufacturer's instructions. The concentrations of purified plasmid DNAs were determined by UV absorption using a NanoDrop 8000 spectrophotometer by. Eluted DNA samples were stored at -80°C until further use.

2.2.8 Plasmid purification using lysozyme and chemical solutions

2.2.8.1 Harvesting of bacteria

Thirty millilitres of LB broth containing 150 µl/ml ampicillin was inoculated with a single colony of DH5α carrying the plasmids pVSV-ΔG-luc, and the bacterial culture was incubated in a shaking incubator at 37°C and 290 rpm for exactly 14 hours overnight. Twenty-five millilitres of the overnight bacterial culture was added to a pre-autoclaved 2L flask containing 500 ml of pre-warmed LB broth and 1ml ampicillin. The bacterial culture was incubated in a shaking incubator at 37°C and 300 rpm for 2.5 hours. Then, 250 ml of bacterial culture was transferred to five 50 ml Falcon tubes, which were centrifuged at 4000 rpm and 4°C for 15 minutes. Supernatant from all tubes was discarded completely, and bacterial pellets were resuspended into one 50 ml Falcon tube with 50 ml of ice-cold STE buffer. Bacteria cells were collected by centrifugation at 4000 rpm and 4°C for 15 minutes.

2.2.8.2 Lysis by alkali

The washed bacterial pellet was resuspended with 9 ml of Solution I (Appendix 1). Next, 2 ml of freshly made lysozyme solution and 30 ml of freshly prepared Solution II (Appendix 1) were added to the bacterial suspension, which was then mixed thoroughly by inverting the tube several times. The mixture was incubated at room temperature for 8 mins. After that, 10 ml of ice-cold Solution III (Appendix 1) was added to the mixture and mixed by shaking and also incubated on ice for 10 min. The bacterial lysate was centrifuged at 4000 rpm and 4°C for 15 minutes. The supernatant was filtered through 4 layers cheesecloth into a 50 ml Falcon tube and 0.6 volume of isopropanol was added to the supernatant and mixed immediately and thoroughly. The mixture was stored at room temperature for 10 min before centrifugation at 5000 rpm for 10 min at room temperature. The supernatant was discarded carefully, and the DNA pellet was rinsed with 5 ml of 70% ethanol. Finally, the ethanol was removed, and DNA pellet was air-dried for 5—10 mins before dissolving in 0.5 ml TE buffer (Appendix 1) and stored at -20°C.

2.2.9 Restriction digestion of plasmid DNA

According to the purpose of the experiment and the DNA to be digested, appropriate restriction enzymes were selected by Restriction Mapper 3. An example of the amounts of restriction enzyme, DNA plasmid, and buffers used for samples and controls is listed in Table 2. 1. They were gently mixed with the DNA in 1.5ml Eppendorf tubes and incubated for 1 hour at 37°C.

Master Mix #1 for pcDNA VSV-G (X2) – 50 µl	Master Mix #2 (x4) –196 µl
10.0 µl Cutsmart	20.0 µl Cutsmart
1.0 µl *Nhe* I	2.0 µl BSA
1.0 µl *Pme* I	174.0 µl dH_2O
1.0 µl BSA	
37 µl dH_2O	
Control #1 no enzyme for pcDNA VSV-G	Control #3 *Pme* I digest for pcDNA VSV-G
49.0 µl Master Mix #2	49.0 µl Master Mix #2
1.0 µl pcDNA VSV-G	1.0 µl pcDNA VSV-G
	0.5 µl *Pme* I enzyme
Control #2 *Nhe* I digest for pcDNA VSV-G	Sample #1 pcDNA VSV-G double digest
49.0 µl Master Mix #2	25.0 µl Master Mix #1
1.0 µl pcDNA VSV-G	1.0 µl pcDNA VSV-G (672.4 ng/µl) 672.4ng
0.5 µl *Nhe* I enzyme	24.0 µl dH_2O

Table 2. 1 An example of mastermix and sample preparation for restriction digestion.

2.2.10 Agarose gel electrophoresis

For gel preparation, 0.5 g of agarose was weighed out and added to a 250 ml conical flask containing 50 ml of 1XTBE buffer (Appendix 1). Agarose was dissolved by microwaving it under 'mid-low' setting for 2 min. While the gel was cooling, both ends of a gel rig were sealed by autoclave tape. Two microlitres of Nancy-520 was added to the agarose solution and mixed by gently swirling the flask. The gel mixture was poured into a casting gel rig slowly to avoid bubbles, and a well-forming comb was put in place. After the gel was fully set, autoclave tape and comb were removed; the gel rig was transferred to a gel running

tank, and 1x TBE buffer was added to the tank until the gel and all the wells were completely covered.

For sample preparation, digested DNAs were mixed with 6X loading dye (NEB) in a ratio of 5:1. One kb DNA ladder (NBE) was also mixed with the loading dye in a ratio of 1:1. Twenty microlitres of each sample and DNA ladder were loaded to appropriate wells. The gel was run for 90 minutes at 110V on constant voltage. The result of restriction digestion was viewed using the UV transilluminator.

2.2.11 Ligation

The vector pEAQ-HT and the insert PCR-amplified ZIKV NS1 were ligated using T4 DNA ligase (NEB) according to manufacturers' instruction and transformed into DH5α competent *E.coli* cells.

2.3 Virology methods

2.3.1 Propagation of Zika Virus (ZIKV)

ZIKV mRNA was obtained from the University of Glasgow (Dr Alain Kohl). RNA concentration (54.18ng/µl) was determined by UV spectrophotometry using a NanoDrop 8000. A T75 flask of Vero cells was sub-cultured 24 hours before the transfection. Transfection of ZIKV mRNA was performed using TransIT®-mRNA transfection kit according to the manufacturer's instruction. Vero cells were observed daily. The cell suspension was harvested when a cytopathic effect (CPE) was observed. The cell suspension was aliquoted, labelled as P1 ZIKV and stored at -80°C.

2.3.2 Infection of Vero cells with ZIKV

Vero cells were seeded in a T75 flask and allowed to grow to a confluence of approximately 90% at the time of infection. ZIKV virus suspension was prepared in a 50 ml Falcon tube

using 2 ml of P1 virus stock and 3 ml of serum-free DMEM. The cell culture medium was removed, and the prepared virus suspension was added to the flask carefully. Vero cells were then incubated in a 37°C incubator with 5% CO_2 for 4 hours. A 15 ml cell growth medium of 2% fetal bovine serum (FBS) was prepared in advance. After 4 hours of incubation, virus suspension was removed and replaced with the cell growth medium. The infected Vero cells were observed daily, and the supernatant was harvested when CPE was observed. The supernatant was aliquoted, labelled as P2 ZIKV and stored at -80°C.

Chapter 3 Generation of pseudotyped Zika Virus (ZIKV)

3.1 Introduction

3.1.1 Background

Zika virus (ZIKV) is a mosquito-borne flavivirus. It was first isolated in a sentinel rhesus macaque in 1947 in the Zika forest of Uganda. In 1954, three cases of human infection caused by ZIKV were reported in Nigeria for the first time. Up until 2007, the virus remained in relative obscurity and caused only sporadic symptomatic human infections in tropical Africa and some countries in Southeast Asia. However, several major outbreaks of ZIKV have occurred since 2007 across the Pacific Islands including the islands of Yap, French Polynesia, Cook Islands, Easter Island, and New Caledonia (Plourde and Bloch, 2016). The 2007 ZIKV outbreak on the island of Yap had an estimated infection rate of 73% in the 6892 Yap residents aged three years or older, although only mild symptoms were reported (Duffy et al., 2009). In 2013—2014, ZIKV caused a larger outbreak in French Polynesia. During this outbreak, an unusual increase in another condition called Guillain–Barré (GB) syndrome, and cases of microcephaly were observed (McNeil and Shetty, 2017). Subsequently, ZIKV was identified in Brazil in March 2015. It spread rapidly to 14 Brazilian states within several months, at least 33 countries and territories in the Americas, and 70 countries and territories globally within a year (Plourde and Bloch, 2016, McNeil and Shetty, 2017). In February 2016, the World Health Organization declared ZIKV infection a public health emergency of international concern (McNeil and Shetty, 2017). Although it mostly causes subclinical or mild influenza-like illness in humans, severe manifestations have increasingly been associated with ZIKV, including GB syndrome in adults and congenital malformations including microcephaly in infants born to infected mothers (Plourde and Bloch, 2016).

3.1.2 Pseudotyped viruses (PV)

Pseudotyped viruses (PV), also referred to as pseudotypes or pseudotype particles, are chimeric 'viruses' consisting of a virus core surrounded by a host cell-derived lipid membrane with the envelope proteins from another virus (Carnell et al., 2015). Generally, the envelope proteins drive the assembly and budding of enveloped viruses and are crucial in the initiation of the infection of a target cell. They are also the primary determinants of the host range and tissue tropism of the virus. In a PV, its genetic material is modified whereby a suitable reporter gene, such as luciferase or green fluorescent protein (GFP) gene, will replace the envelope protein gene of the core virus. As a result, the virus can only undergo a single cycle of infection in the target cells; it is deficient in completing a full replication cycle and producing infectious progeny viruses (see Figure 3. 1). This is one of the most appealing advantages of PV, as it provides a safer platform for researchers to study highly pathogenic viruses such as West Nile virus (WNV) without the need for access to restrictive, expensive and high-category biosafety facilities (Carnell et al., 2015).

The viral core and reporter are the two key components of a PV. The core and its related genome, including the reporter gene, are considered the backbone of a PV. The replication properties of a PV remain the same as its backbone. However, some other properties of the PV may differ from its parent virus when the envelope proteins are added, which can be used to study properties of the envelope proteins of interest. The most commonly used PV backbones are from lentiviral human immunodeficiency virus (HIV) and gammaretroviruses such as murine leukaemia virus (MLV). They were discovered independently to have the natural ability to incorporate envelope proteins from other viruses.

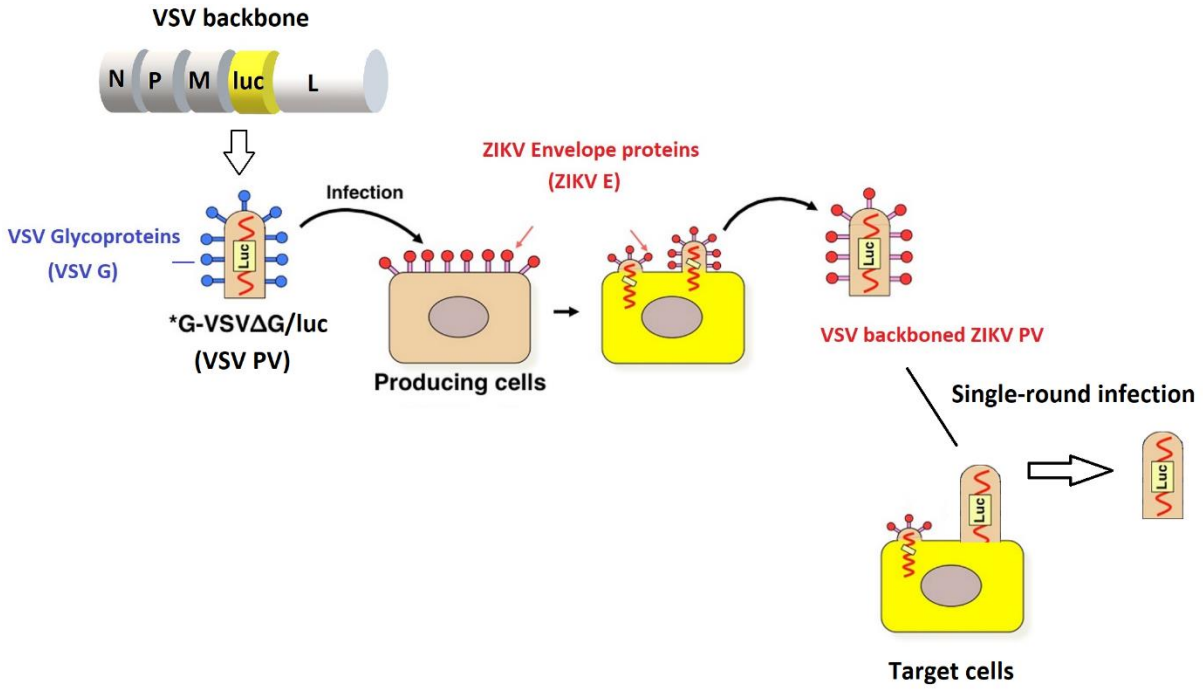


Figure 3. 1 Schematic representation of the production of ZIKV PVs (Adapted from (Tani, 2014)).

**G-VSVΔG/luc is pseudotyped VSV where the VSV glycoprotein gene is replaced by the luciferase gene, and the virus core is complemented with VSV glycoproteins for virus entry by co-transfection of a plasmid encoding VSV-G gene. It is referred to as VSV PV hereinafter.*

Furthermore, rhabdoviruses such as the vesicular stomatitis virus (VSV) are also a promising candidate as pseudotype backbones (Carnell et al., 2015). It was found that when cells were co-infected with VSV and other enveloped viruses, VSV forms PV readily. The VSV virions are very flexible in the type of membrane proteins that can be incorporated into the viral membrane.

Additionally, the 'naked' VSV viral particle can be produced in the absence of its envelope protein, G protein, although at a much lower efficiency than when G protein is present. Therefore, a recombinant VSV (*G-VSVΔG/luc) was developed in which the G protein gene is deleted and replaced with the reporter gene. When heterologous envelope proteins are transiently expressed by the cells infected with *G-VSVΔG/luc, VSV backboned PVs can be produced (Whitt, 2010) (see Figure 3. 1).

Because the reporter gene is incorporated into the viral genome where the envelope protein gene was, it will naturally be transcribed or, in the case of HIV or MLV backbones, reverse transcribed and integrated into the host cell genome after host cells are transduced. The host cell itself will then produce the reporter proteins, and this can be used to check transduction efficiency. Firefly-derived luciferases are primarily used as the reporters. The transduced cells are lysed, luciferase substrates are added, and the relative luminescence units (RLU) measured by a luminometer. GFP is also very often used; the transduction efficiency is measured by counting the number of cells emitting fluorescent light under fluorescence microscopy or by fluorescence-activated cell sorter (FACS). Sometimes other reporters are also used, such as lacZ as well as Gaussia and Renilla luciferase (Carnell et al., 2015).

The most commonly used system for generating a PV is by multiple plasmid co-transfection of the 'producer' cells. For example, to make influenza PV, the 'producer' cells are co-transfected with separate plasmids encoding the envelope protein haemagglutinin (HA) gene, the reporter luciferase or GFP gene, and the HIV backbone genes including *gag* and *pol*. Gag provides the structural proteins p18, p24 and p15, whereas *pol* provides the integrase, reverse transcriptase as well as the protease p10. When making VSV PVs, the producer cells are co-transfected with plasmids encoding the VSVΔG/luc, the reporter gene, and different components of the VSV genome, for example, the structural proteins including VSV-G, and proteins needed for initiation of the replication cycle. A range of expression plasmids, such as pI.18, pcDNA3.1, phCMV, and pCAGGS, are used for cloning of these genes. The plasmids should be added in a ratio that can achieve the highest quality and yields, therefore, optimisation is required (Carnell et al., 2015).

PVs have a wide range of applications due to their flexibility; one of them is being used as surrogates of highly pathogenic wild-type viruses in a pseudotyped virus neutralisation test (PVNT) for measuring antibodies. PVNT is also called pseudotype micro-neutralisation assay (pMN). It is usually performed in a 96-well white plate. The test serum is serially

diluted and added to appropriate wells. Cell only/negative control and a known positive control serum should also be included. The serum is then incubated with a standardised amount of PV for a period of between 30 min to 2 hours. Target cells are then added to each well and incubated at 37°C in 5% CO_2 for 48 or 72 hours. The neutralising antibody titre can be determined as an inhibitory concentration; IC50 or IC90 are typically used, which represent the highest dilution of the sample that reduces RLU readings by 50% or 90% when compared to 100 and 0% transduction controls (Carnell et al., 2015). Additionally, recombinant VSV-based chimeric viruses that include genes from other viruses have great potentials in applications such as vaccines (Ma et al., 2019) and oncolytic viruses (van den Pol et al., 2017).

3.2 Aim

Except for ZIKV, the majority of the flaviviruses are classified as human hazard group 3 or above. Correspondingly, they need to be handled in containment level 3 (CL3) or 4 laboratories (HSE, 2013), whereas ZIKV can be handled at CL2, which makes it an ideal model for other more pathogenic flaviviruses. Despite two publications suggesting that flavivirus envelope proteins could be successfully expressed on an HIV/MLV backbone (Lee et al., 2009, Lee et al., 2014), previous attempts in our and other laboratories were unsuccessful. Therefore, this project aimed to generate pseudotyped ZIKV using VSV as the backbone to use as a surrogate for wild-type ZIKV in serological tests.

3.3 Materials and methods

3.3.1 Plasmids, virus and cell lines

Plasmids pVSV-ΔG-Luciferase and helper plasmids pBS-N-ΦT, pBS-P-ΦT, pBS-L-ΦT, pBS-G-ΦT (see Figure 3. 2) made by Dr Michael A. Whitt (University of Tennessee) were provided by Dr Edward Wright (University of Sussex). All of these plasmids were regrown and purified using an EndoFree Plasmid Maxi kit following the manufacturer's instructions. The concentrations of purified plasmid DNAs were determined by UV absorption using a

NanoDrop 8000 spectrophotometer. Eluted DNA samples were stored at -80°C until further use.

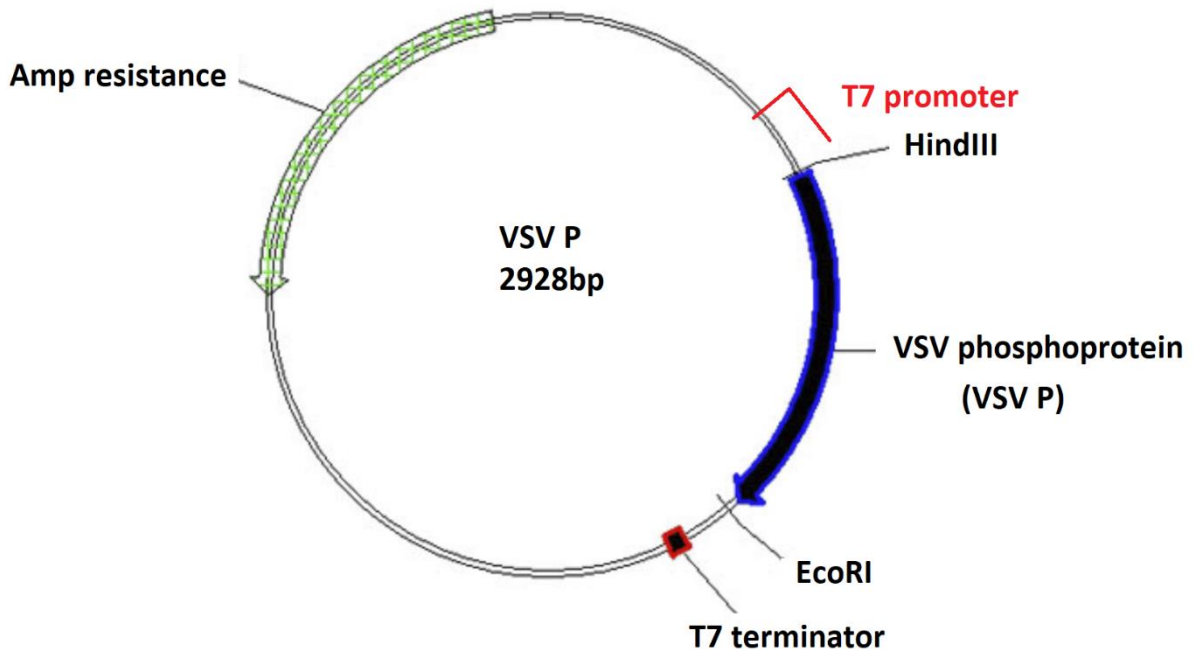


Figure 3. 2 The plasmid map of VSV P as an example of plasmids encoding VSV structural proteins (adapted from https://www.kerafast.com/product/701/pbs-p-t-plasmid).

The Zika envelope protein (ZIKV-E) was chemically synthesised and provided in plasmid pI.18 (GenScript Corp., Piscataway, NJ). The ZIKV-E sequence was designed by Dr Simon Scott (University of Kent) based on Zika virus strain ZikaSPH2015, complete genome (GenBank: KU321639.1) (see Figure 3. 3).

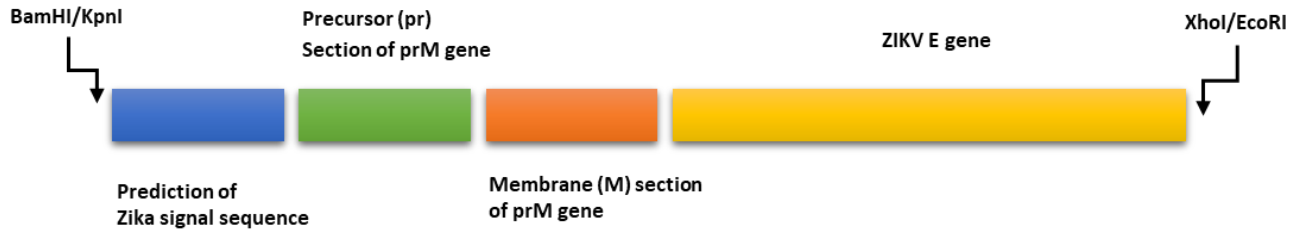


Figure 3. 3 Sequence designed for ZIKV-E synthesis in pI18 plasmid. Prediction of Zika signal sequence was done by Dr Simon Scott based on various prediction programs.

pMD2.G was given by Dr Cinzia Allegrucci (University of Nottingham). Fowlpox virus-T7 (FPV-T7) was kindly given by Dr Mike Skinner (Imperial College London). Chicken embryonic fibroblast (CEF) cells were prepared and kindly given by Dr Sanjeeva Kumar (University of Nottingham). Baby hamster kidney (BHK-21) cells were kindly given by Dr Edward Wright (University of Sussex). For some envelope proteins that do not form PVs readily in their native form, chimeric proteins have been used with the C-terminal tail from VSV-G (Matsuura et al., 2001). A chimeric protein (C2) in which the C terminus of WNV E protein was replaced with the C terminus of VSV G was made by Dr Barney King (University of Nottingham) (see Figure 3. 4).

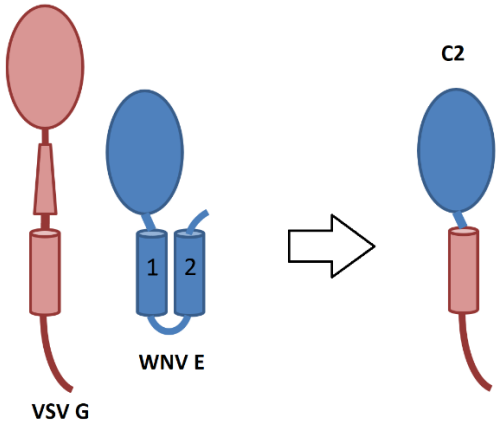


Figure 3. 4 Construction of C2 by replacing of the WNV E transmembrane domains (TM) with the TM and c-tail of VSV G, which contains the export signal sequence. (Figure is drawn by Dr Barney King (University of Nottingham))

3.3.2 Transfection of pI.18ZIKV-E in 293T cells

Transfection of pI.18ZIKV-E in 293T cells in a T75 flask was achieved using a TransIT-X2 Dynamic Delivery System according to the manufacturer's instruction.

3.3.3 Detection of Zika envelope (E) protein using Western Blot

3.3.3.1 Sample preparation

A T75 flask of 293T cells transfected with pI.18ZIKV-E was lysed using RIPA buffer at day two post-transfection according to the manufacturer's instruction. Protein concentration (1.139 mg/ml) was determined by Nanodrop 8000.

3.3.3.2 Native SDS PAGE

Protein samples were mixed with 4X LDS sample buffer 3:1, and directly loaded to Mini-PROTEAN® TGX pre-cast gel without heating or adding beta-mercaptoethanol (BME). The gel was run at 200V for 30—45 min.

3.3.3.3 Membrane preparation and wet transfer

PVDF membrane was cut to the right size, activated by soaking in methanol for 1 min and equilibrated in transfer buffer (Appendix 1). The protein samples were transferred to PVDF membrane by tank transfer. A 'sandwich' was made as shown below (see Figure 3. 5). Proteins were transferred in the tank at 30 V for 1 hour.

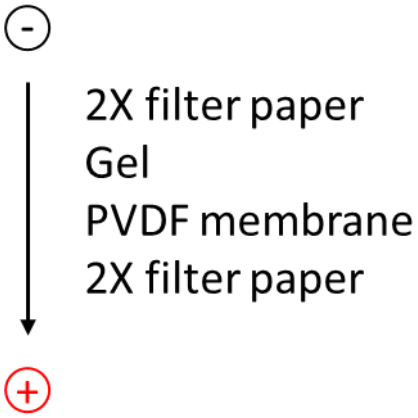


Figure 3. 5 'Sandwich' method for protein transfer.

3.3.3.4 Blocking

The membranes were then blocked in 5% (w/v) bovine serum albumin (BSA) for 1 hour at room temperature in a shaking platform or 4°C overnight.

3.3.3.5 Primary antibody incubation

After blocking, the membrane was incubated with human anti-ZIKV-E antibody (Kerafast) 1:5000 diluted with blocking buffer for 1 hour at room temperature in a shaking platform. After incubation, the membrane was washed with TBST (Appendix 1) three times, five min each time.

3.3.3.6 Secondary antibody incubation

After washing, the membrane was incubated with secondary antibody sheep anti-human antibody 1:10000 diluted in blocking buffer at room temperature on a shaking platform. The membrane was washed three times, 5 min each time, after secondary antibody incubation.

3.3.3.7 Imaging

An equal amount of solution A and solution B from ECL prime western blotting detection reagent were mixed and added on top of the blots to cover the whole area, which was then incubated for 5 min. Excess reagents were drained off from the blots, and the membranes were carefully wrapped with cling film to avoid drying out. Lastly, the blots were imaged using an X-ray film (Kodak) and a developing machine (brand unknown) in a dark room.

3.3.4 Propagation of Fowlpox-T7 helper virus (FPV-T7)

Chicken embryonic fibroblast (CEF) cells were 80—100% confluent at the time of infection. FPV-T7 was diluted 1:100 in SF DMEM and incubated on cells for 4 hours before removal and addition of 2% complete growth media (Appendix 1). For the following five days, cells were incubated in a 37°C incubator with a humidified atmosphere of 5% CO_2 and imaged every day to record changes of CPE. After five days, cells and supernatants were harvested by scraping and aliquoted into 1.5 ml Eppendorf tubes which were all subjected to 5 cycles of freeze/thawing 10 mins at -80°C, 10 mins at 37°C. After that, samples were pooled and

centrifuged at 4,000 *g* for 10 mins at room temperature. The supernatant was passed through a 0.45 µm filter and stored as 1 ml aliquots in 1.5 ml Eppendorf tubes at -80°C.

3.3.5 Primary virus rescue of VSV PV from plasmids using FPV-T7

BHK-21 cells were seeded into 6-well plates 16—24 hours before starting the primary recovery. Different seeding densities were used depending on how confluent cells were before plating and how soon the 6-well plates of BHK-21 cells were intended to be used. BHK-21 cells were incubated at 37°C in a humidified incubator containing 5% CO_2 until they reached 80–90% confluence.

Primary recovery of VSV PV started with infection of the BHK-21 cells with FPV-T7 helper virus. A stock of FPV-T7 virus was removed from -80°C freezer and thawed rapidly in a 37°C water bath. For each well, 500µl of FPV-T7 inoculum was prepared by diluting 13.6µl of virus stock with 486.4µl of pre-warmed SF DMEM. Growth medium was removed from the 6-well plates, and each well was rinsed with 3ml of pre-warmed SF-DMEM. Subsequently, to each well, 500µl of FPV-T7 inoculum was added and then incubated on cells at 37°C in a humidified incubator containing 5% CO_2 for 45—60 min.

The transfection mix was prepared using Lipofectamine according to manufacturer's instructions. For each well, the plasmid ratio of N: P: G: L: pVSV-ΔG-Luciferase was 3:5:8:1:5 µg. Therefore, a final amount of 22µg of plasmids was transfected per well. The volume of Lipofectamine was also titrated to achieve the best transfection efficiency. When the incubation of FPV-T7 was finished, it was removed, and 2ml fresh 5% complete growth medium (Appendix 1) was added to each well in addition to the transfection mix. The 6-well plate was then incubated in a 37°C incubator containing 5% CO_2 for 3—5 hours. The transfection mix was then removed and replaced with 2ml fresh D-5, and the plate was further incubated for 16—24 hours. When harvesting, supernatants were filtered using a 0.45µm filter and stored at -80°C for future use or added to target cells for further analysis. The luciferase activity of producer cells from the plate was tested as well. A mixture of

250µl of SF DMEM (Appendix 1) and 250µl of SteadyGlo® reagent was added to each well. The plate was incubated on a shaking platform at room temperature for 5—10 min or until all cells were detached from the bottom of the plate. The cell suspension was transferred to a white plate and analysed in an Orion L microplate luminometer.

3.3.6 Plaque purification of VSV PV

A 10cm dish of BHK-21 cells was transfected with 16µg of pMD2.G using Lipofectamine as per the manufacturer's instructions. Approximately 24 hours after transfection, cells were trypsinised and divided between two 6-well plates and allowed to attach to plates for at least 6 hours. VSV PV stock was 10-fold diluted up to 10^{-7} using SF DMEM as a diluent (see Figure 3. 6). The medium was removed, and 0.3ml SF DMEM was added to each well, then 100µl of serial diluted VSV PV stock was added to the appropriately labelled well. The plates were incubated in a 37°C incubator containing 5% CO_2 and manually rocked every 10 min for 60 min. After incubation, agar-overlay (5% complete medium containing 0.9% agar) was added directly onto each well and allowed to solidify. The plates were further incubated in the 37°C incubator containing 5% CO_2 until plaques were visible at around 48—60 hours. Subsequently, 1 ml pipette tips were used to isolate the plaques. The tip of the 1ml pipette was inserted to the bottom of the agar where plaques were observed, and the agar plugs were aspirated and placed in 0.5ml D-5 at 4°C for 1—2 hours for the viruses to be eluted. Finally, the eluted plaque isolates were stored at -80°C, and one aliquot was used to amplify the virus to make a working stock.

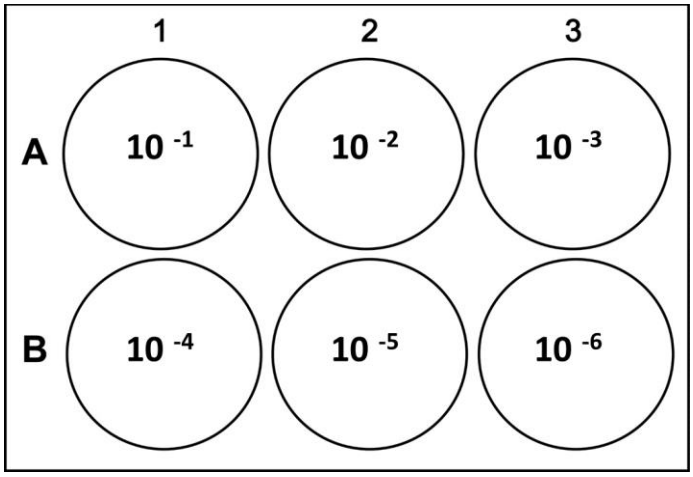


Figure 3. 6 Six well plate layout for dilution factors of VSV PV original stock for plaque purification.

3.3.7 Amplification of VSV PV plaque isolates and generation of VSV PV working stocks

To amplify virus from plaque isolates, 6-well plates of BHK-21 cells were transfected with pMD2.G at 2µg/well using Lipofectamine according to manufacturer's instructions. Approximately 24—30 hours after transfection, cell medium was removed and replaced with 1 ml SF DMEM per well. In each well, transfected cells were then infected with 15µl of the eluted virus and incubated in a 37°C incubator containing 5% CO_2 for 1—2 hours. Lastly, 1ml of D-5 was added directly to each well. The plates were further incubated overnight, and the development of VSV-induced cytopathic effect (CPE) was monitored carefully. When most of the cells showed CPE, supernatants were harvested and centrifuged at 450 *g* for 10 min. The clarified supernatants were then stored in 1ml aliquots in a -80°C freezer.

3.3.8 Pseudotyping ΔG-VSV with heterologous envelope proteins

To make pseudotyped VSV with heterologous envelope proteins, 6-well plates of BHK-21 cells were transfected with 2µg of heterologous envelope proteins per well using Lipofectamine according to manufacturer's instructions and further incubated for 24—30 hours. When cells began to show CPE due to the expression of the envelope proteins, they were infected with VSV PV 20µl/well and incubated for 24 hours or until the majority of

cells showed VSV-induced CPE. Then supernatants were collected, centrifuged at 1320 *g* for 10min and stored at -80°C for further analysis. Cells left in the plates were also analysed for their luciferase activity using SteadyGlo® reagent and an Orion L microplate luminometer.

3.3.9 Cell surface expression assay using a flow cytometer

BHK-21 cells were seeded into a 12-well plate, 48 hours before the experiment, at a seeding density of 1×10^5 cells/well, and cells were transfected with pI.18 empty vector, pI.18-HA, or pI.18-ZIKV-E at 2µg/well approximately 16—24 hours before the assay using Lipofectamine according to manufacturer's instructions (see Figure 3. 7). Growth media was removed from the plate, and each well was washed gently once with PBS. To each well, 200µl of 10 mM EDTA in PBS was added. The plate was gently rocked until all cells were detached. Cell suspensions from each well were transferred to labelled 1.5ml Eppendorf tubes. Eppendorf tubes were then centrifuged at 2000 rpm for 5 min, which was kept the same for all centrifuge steps throughout this experiment. After centrifugation, supernatants were removed, and cell pellets were washed with FACS buffer (Appendix 1) once and kept on ice. Both rabbit anti-HA (raised against influenza A/equine/Sussex/89 (H3N8) kindly provided by Dr Debra Elton, Animal Health Trust) and human anti-ZIKV-E primary antibodies (Kerafast) were diluted 1 in 100 with PBS. Fifty microlitres of rabbit anti-HA primary antibodies were added to tube 3 and tube 4, which contained cells transfected with pI.18-HA, and incubated at 4°C for 30—60 min. The same procedure was done for tubes 5 and 6 with human anti-ZIKV-E antibodies. After primary antibody incubation, cells were washed three times with FACS buffer. Alexa Fluor™ 594 goat anti-rabbit and Alexa Fluor™ 546 goat anti-human (Invitrogen) secondary antibodies were diluted 1:100 with PBS. Fifty microlitres of anti-rabbit secondary antibody were added to tube 3, tube 4 and tube 8 containing untransfected cells. Fifty microlitres of anti-human secondary antibody were added to not only tube 5 and tube 6 but also tube 2 and tube 9 for background control. After 30—60 min secondary antibody incubation, cells were

washed with PBS for five times and resuspended in 100µl PBS ready to be analysed. Cells were analysed using a cytometer and FlowJo software.

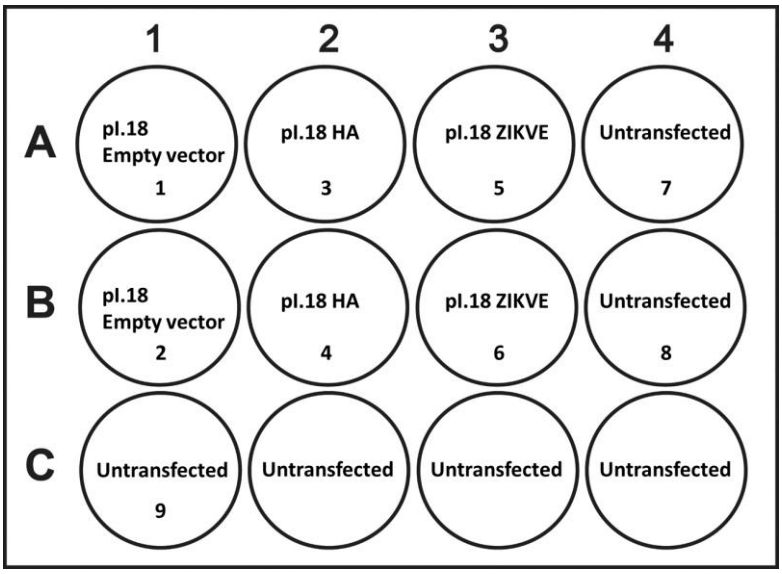


Figure 3. 7 Twelve-well plate layout for transfecting the cells with different plasmids.

Cells were transfected with three different plasmids at 2µg/well: pI.18 empty vector, pI.18-HA and pI.18-ZIKV-E in duplicate wells and 3 of the untransfected wells were used as background control as well.

3.4 Results

3.4.1 Restriction Digestion

According to its plasmid map, pBS-P-ΦT only has two restriction sites: *Hin*dIII and *Eco*RI. When digested by either of these two restriction enzymes, only one band was observed in the gel indicating the linearization of the plasmid. When cut by both enzymes, two bands with different size (2 kb, and 4 kb) were seen. However, the sizes of the bands were both bigger than expected (841 bp and 3105 bp) according to its original plasmid map. pBS-N-ΦT has two restriction sites: *Xho*I and *Eco*RI. When digested with both restriction enzymes, the sizes of the two bands were similar to their expected sizes (1372 bp and 3105 bp) (see Figure 3. 8).

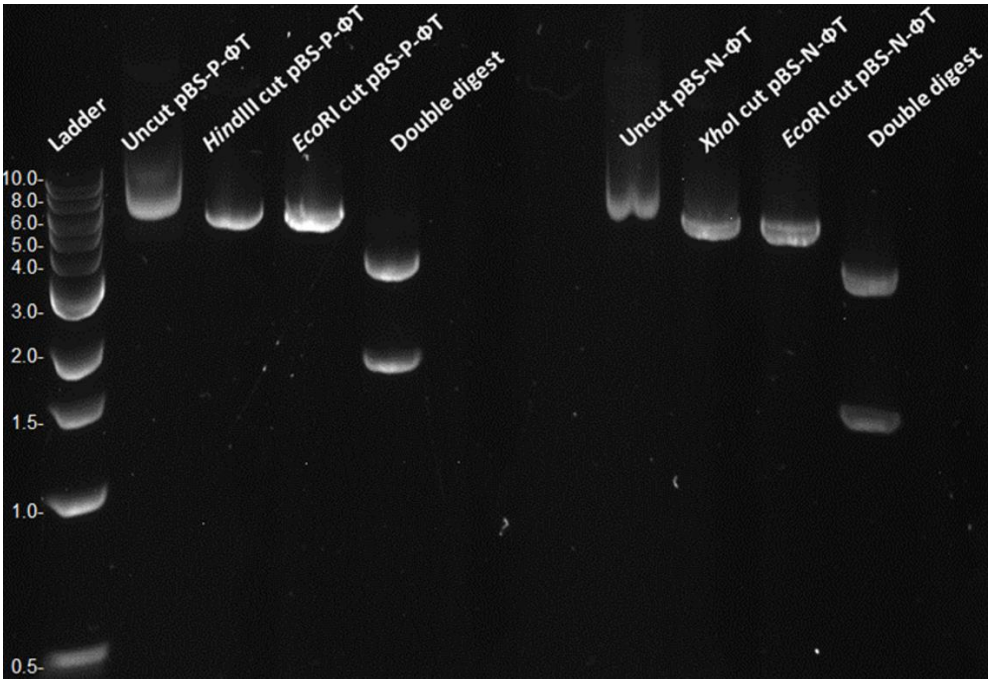


Figure 3. 8 Restriction Digestion of pBS-P-ΦT and pBS-N-ΦT to confirm their identity.

From left to right: 1kb DNA ladder (NEB); undigested pBS-P-ΦT; when pBS-P-ΦT was digested with only HindIII, one band was observed; when pBS-P-ΦT was digested with only EcoRI, one band was also observed; when pBS-P-ΦT was digested with both HindIII and EcoRI, two bands were observed. Similar pattern was seen when digesting pBS-N-ΦT with XhoI and EcoRI, individually and simultaneously. The patterns of bands were as expected after restriction digestion with specific restriction enzymes, which confirms the identity of each plasmid.

According to the plasmid map of pBS-G-ΦT, it has two restrictions sites: *Apa*I and *Bam*HI. The expected band sizes after restriction digestion are 1700 bp and 3105 bp, which are similar to the band sizes observed (see Figure 3. 9).

Based on the entire sequence of pI18-ZIKV-E, *Bam*HI/*Kpn*I and *Xho*I/*Eco*RI are at either end of ZIKV-E gene in the pI18 plasmid vector, and the size of the ZIKV-E gene is 2163 bp. Hence, *Bam*HI, *Xho*I and *Eco*RI are chosen to digest the plasmid. The digestion result corresponded to what was expected. One band was observed when pI18-ZIKV-E was digested with *Bam*HI; two bands occurred when the plasmid was cut with *Bam*HI and *Xho*I or *Bam*HI and *Eco*RI (see Figure 3. 10).

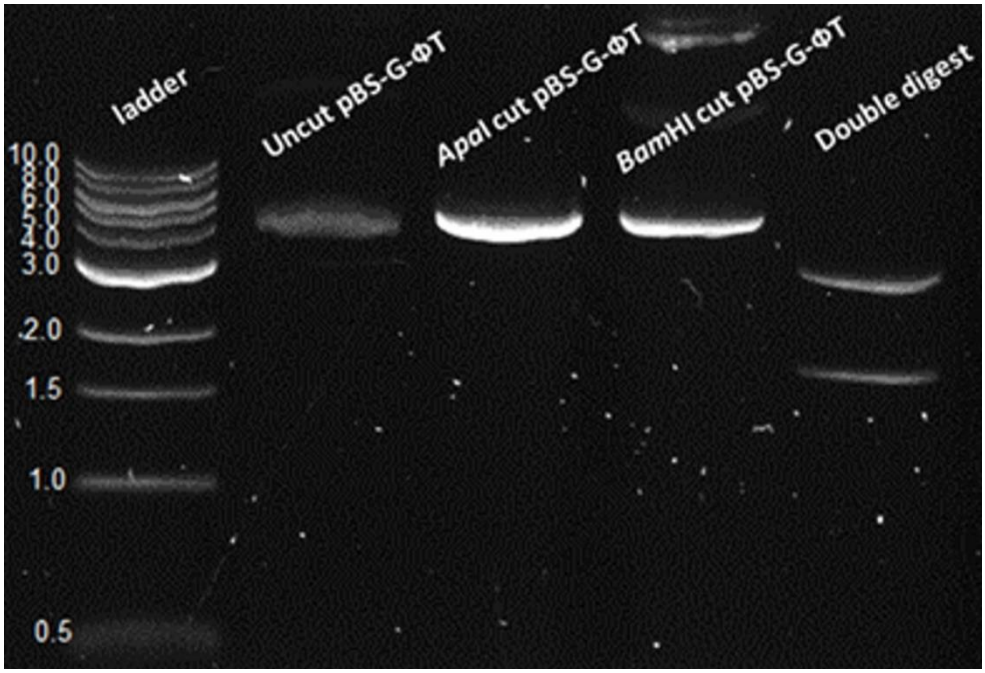


Figure 3. 9 Restriction Digestion of pBS-G-ΦT. From left to right: 1kb DNA ladder (NEB); undigested pBS-G-ΦT; pBS-G-ΦT digested with ApaI; pBS-G-ΦT digested with BamHI; pBS-G-ΦT digested with both ApaI and BamHI. Gel electrophoresis confirms the plasmid is pBS-G-ΦT.

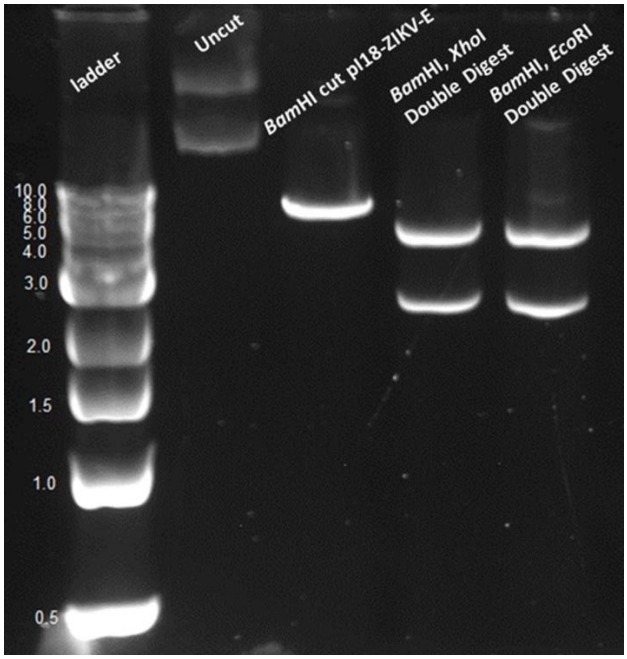


Figure 3. 10 Restriction Digestion result of pI18-ZIKV-E. From left to right: 1kb DNA ladder (NEB); undigested pI18-ZIKV-E; pI18-ZIKV-E digested with BamHI; pI18-ZIKV-E digested with both BamHI and XhoI; pI18-ZIKV-E digested with both BamHI and EcoRI. Gel electrophoresis confirms the plasmid is pI18-ZIKV-E.

3.4.2 Western blot

Western blot result confirmed the successful expression of ZIKV-E in 293T cells and the expressed ZIKV-E proteins are of the correct size which is approximately 52 kDa (Dai et al., 2016). The negative control: cell lysate from 293T cells which were not transfected with pI18-ZIKV-E did not express ZIKV-E proteins as expected (see Figure 3. 11).

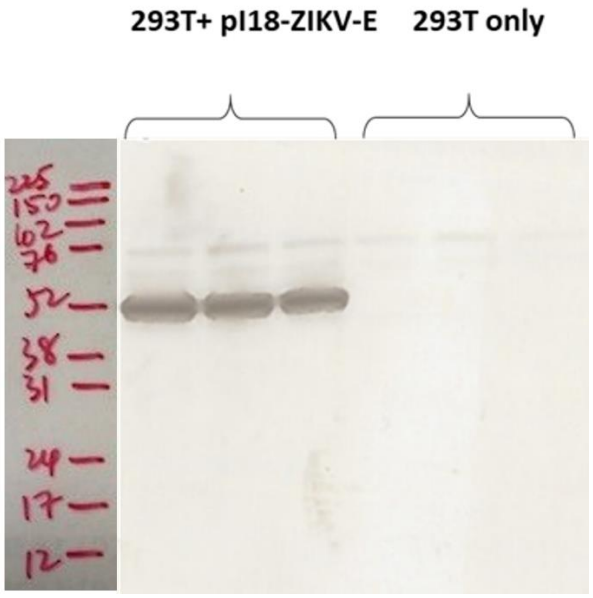


Figure 3. 11 Western blot result shows the ZIKV-E was expressed by 293T cells and the size was correct. Full range rainbow molecular weight marker (Fisher Scientific) was used. Strong bands were observed in the first three lanes which were loaded with samples produced by transfecting 293T cells with plasmid pI18-ZIKV-E, whereas no bands were shown in the negative control lanes where the samples were untransfected 293T cells.

3.4.3 Propagation of FPV-T7

CEF cells infected with FPV-T7 viruses were observed five days post-infection. CPE of the cells were observed (see Figure 3. 12). Dead cells became rounded in shape and detached from the bottom of the flask.

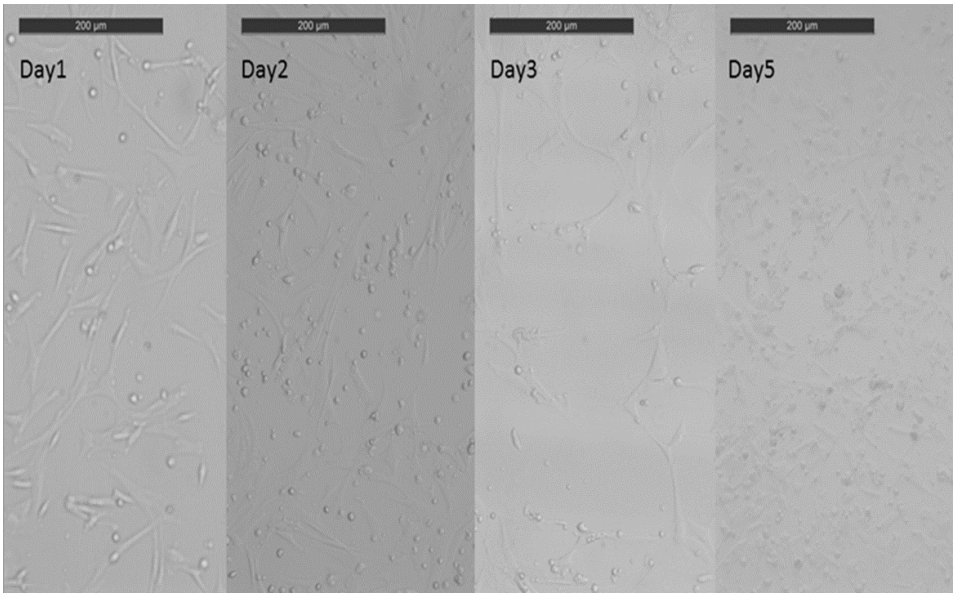


Figure 3. 12 Observations of cytopathic effect (CPE) in chicken embryonic fibroblast (CEF) cells infected with Fowlpox T7 helper (FPV-T7) virus.

3.4.4 Primary recovery of VSV PV

During initial attempts of primary recovery of VSV PV, the total amount of plasmids transfected in each well (22µg), helper plasmids ratio (N: P: G: L=3:5:8:1) and volume of FPV-T7 (13.6µl) were kept the same. However, the volume of Lipofectamine used per well was titrated for the best transfection result. Five different volumes were tested, which were 5µl, 7µl, 9µl, 12µl, and 15µl. After incubation, the supernatants from each well were collected, filtered and added to fresh BHK-21 cells, referred to as target cells, for further incubation. The cells left in the wells, referred to as producer cells, were tested for luciferase activity, which directly reflects the PV titres. Producer cells from wells in which Lipofectamine used up to 12µl had similar low luciferase activities of less than 1×10^5 RLU/ml. Surprisingly, when the Lipofectamine volume was increased to 15µl per well, a dramatic increase of luciferase activity in the producer cells was observed (see Figure 3. 13). Lipofectamine >15 was not tested to keep cost-effective with the usage of reagent, and the preliminary result was already satisfactory. However, in hindsight, even higher luciferase activities may be achieved if higher volume of lipofectamine was used. Finally, 15µl/well Lipofectamine was decided to be the optimal amount for transfection.

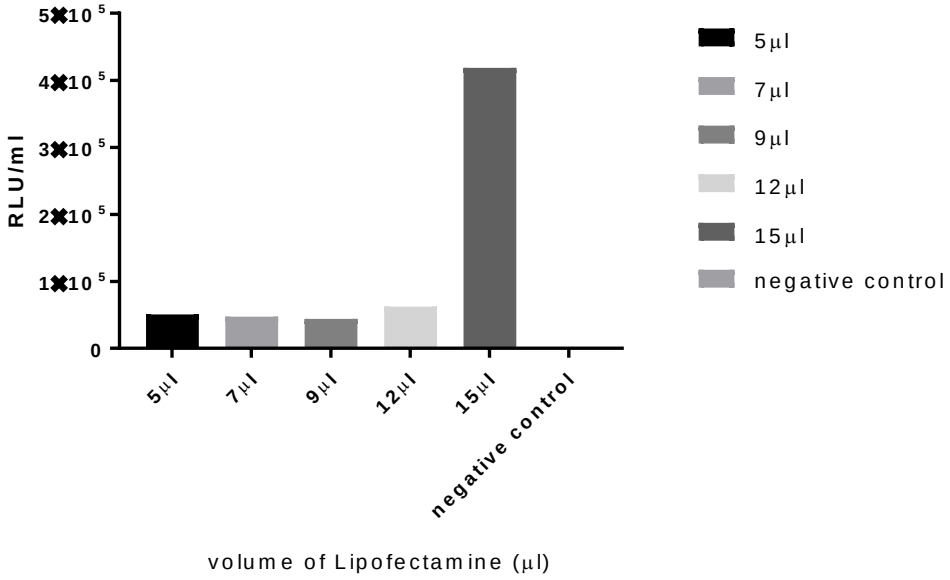


Figure 3. 13 Luciferase activities in producer cells transfected with the same amount of plasmids, FPV-T7 helper virus and helper plasmid ratio but using different volumes of Lipofectamine. A large difference in luciferase activity was observed between Lipofectamine. This experiment was not performed in replicates; therefore, no error bars were presented.

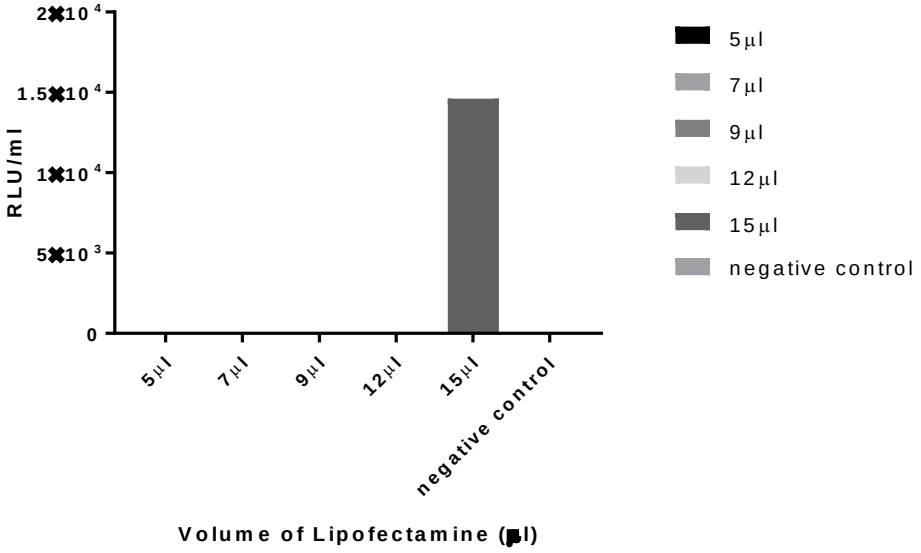


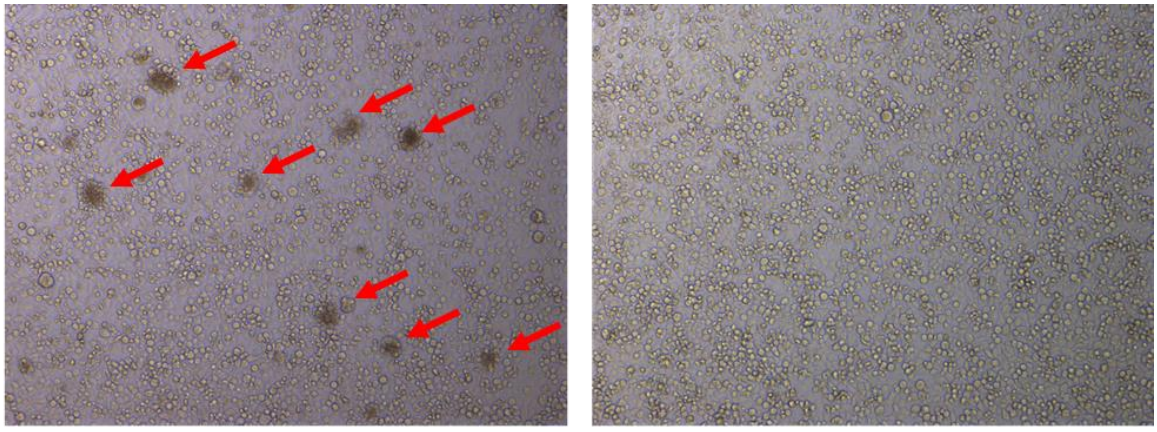
Figure 3. 14 Luciferase activities in target cells infected with recovered VSV PV supernatant. Only target cells in the '15µl' well showed luciferase activity. This experiment was not performed in replicates; therefore, no error bars were presented.

After the supernatants containing recovered VSV PV were incubated on target cells, target cells were also harvested and tested. As expected, only the '15µl well' target cells showed evidence of luciferase activity (see Figure 3. 14), which confirmed that the primary rescue of VSV PV was successful.

The rescued VSV PV was then used in plaque purification to remove the FPV-T7 helper virus input used in the primary recovery stage. Two 6-well plates were used, and 12 wells of BHK-21 cells in total were infected with primarily recovered VSV PV. Only one well showed viral plaques after at least 48 hours of incubation (no images were taken). Sixteen plaque isolates were individually harvested using the tip of a 1ml pipette and eluted in 0.5ml D-5 in an appropriately labelled 1.5ml Eppendorf tube. Out of 16 tubes of purified VSV PV, 15 of them caused CPE in fresh target cells; one sample had no effects on target cells (no images were taken).

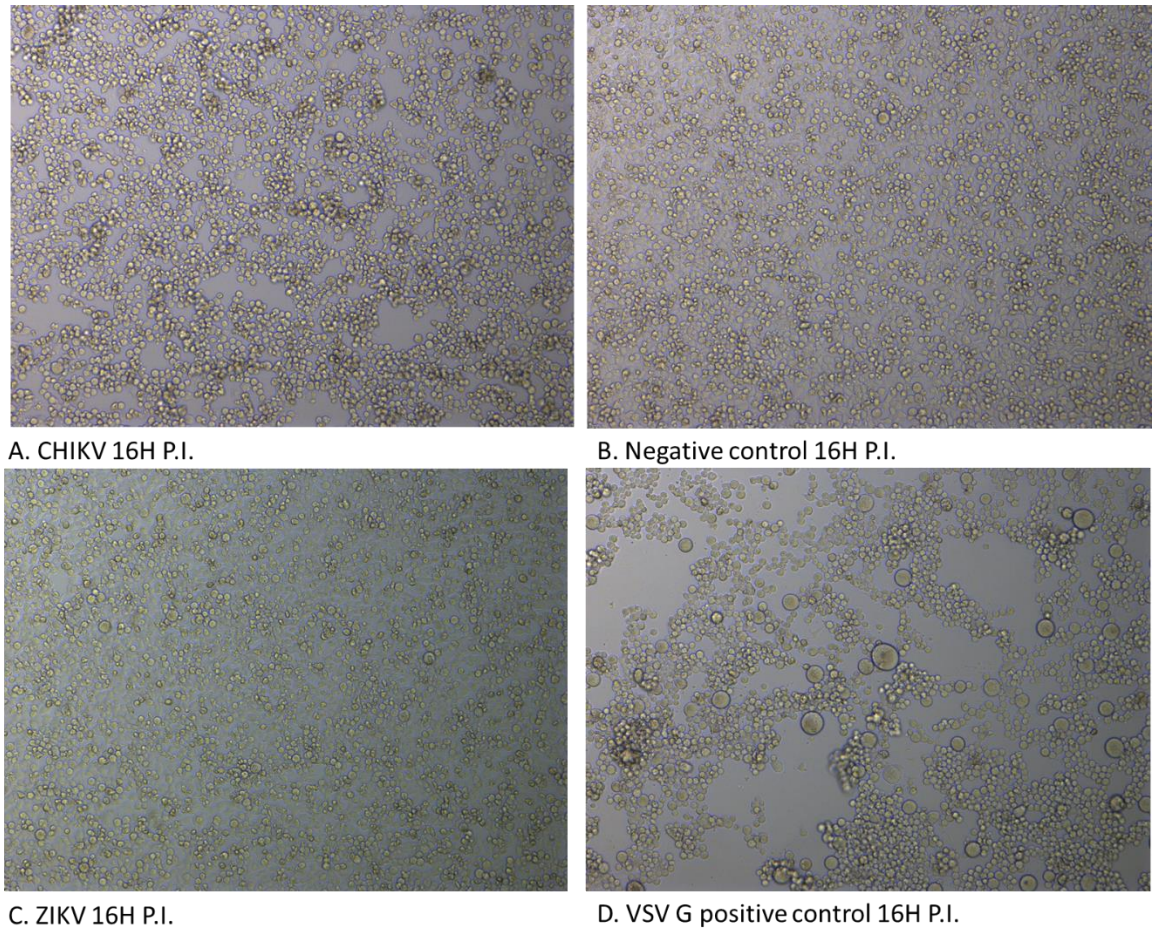
Subsequently, the plaque-purified VSV PV was used to make VSV backboned PV with heterologous envelope proteins. Attempts were made using envelope proteins of chikungunya virus (CHIKV), C2 (WNV envelope with VSVG signalling peptide) and ZIKV. Producer cells transfected with C2 showed a certain degree of CPE, cell death and aggregations were observed (see Figure 3. 15).

When producer cells transiently expressing CHIKV-E were infected with VSV PV, they showed similar CPE to the VSV-G positive control, at a relatively reduced level at 16 hours post-infection. However, after 24 hours, as for the positive control, all 'CHIKV E' producer cells were all dead. ZIKV-E expressing producer cells showed no obvious difference compared to negative control cells at the time point when the images were taken or after 24 hours (see Figure 3. 16).



A. C2 16H P.I. B. Negative control 16H P.I.

Figure 3. 15 Image of producer cells transiently transfected with C2 and infected with VSV PV taken 16H P.I.. The red arrow shows possible aggregations of dead cells, which were not observed in negative control cells which were untransfected producer cells and infected with VSV PVs (B).



A. CHIKV 16H P.I. B. Negative control 16H P.I.

C. ZIKV 16H P.I. D. VSV G positive control 16H P.I.

Figure 3. 16 Images of producer cells A. transiently transfected with CHIKV-E and infected with VSV PV taken 16 hours post-infection. B. negative control cells. C. producer cells transiently transfected with ZIKV-E. D. producer cells transiently transfected with VSV-G.

Producer cells transiently transfected with heterologous envelope proteins were harvested when CPE was observed. Five different heterologous envelope proteins were used in attempts to form PVs with G*ΔG-VSV. Only producer cells transfected with chikungunya envelope proteins showed luciferase activities as high as a positive control. Supernatants harvested and filtered from attempts to generate ΔG-VSV PVs with foreign glycoproteins were passed directly onto fresh target cells. After 24 h incubation or cells started to show CPE, target cells were again harvested and tested for luciferase activity. High levels of luciferase activity were observed from only those target cells infected with G*ΔG-VSV pseudotyped with chikungunya envelope proteins and VSV-G proteins. This result indicated that chikungunya PVs were produced. No signal was observed in target cells infected with G*ΔG-VSV pseudotyped with ZIKV envelope protein (see Figure 3. 17).

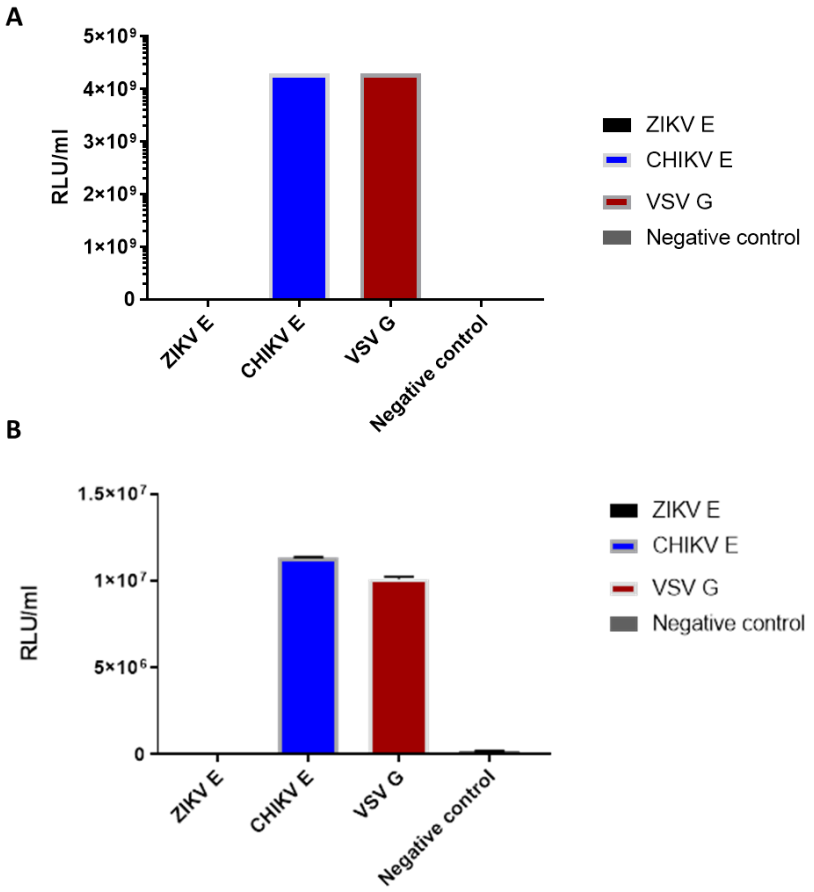


Figure 3. 17 A producer cell luciferase activity when attempting to generate ΔG-VSV PVs with foreign glycoproteins, no error bars were presented because data was collected from single well; B target cell luciferase activity after they were infected with ΔG-VSV PVs formed with foreign glycoproteins.

3.4.5 Cell surface expression using a flow cytometer

It was found that BHK21 cells support productive ZIKV replication (Chan et al.,2016). However, flow cytometry results showed that only 5% of cells transfected with pI18-ZIKV-E expressed ZIKV envelope proteins on their cell surface (see Figure 3. 18).

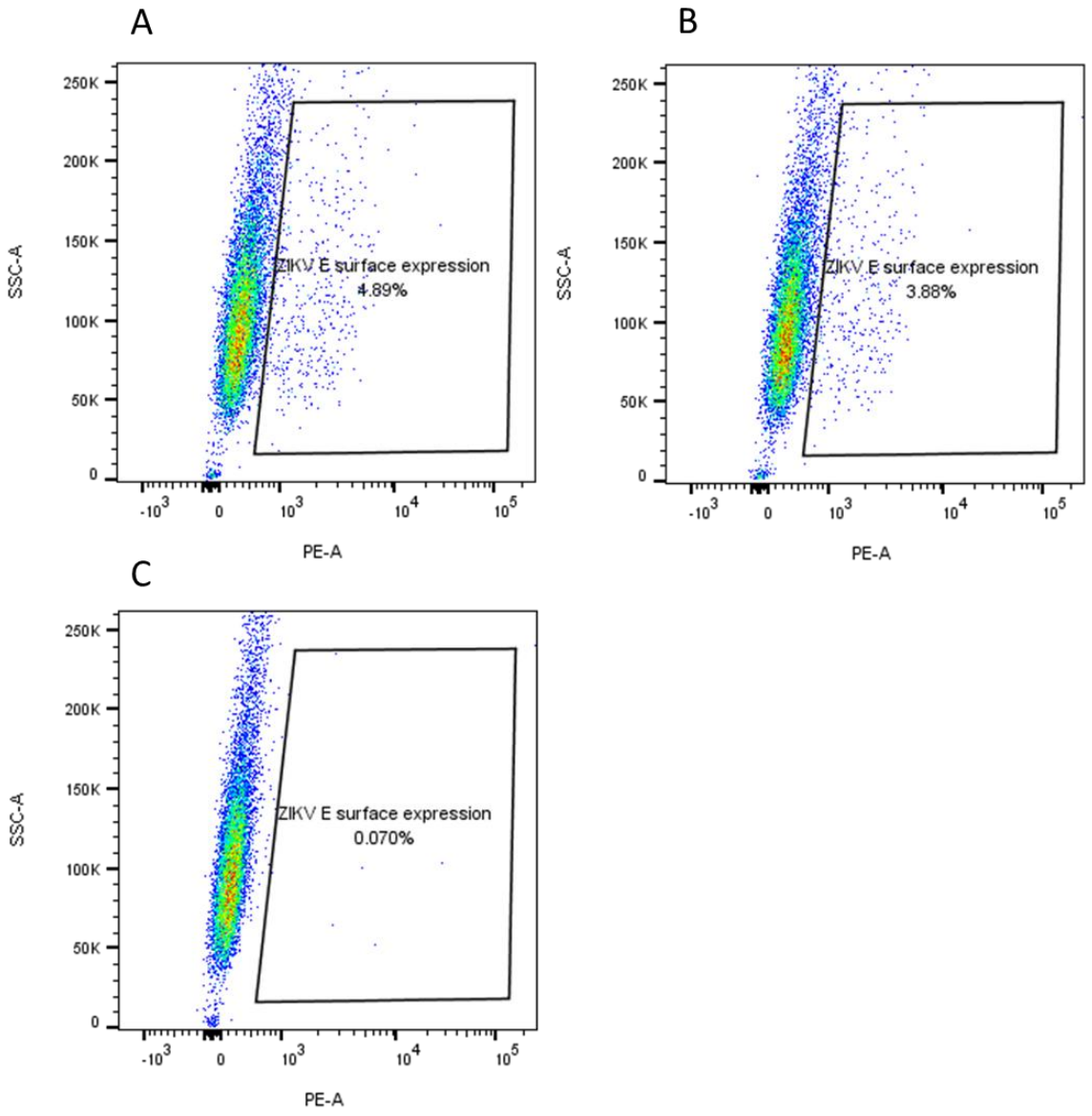


Figure 3. 18 Cell surface expression of ZIKV envelope proteins on BHK-21 cells.

BHK-21 cells were immunostained with anti-ZIKV-E antibody and Alexa Fluor™ 546 goat anti-human IgG (H+L) and analysed by flow cytometer. The level of cell surface expression is indicated inside the gate. A and B are two replicates, sample A had a percentile of 4.89%, whereas sample B had a percentile of 3.88%; C shows the percentile of untransfected BHK-21 cell control immunostained with the same secondary antibody.

Influenza HA was expressed as a control in parallel with ZIKV E surface expression experiment. Approximately 60—70% of BHK-21 cells transfected with HA containing plasmid expressed influenza HA on their cell surfaces (see Figure 3. 19), which probably explained why pseudotyping with influenza HA was successful (Carnell et al., 2015).

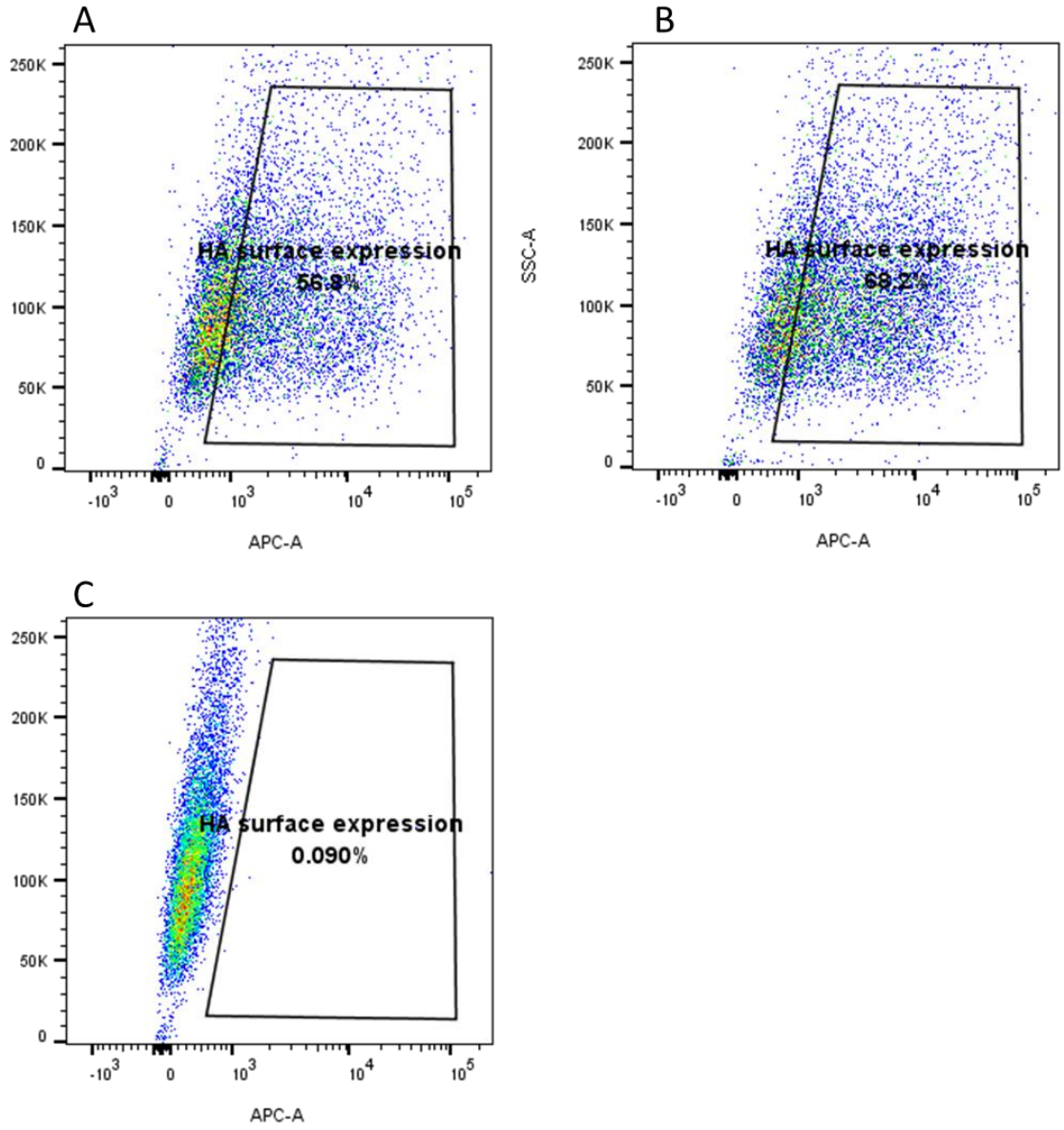


Figure 3. 19 Cell surface expression of influenza HA envelope proteins on BHK-21 cells.

BHK-21 cells were immunostained with anti-HA antibody and Alexa Fluor™ 594 goat anti-rabbit IgG (H+L) and analysed by flow cytometer. The level of cell surface expression is indicated inside the gate. A and B are two replicates, sample A had a percentile of 56.8%, whereas sample B has a percentile of 68.2%; C shows percentile of untransfected BHK-21 cell control immunostained with the same secondary antibody.

3.5 Discussion

A purified G*ΔG-VSV working stock was successfully generated, and it was able to generate ΔG-VSV PVs further using a heterologous envelope protein. However, only chikungunya PVs were produced. Although VSV PV has many remarkable properties in generating PVs, e.g. readily forming PVs with many different foreign glycoproteins (Matsuura et al., 2001), this study found that G*ΔG-VSV did not form PVs with unmodified ZIKV envelope protein or a chimeric WNV envelope protein.

3.5.1 Virus budding sites

A potential explanation for the failure to produce a ZIKV PV is that there are differences in virus assembly and budding between VSV and ZIKV. VSV buds from the plasma membrane of infected cells. VSV-G protein is synthesised by endosomes bound to the rough ER membranes, post-translationally modified in the Golgi apparatus like most proteins and subsequently transferred to the plasma membrane where it is grouped into clusters or microdomains. The majority of its sequence (446 amino acids) forms the ectodomain of the protein, whereas 29 amino acids in the C-terminal form the cytoplasmic domain, which remains on the cytoplasmic side of the ER. The G protein is one of the most rapidly transported integral membrane proteins, requiring approximately 15 minutes to be transferred from ER to Golgi membranes and 15 minutes from Golgi membranes to plasma membranes. This rapid transport is dependent on a 6-amino acid sequence in the cytoplasmic domain, which is responsible for concentrating G protein at sites of vesicle budding. Also, the virus budding site is formed by clustering of VSV-G-containing microdomains, which are up to 4 times larger than microdomains outside the virus budding site (Lyles, 2007).

As mentioned previously, flavivirus replication and assembly occur on ER membranes where viral genomes assemble with C, prM and E proteins and bud into the ER lumen, taking ER membranes with the developing virion (Barrows et al., 2018). Flavivirus

assembly process happens rapidly and/or simultaneously with replication and budding, evidenced by failure to visualise assembly intermediates (Apte-Sengupta et al., 2014). Although budding at the plasma membrane has been observed occasionally, it is not a crucial mechanism for flavivirus virion formation (Lindenbach, 2007). These studies underline the fact that either the efficiency of flavivirus envelope proteins transported to the cell surface or the possibility of flavivirus envelope proteins accumulated on the plasma membrane is extremely low. This is consistent with the cell surface expression results in this report, which has shown that less than 5% of cells transfected with pI18-ZIKV-E plasmid express the envelope protein on their surface, also evidenced in Ciczora et al. (2010)'s experiment, whereas approximately 60%—70% of cells transfected with influenza HA plasmid express HA on cell. Additionally, pulse-chase experiments and endoglycanase treatments have also revealed that only a small fraction of glycoproteins from hepatitis C virus (HCV), which is phylogenetically related to flaviviruses, are translocated to the plasma membrane (Tani et al., 2007).

Different virus budding sites were thought to attribute to the failure in pseudotyping flavivirus, considering budding is the process where foreign glycoproteins are incorporated into VSV virions. Nonetheless, production of pseudotyped VSVs bearing unmodified envelope glycoproteins of bunyaviruses has been reported, in spite of the lack of glycoproteins transferred to the plasma membrane. Therefore, cell surface expression of foreign glycoproteins may not necessarily be a 'must' for generating pseudotype particles based on VSV (Tani et al., 2007).

On the other hand, similar to VSV, CHIKV buds through the cell membrane (Solignat et al., 2009). CHIKV enters the cell by clathrin-dependent endocytosis. Once inside the host cell cytoplasm, capsid protein binds to large ribosomal subunit. Then replication occurs in the cytoplasm. Non-structural proteins (nsPs) are produced by a polyprotein precursor termed nsP123. The subgenomic positive-strand mRNA serves as a template for viral structural proteins which are also encoded by a polyprotein, co- and post-translationally

cleaved into C, PE2, E1 and a small peptide called 6K (possibly function as a signal sequence for the translocation of E1). The cleavage of PE2 and 6K are catalysed by signalase in the lumen of the ER. Once transported to the trans-Golgi, the PE2-E1 moves to the cell surface, meanwhile PE2 is cleaved by a cellular furin or furin-like proteinase to form E2 and E3. CHIKV virion assembly starts with nucleocapsid assembly in the cytoplasm, which then freely distribute to the plasma membrane. Virions take up a lipid bilayer envelope containing E1 and E2 glycoproteins. The mature envelope glycoprotein spikes consist of trimers of E1-E2. During budding, the nucleocapsid appears to go through a maturation event and requires binding to E2 for appropriate targeting to the cell membrane (Solignat et al., 2009). All in all, this aspect probably contributes to the successful pseudotyping of CHIKV with VSV backbone.

3.5.2 ER retention signal

Pseudotyped VSVs bearing glycoproteins of HCV, another member of the family *Flaviviridae*, were generated previously (Matsuura et al., 2001). Both HCV E1 and E2 proteins have C-terminal retention signals. In their studies, chimeric proteins containing the signal sequence, transmembrane domain, and cytoplasmic tail of VSV G glycoprotein and the ectodomain of HCV E1 or E2 protein were generated to overcome the retention of envelope proteins in the ER/lack of translocation of envelope proteins to the plasma membrane (Matsuura et al., 2001, Takikawa et al., 2000).

Although few studies on ZIKV envelope protein ER retention signal can be found, extensive research on other flavivirus envelope proteins such as yellow fever virus (YFV) has been done. ER-retention signals in the transmembrane domains of YFV envelope proteins have been well characterised. The prM and E envelope proteins contain a large ectodomain and a C-terminal membrane anchor. The C-termini of prM and E form two anti-parallel transmembrane α-helices. It was found that the prME heterodimer contains at least three ER-retention signals, two in the transmembrane region of prM and at least one in the transmembrane region of E (see Figure 3. 20). Furthermore, the first transmembrane

segment of prM (TM1prM) is a dominant retention signal as adding a VSV-G export signal in the C-terminal cannot outweigh its retention effect. VSV-G cytosolic tail contains a DIE motif corresponding to an export signal (Nishimura and Balch, 1997). The presence of this motif led to an export of a chimeric protein containing the ectodomain of CD4 in fusion with the first transmembrane segment of YFV E protein (TM1E) at the plasma membrane. However, when adding an export motif at the C-terminus of the prME heterodimer or adding an export signal at the C-terminus of TM1prM fused to CD4, the prME and CD4 were not exported to the plasma membrane in both occasions, which indicates the export motif in VSV-G is not strong enough to compete with the ER retention of the TM1prM. There is a balance of forces between retention and export signals that will provide different outcomes depending on the strength of the retention signals (Ciczora et al., 2010). This probably explains why chimeric WNV envelope protein C2, which did not form PVs with VSV backbone successfully in this study. Additionally, it was necessary to delete the second transmembrane segment of the E protein (TM2E) to place the export motif of VSV-G into the cytosol. The deletion does not affect the functions of the prME heterodimer.

Another way Ciczora et al. (2010) used to identify ER-retention signal was to add a stretch of hydrophobic residues in the middle of TM1E and compared the subcellular localisation of this protein (CD4-TM1E$_{(AL)3}$) with that of CD4-TM1E and wild type CD4, based on the existing knowledge that increasing the length of transmembrane domains can disrupt ER retention of certain proteins. The ALALAL sequence was chosen, as both alanine and leucine residues are observed frequently in transmembrane domains. As a result, this insertion led to the export of the chimeric protein at the plasma membrane. The same method was applied to identify the ER-retention signal in TM1prM and TM2prM.

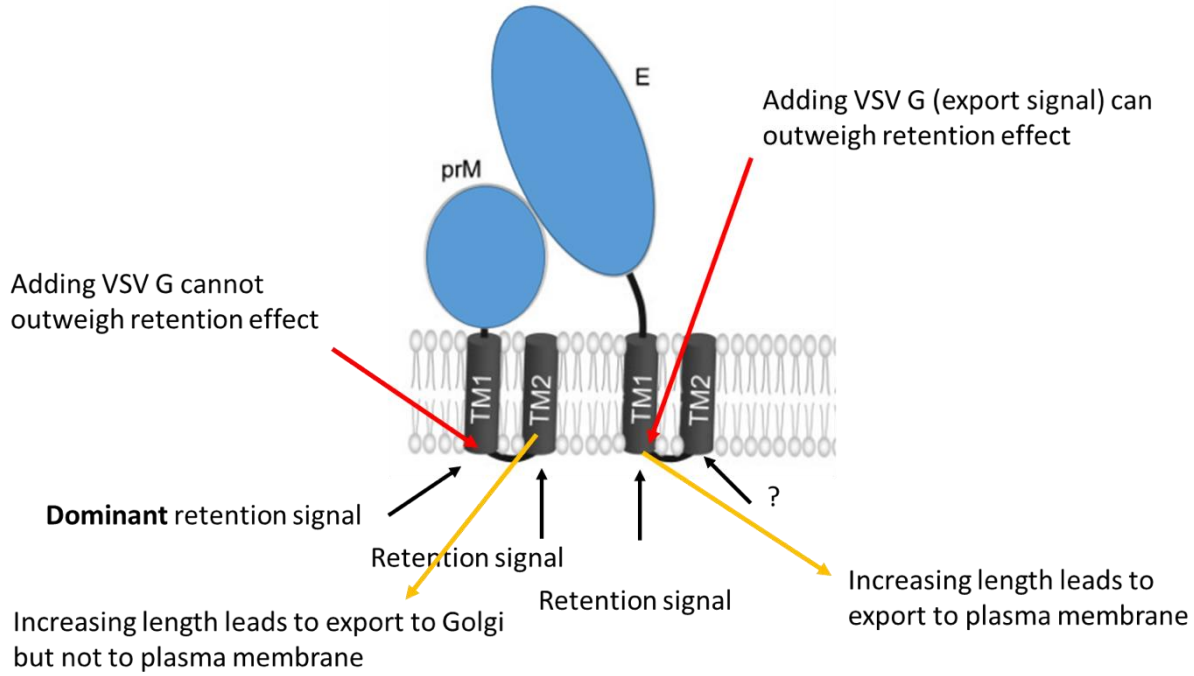


Figure 3. 20 Topology of yellow fever virus (YFV) envelope proteins (Adapted from (Ciczora et al., 2010)).

prM and E contain a large luminal domain and a C-terminal membrane anchor. The C termini of these proteins form two antiparallel transmembrane α-helices (TM1 and TM2).

In future experiments, to produce VSV PVs bearing ZIKV envelope proteins, a large fraction of ZIKV-E must be exported to cell surface first. It is recommended to construct a chimeric protein containing the ZIKV signal sequence, the ectodomain of ZIKV prM, mutated TM1prM and TM2prM, the ectodomain of ZIKV-E and mutated TM1E, together with the stem, transmembrane domain and the cytoplasmic tail of VSV-G. The TM1prM, TM2prM and TM1E were mutated to remove their ER-retention function. In addition, the VSV-G stem region is included in the chimeric protein because its possible ability to improve glycoprotein uptake by inducing membrane curvature at sites where budding occurs (Hanika et al., 2005) (see Figure 3. 21). Intracellular staining of transfected cells for ZIKV E could be used to confirm the successful export of the genetically modified ZIKV E to cell surface.

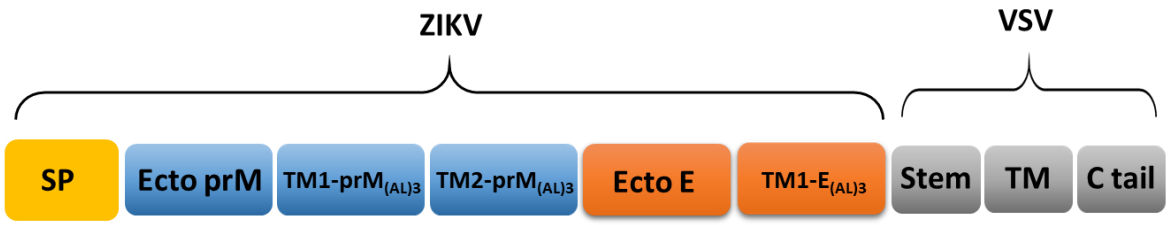


Figure 3. 21 Schematic diagrams of a recommended chimeric protein construct for pseudotyping ZIKV by the author.

3.5.3 Cell lines

Protein molecules and glycosaminoglycans (GAGs) on the cell surface play a vital role in the binding and/or entry of the pseudotyped VSV particles. These cell surface components presumably serve as cellular receptors or cofactors for the virus. In the same HCV study mentioned earlier, it was reported that the infectious titres were lower when using a transient expression system with 293T cells than those from CHO cell line. Additionally, their pseudotyped HCV showed no infectivity in BHK cells (Matsuura et al., 2001). Unfortunately, all results obtained in this report were only from using BHK-21 cells. Using alternative cell lines may provide some different results.

Chapter 4 Development of a ZIKV NS1-based enzyme-linked immunosorbent assay (ELISA) using plant expressed NS1 protein

4.1 Introduction

Co-transmission of Zika (ZIKV), Dengue (DENV), and chikungunya (CHIKV) in their endemic regions has resulted in co-infection of humans with these viruses which exhibit similar acute symptoms. Improvements in the differential diagnosis in terms of accuracy and efficiency are needed for better patient management and epidemiological data collection. (Ohst et al., 2018).

4.1.1 ZIKV diagnosis

Diagnosis of Zika virus (ZIKV) infection is currently performed using either molecular methods, for example, reverse transcription-polymerase chain reaction (RT-PCR), for the detection of viral RNA or serological methods, e.g. plaque-reduction neutralization tests (PRNTs) or enzyme-linked immunosorbent assays (ELISAs), for the detection of virus-specific antibodies (Wong et al., 2017). Serological methods have a longer diagnostic window than molecular methods and are suited for diagnosing both acute and past infections (Ohst et al., 2018).

Accurately diagnosing Zika infection is sometimes not straightforward. Firstly, the duration of viraemia is usually less than seven days before and after symptom onset (Rabe et al., 2016). Around 80% of ZIKV infections are asymptomatic (Wong et al., 2017). Therefore, with a narrow testing window, a negative real-time RT-PCR (rRT-PCR) result does not exclude infection, which still requires a confirmation from serological tests. Secondly, when a person who has previously had a flavivirus infection is subsequently exposed to ZIKV,

there will be a rapid rise in the neutralising antibodies against multiple flaviviruses. The titre of neutralising antibody against flavivirus, causing the previous infection is higher than that against the virus causing the recent infection (Rabe et al., 2016) (see Figure 4. 1). PRNTs can measure virus-specific neutralising antibodies. However, PRNTs do not discriminate between virus-specific neutralising antibodies and cross-reactive neutralising antibodies, especially in secondary flavivirus infections. Additionally, PRNTs are time-consuming, difficult to perform, unscalable and only suitable for use in highly specialised laboratories. On the contrary, ELISAs are rapid, scalable and widely accessible. Even so, the cross-reactivity between multiple co-circulating flaviviruses is limiting the current ELISAs (Steinhagen et al., 2016).

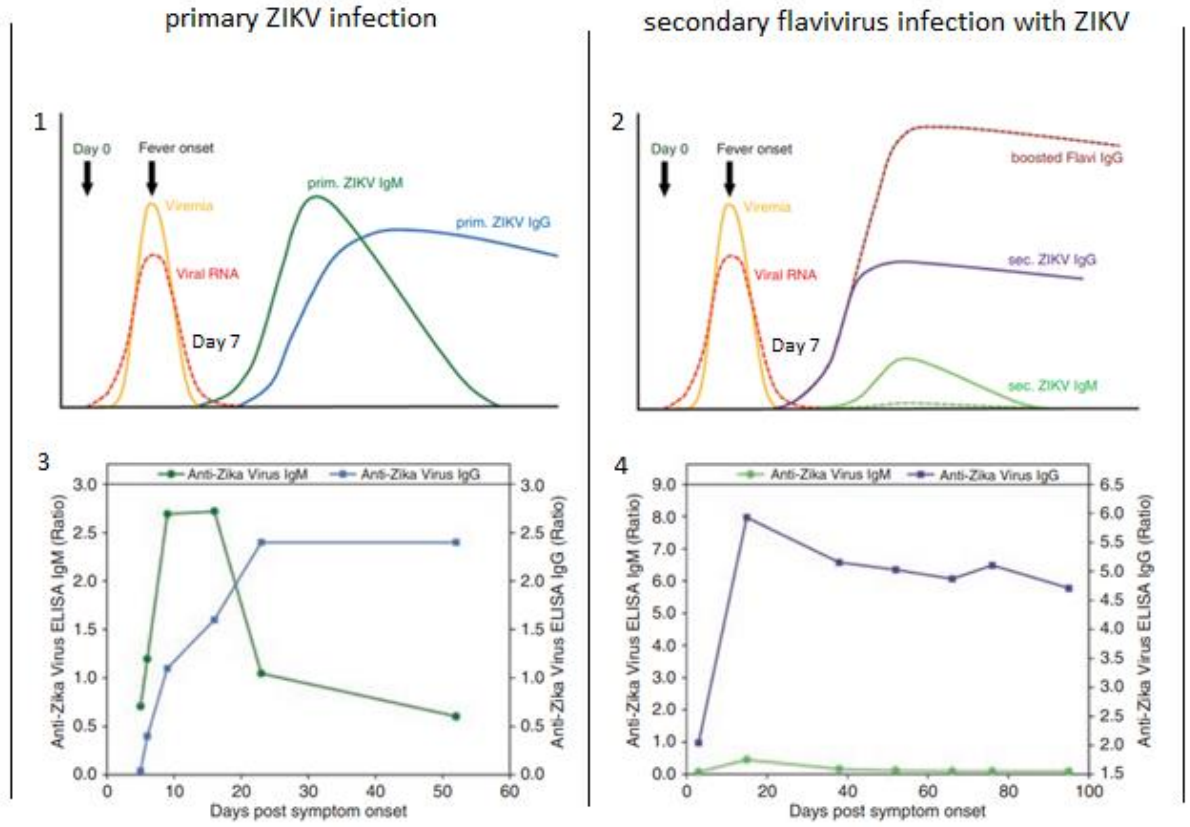


Figure 4. 1 The significant laboratory diagnostic markers in (1) primary ZIKV infections and (2) secondary flavivirus infections with ZIKV. Titer course of anti-ZIKV IgM and IgG in (3) a traveller from the non-endemic area after primary infection with ZIKV, and (4) a resident from the endemic region of multiple flaviviruses who contracted ZIKV as secondary flavivirus infection (Adapted from (Ohst et al., 2018)).

4.1.2 ZIKV-NS1

Knowledge of flavivirus nonstructural protein 1 (NS1) has primarily accumulated from well-studied flaviviruses such as DENV, WNV and YFV. However, little is known about ZIKV-NS1, which exhibits different pathogenesis from that of typical flaviviruses. Flavivirus NS1 proteins (46–55kDa) are transferred into the endoplasmic reticulum (ER) during synthesis. They are cleaved from E protein by host signal peptidase, whereas an unknown ER-resident host enzyme cleaves the NS1/NS2A junction. Around 30 minutes after synthesis, NS1 forms highly stable homodimers and acquires an affinity for intracellular membranes, such as the ER, vesicle packets and cell surfaces (Lindenbach, 2007). These NS1 are also called membrane associated NS1. DENV NS1 protein is retained within infected cells, but it can be secreted from mammalian cells as a barrel-shaped hexameric lipoprotein consisting of three dimers (Gutsche et al., 2011).

NS1 has an important yet unclear role in RNA replication. Mutation of NS1, which localises to the sites of RNA replication, can lead to dramatic defects in RNA replication and virus production. It was revealed that NS1 functions at a very early stage in RNA replication. Interactions between NS1 and NS4A are essential for replicase function (Lindenbach, 2007).

Extracellular NS1 interacts with components from both the innate and adaptive immune systems and plays a critical role in immune evasion and pathogenesis (Song et al., 2016). During infection, strong humoral responses are made against this protein, and antibodies against membrane-associated NS1 can lead to complement-mediated lysis of virus-infected cells. The secreted NS1 was originally identified as the soluble complement-fixing antigen in the serum and tissue of infected animals, which peaks during the acute phase of infection (Lindenbach, 2007). In the case of DENV and WNV, NS1 is secreted into serum,

eliciting antibody production against NS1; this acute-phase release of ZIKV-NS1 into serum has not yet been evidenced (Steinhagen et al., 2016).

Furthermore, ZIKV NS1 was structurally compared with that of DENV1, DENV2 and WNV. The NS1 structure of ZIKV was very similar to DENV1, DENV2 and WNV NS1 structure, despite sharing a protein sequence identity of only 53%—56% (Song et al., 2016). It was also found that the electrostatic potential of the outer surface of ZIKV NS1 is distinctly different from those of DENV and WNV, which may lead to different binding properties when interacting with host factors and known protective antibodies to flavivirus NS1 (Song et al., 2016).

Moreover, traditionally, serological assays were designed to detect antibodies against flavivirus structural proteins, especially envelope proteins. However, Stettler et al. (2016) reported that the ZIKV E protein, primarily domain I and domain II, elicits flavivirus cross-reactive neutralisation antibodies and the ZIKV NS1 protein induces a non-neutralising yet virus-specific antibody response. Considering all the aforementioned characteristics of ZIKV NS1, it is an excellent candidate for developing novel diagnostic tools for ZIKV infection.

4.1.3 Plant expression system

Compared with bacteria, yeast and animal cell production systems, using plants for the transient production of recombinant proteins give the benefits of lower cost, lower contamination risks when producing pharmaceutical proteins, and higher biomass yields in a shorter amount of time.

To transiently express proteins in plants, either modified plant viruses or the combination of *Agrobacterium tumefaciens* and an expression plasmid can be used. In the latter case, agro-infiltration is performed to flood the intercellular space within the plant leaves with a suspension of bacteria carrying the expression vectors. pEAQ expression vectors were developed based on a deleted version of cowpea mosaic virus (CPMV) RNA-2, CPMV-HT (see Figure 4. 2). The system is highly effective at producing a high yield of a variety of recombinant proteins in plants in a matter of days (Sainsbury and Lomonossoff, 2008). This system works by inserting the gene to be expressed between a modified 5'-untranslated region (UTR) and the 3'-UTR from CPMV RNA-2 in a plant expression cassette consisting of the cauliflower mosaic virus (CaMV) 35S promoter and nopaline synthase (nos) terminator (Sainsbury et al., 2009).

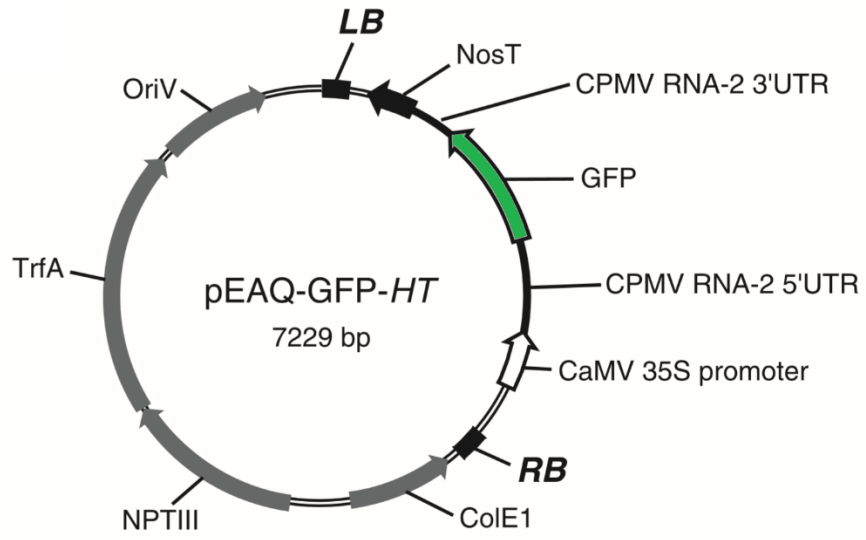


Figure 4. 2 pEAQ vector with a GFP insert.

Black boxes represent T-DNA left (LB) and right (RB) borders. Regions essential for plasmid growth and replication include oriV (pRK2 replication origin); ColEI (pBR322 replication origin); NPT(neomycin phospho-transferase); TrfA (replication-essential locus) (Adapted from (Sainsbury et al., 2009)).

4.2 Aim

This project aimed to produce plant-expressed ZIKV NS1 protein and use it to establish an ELISA to detect serum antibodies.

4.3 Materials and methods

4.3.1 General materials

4.3.1.1 Molecular cloning

Plant expression vector pEAQ-HT was kindly given by Professor George Lomonossoff (John Innes Centre) (see Figure 4. 3). Zika virus (ZIKV) (GenBank: KX197192.1) was kindly provided by Dr Alain Kohl (University of Glasgow). Oligonucleotide primers used for PCR amplification were purchased from Sigma-Aldrich (Appendix 1). The transformation was performed using DH5α competent *E. coli* cells.

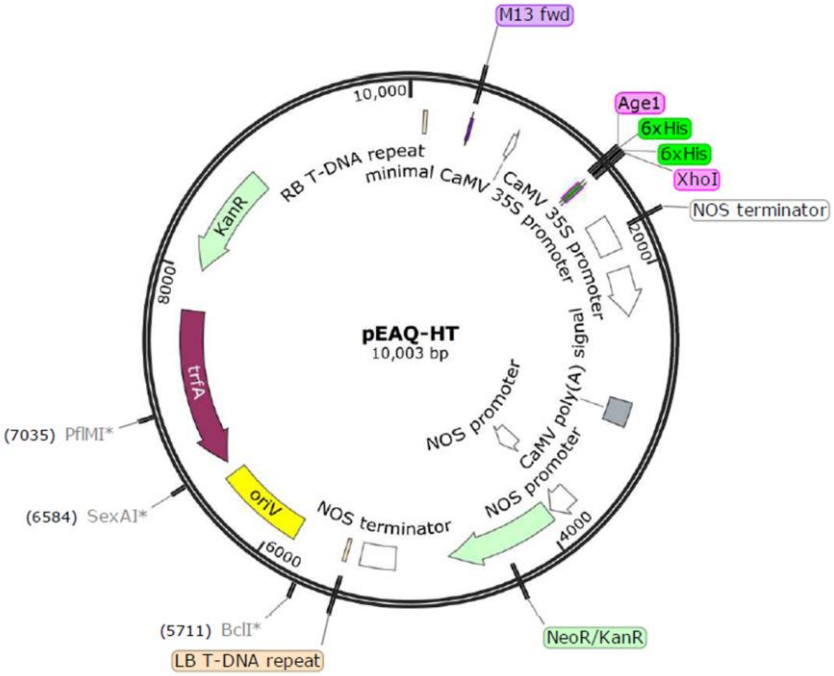


Figure 4. 3 Plasmid map of pEAQ-HT. The insert region is flanked by two 6×His tags and two AgeI restriction sites.

4.3.1.2 Plant expression

Nicotiana benthamiana plants were used for ZIKV NS1 protein expression, and they were grown in greenhouses with controlled supplementary light (16 hours per day) and temperature (23—25°C). *Agrobacterium tumefaciens* (*A.tumefaciens*) strain LBA4404 was used as host cells for pEAQ-HT vector. A list of buffers used for extraction and purification was included in Appendix 1.

4.3.2 PCR cloning of pEAQ-HT-ZIKV-NS1-His by conventional PCR cloning

A first attempt to clone the ZIKV NS1 gene into pEAQ-HT used conventional PCR cloning methods. ZIKV RNA was extracted from cell culture supernatant using QIAamp® Viral RNA Mini Kit (Qiagen) and converted to cDNA by reverse transcription using SuperScript™ IV VILO™ Master Mix according to the manufacturers' instructions. ZIKV NS1 was then PCR amplified using Q5 DNA polymerase (New England Biolabs). In order to determine the best annealing temperatures for each set of PCR primers, gradient PCRs were performed and the PCR programs were shown in Table 4. 2.

In order to amplify ZIKV NS1 as well as adding a hexa His-tag at its C-terminal end, the template for Round 1 PCR was ZIKV cDNA achieved by reverse transcription; however, the template for Round 2 was the PCR products from Round 1 reaction (see Figure 4. 4). PCR reaction mix was shown in Table 4. 1. End products of Round 2 PCR were gel purified using NucleoSpin® Gel and PCR Clean-up (MACHEREY-NAGEL) and double restriction digested by AgeI and XhoI (New England Biolabs). Subsequently, it was cloned into the plant expression vector pEAQ-HT, which was purified from glycerol stock using Plasmid Miniprep Kit (Qiagen) and double restriction digested using *AgeI* and *XhoI* to create sticky ends. Finally, the vector (pEAQ-HT) and the insert (amplified ZIKV NS1) were ligated using T4 DNA ligase (New England Biolabs) and transformed into DH5α competent *E. coli* cells. Schematic illustration of the end product was shown in Figure 4. 5.

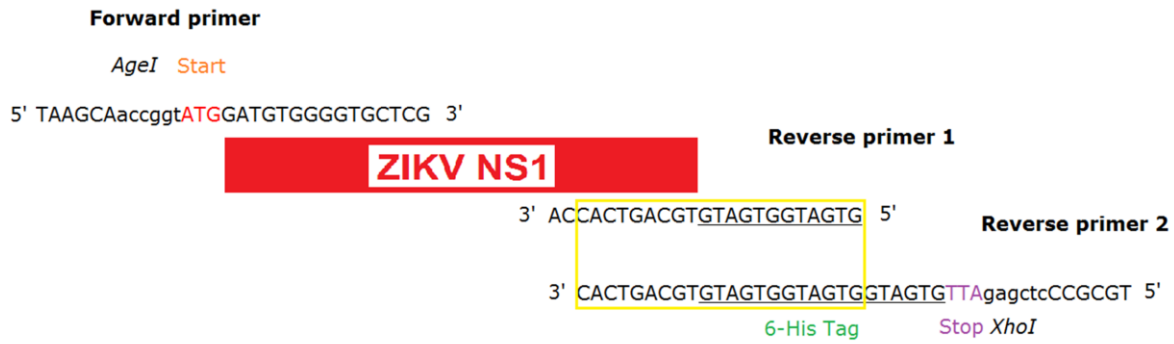


Figure 4. 4 PCR amplification of ZIKV NS1. Restriction site AgeI and a start codon were added to ZIKV NS1 N-terminus by a forward primer. Also, restriction site XhoI, a stop codon and a 6-Histidine tag were added to C-terminus of ZIKV NS1 by two reverse primers in two separate PCR reactions.

Component	Volume (µl)
5XQ5 reaction buffer	5
25mM MgCl2	1.5
10mM dNTP	0.5
10mM Forward primer	0.5
10mM Reverse primer	0.5
Q5 DNA polymerase	0.125
Nuclease-free water	11.875
Template cDNA	5

Table 4. 1 PCR reaction mix for a 25 µl reaction.

	Primer sets	Purpose	Temperature (˚C)	Time (min)	Cycles
Round 1	ZIKV NS1 forward primer and His tag Rev 1	Initial denaturing	95	0.5	1
		Denaturing	95	0.5	30
		Annealing	60-70	1	
		Extension	72	1	
		Terminal extension	72	5	1
Round 2	ZIKV NS1 forward primer and His tag Rev 2	Initial denaturing	95	0.5	1
		Denaturing	95	0.5	30
		Annealing	80-90	1	
		Extension	72	1	
		Terminal extension	72	5	1

Table 4. 2 Gradient PCR programs for different sets of primers

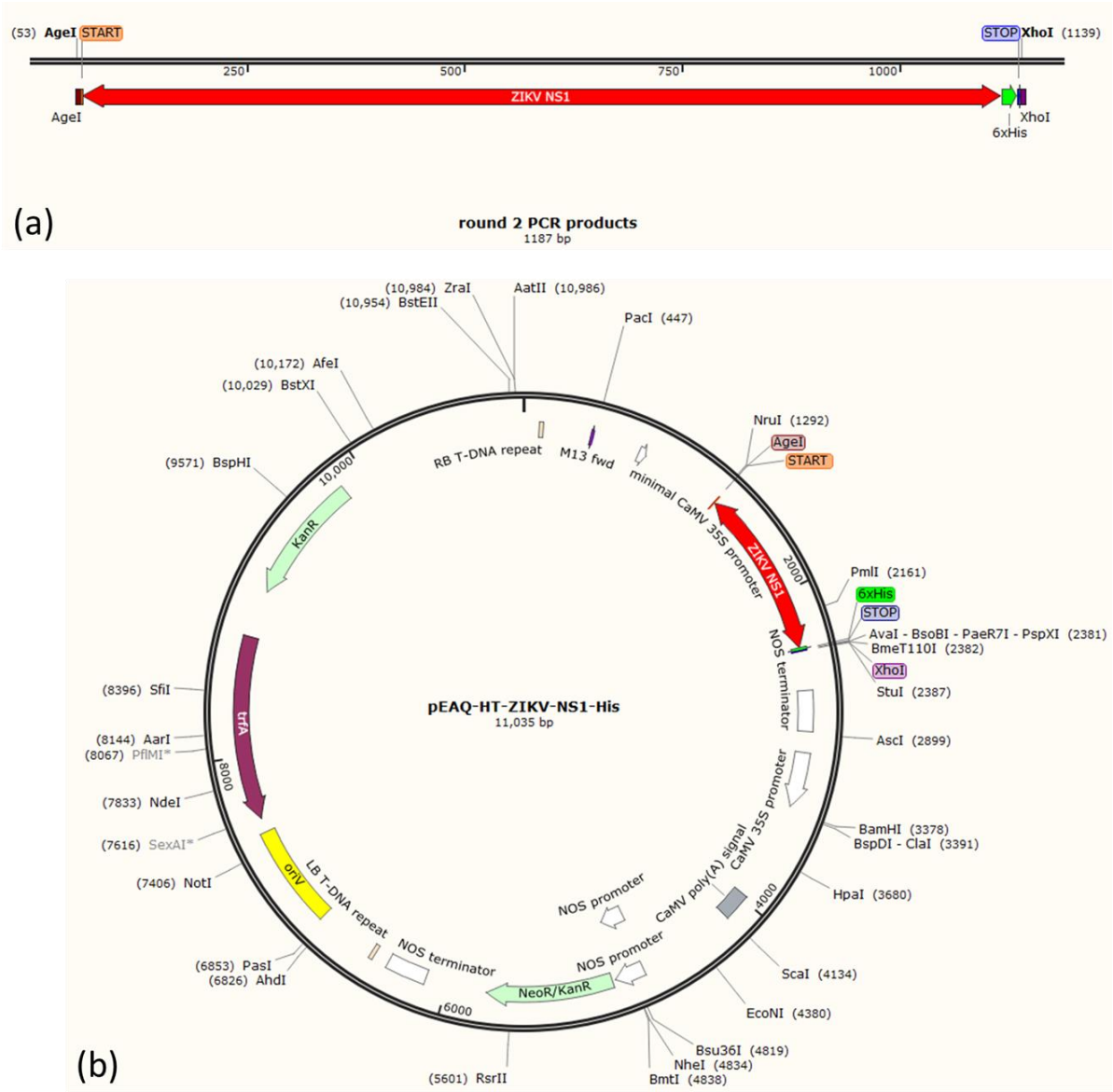


Figure 4. 5 (a) estimated Round 2 PCR products, features including an upstream AgeI restriction site and a downstream Xhol restriction site, ZIKV NS1 sequence followed by a hexa his-tag. (b) Theoretical PCR cloning end product.

4.3.3 Second attempt—Gibson Assembly® Cloning of pEAQ-HT-ZIKV-NS1-His

ZIKV NS1 were also cloned into its plant expression vector pEAQ-HT by Gibson Assembly® Cloning (New England Biolabs). Gibson Assembly is a recently developed cloning technique that allows the cloning of any two fragments without the need for restriction enzyme digestion or compatible restriction sites. The Gibson Assembly mastermix contains exonuclease, DNA polymerase and DNA ligase which allows three different enzymatic activities to occur in a single tube. The exonuclease creates single-stranded 3' overhangs that help the annealing of fragments which have overlap regions. The DNA polymerase fills in gaps within each annealed fragment, and the DNA ligase seals nicks in the assembled DNA.

Forward primer 'MyInsert F1' and reverse primer 'MyInsert R1' were explicitly designed using Gibson Assembly Primer Design Tool (https://tools.sgidna.com/gibson-assembly-primers.html) so that the vector and insert have 20–40 base pair overlapping regions. Amplified ZIKV NS1 was used directly in the next step of cloning without the need for restriction digestion. The vector pEAQ-HT was linearized by restriction enzyme AgeI and purified by NucleoSpin® Gel and PCR Clean-up (MACHEREY-NAGEL). Amplified ZIKV NS1 and purified pEAQ-HT were combined in an equimolar ratio in a final volume of 5 µl in a sterile Eppendorf tube, and 15 µl of Gibson Assembly mastermix was added to the DNAs. After a thorough mix, the tube was centrifuged and incubated at 50 °C for one hour. The final product was transformed into DH5α competent *E.coli* cells, and a schematic illustration is shown in Figure 4. 6.

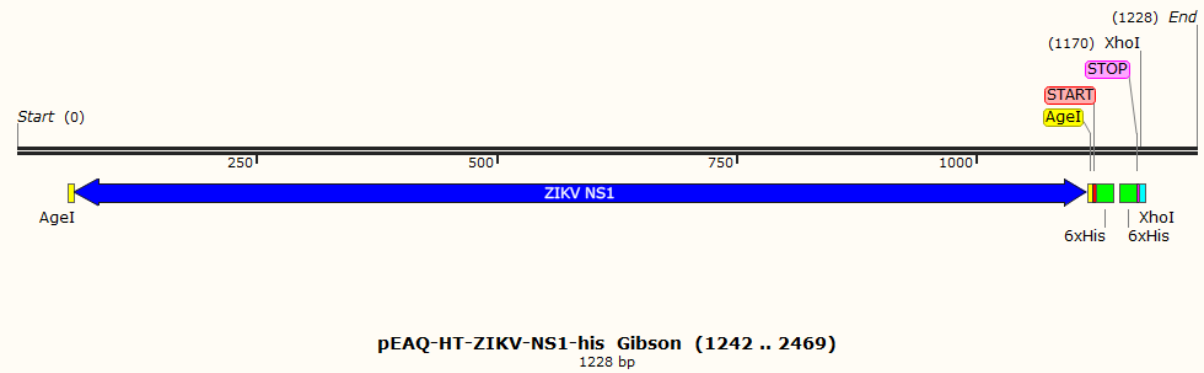


Figure 4. 6 ZIKV NS1 amplified using primers designed for Gibson Assembly® Cloning. It is different from ZIKV NS1 amplified for PCR cloning in two main areas: 1, there are two AgeI restriction sites flanking ZIKV NS1, whereas only one AgeI site was kept in the first attempt; 2, there are two consecutive 6His-tags after ZIKV NS1, whereas there is only one 6 His tag attached to ZIKV NS1 in the previous attempt.

4.3.4 PCR colony screening to confirm successful ligation

GoTaq® DNA polymerase was used for colony PCR. To prepare the colony samples, well isolated colonies from agar plates were individually labelled, picked and transferred to 50 µl of nuclease-free water. For each colony, part of the colony was also transferred to 5 ml LB broth containing 7.5 µl kanamycin. LB cultures were placed in a shaking incubator at 300 rpm, 37˚C for 8 hours. The colony samples in nuclease-free water were boiled for 10 min in a heat block and centrifuged at 16000 g for 5 min. Five microlitres of the supernatant were used as the template in a 25 µl PCR reaction. Insert-specific primers 'ZIKV NS1 forward primer' and 'His tag full reverse' as listed in Table 2 were used as primers for colony screen. The other components in the colony PCR remain the same as shown in Table 3. The annealing temperature was set to 80˚C. PCR products were then analysed on a 1% w/v agarose gel.

4.3.5 Third attempt—ZIKV NS1 expression vector construction by gene synthesis

The ZIKV NS1 gene synthesis was carried out by GenScript, USA (https://www.genscript.com/) with codons optimised for expression in *Nicotiana benthamiana*. The construct was synthesised in the following context: *AgeI* restriction site, Kozak sequence (CGGTGGTACC), signal sequence of tobacco PR1a for pathogenesis-related protein (GenBank: X06930), ZIKV NS1 (GenBank: KX197192.1), hexahistidine sequence for affinity purification, an endoplasmic reticulum (ER) retention signal peptide SEKDEL, a stop codon and *XhoI* restriction site (see Figure 4. 7). The synthesised, codon-optimised ZIKV NS1 gene was cloned into pEAQ-HT by using restriction sites *AgeI/XhoI*, which were then transformed into DH5α competent *E.coli* cells. Finally, the construct was verified by Sanger sequencing.

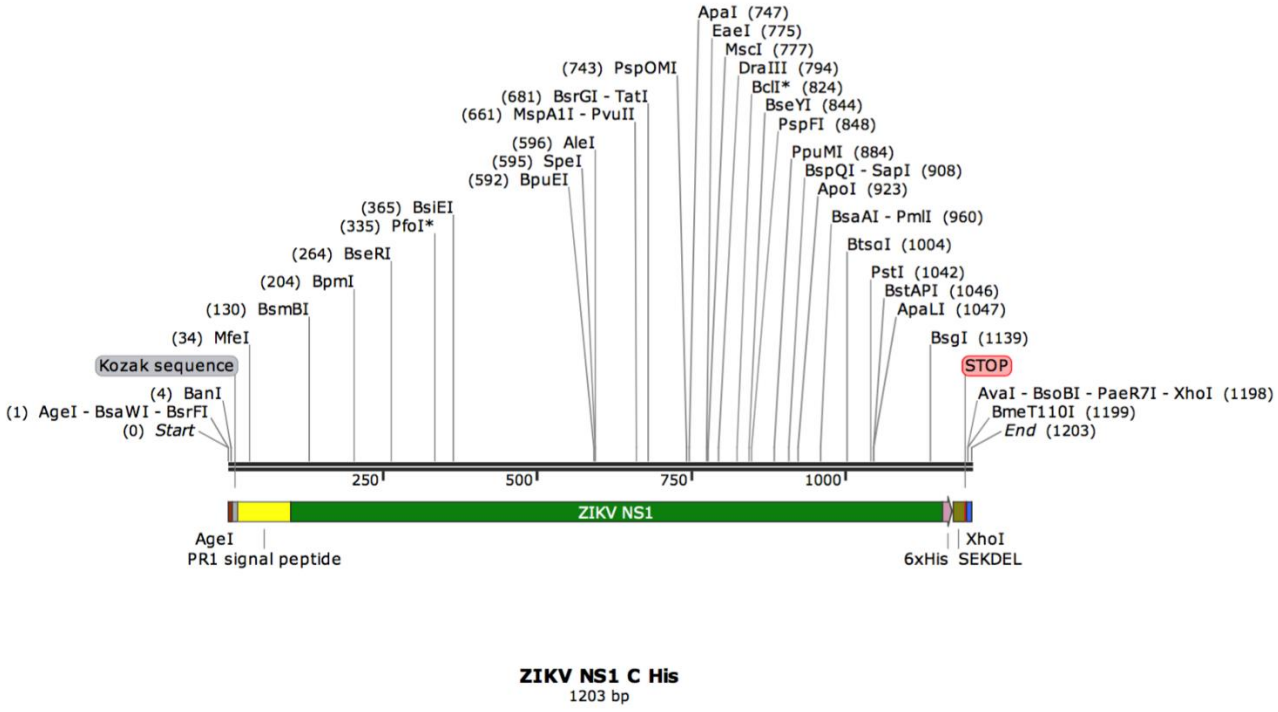


Figure 4. 7 Codon optimised and synthesised ZIKV NS1. N-terminal features include AgeI site, Kozak sequence and PR1a signal peptide. C-terminal features include a 6×His tag SEKDEL sequence and XhoI restriction site.

4.3.6 Transient Expression of ZIKV NS1 proteins in *N.benthamiana*

The author received a brief training of the following procedures, however, the actual work was done by Dr Keith Saunders in the John Innes centre.

4.3.6.1 Preparation of infiltration solution

LBA4404 transformed with pEAQ-HT-ZIKV-NS1-His were grown at 28°C in a shaker until OD600≥1. The infiltration suspension was prepared by checking OD600 of the grown culture and resuspending cells in the required volume of MMA medium to make a solution of OD600=0.4, which was enough to infiltrate the desired amount of plants. The infiltration suspension was incubated at room temperature for 0.5–3 hours.

4.3.6.2 Agroinfiltration

The upper side of the leaf surface was gently nicked in 4–5 places across the whole surface with a sterile needle. Infiltration solution was aspirated into a sterile 1 ml needleless syringe. The syringe was placed over the leaf wound while a finger was placed behind the leaf. The infiltration solution was gently pressed into the intracellular space of the leaf. Three to four leaves were infiltrated per plant.

4.3.6.3 Extraction and purification of ZIKV NS1 protein

Between 6 and 9 days after infiltration, leaves were harvested and weighed. Extraction and purification of ZIKV NS1 protein were carried out in a 4°C cold room. Leaves were transferred to a 1L blender jug, and 3X volumes (g/ml) of extraction buffer was added to the same jug using a measuring cylinder. Leaves were homogenized for 1 min in the blender, and the leaf juice was filtered using mira® cloth and a funnel over a 500ml beaker. Unfiltered leaf matter and used cloth were discarded. The leaf juice was transferred to 250ml centrifuge bottles and centrifuged at 13000g for 20min at 4°C. Next, Ni NTA agarose column (Qiagen) was prepared as follows: a resin/filter was placed into

the tube; 3-4ml Ni NTA agarose was added to the resin, and it was allowed to flow through; 2–3ml of binding buffer was added to the resin, and it was allowed to flow through. All leaf juice was again filtered with sterile EO GF+CA 0.45µm filter and a 50ml sterile syringe. The filtered leaf juice was added to the Ni NTA agarose column. Subsequently, the column was washed once with 25 ml 5mM imidazole wash buffer, once with 25ml 10mM imidazole wash buffer, once with 25ml 20mM imidazole wash buffer and lastly twice with 25ml 30mM imidazole wash buffer. After washing, ZIKV NS1 protein was eluted from the column by adding 1ml elution buffer five times in 5 separate sterile Eppendorf tubes and store at 4°C. Finally, polyacrylamide gel electrophoresis was performed to confirm the existence of the ZIKV NS1 protein.

4.3.7 Testing ZIKV-NS1 based ELISA in detecting antibodies against Zika and Dengue

ZIKV-NS1 based ELISA was performed by a colleague, Anitha Varghese. A total of 40 human serum samples were tested using this ELISA, among which 20 samples were positive for Zika IgG, and 19 samples positive for Dengue IgG and one sample was negative for both Zika and Dengue IgG. They were confirmed by RT-PCR. A 96-well plate (Nunc) was coated with 5µg/ml plant expressed Zika NS1 diluted in carbonate coating buffer (Appendix 1) at a volume of 50µl per well except for negative control wells. The 96-well plate was incubated overnight at 4°C and washed with 200µl PBS-T (0.1%) per well and then blocked with 100µl superblock for an hour at room temperature. Blocking solution was removed and samples, which were diluted 1:100 in Superblock™ buffer was added to the plate at a volume of 50µl per well. Sheep serum was added as a control for the secondary antibody. Serum samples were added in duplicates (see Figure 4. 8). The plate was incubated at room temperature for an hour.

sample	1	2	3	4	5	6	7	8	9	10	11	12
A	no sample, no coating	no sample, no coating	Zika 8	Zika 8	Zika 16	Zika 16	Dengue 4	Dengue 4	Dengue 12	Dengue 12	Dengue 20	Dengue 20
B	Zika 1	Zika 1	Zika 9	Zika 9	Zika 17	Zika 17	Dengue 5	Dengue 5	Dengue 13	Dengue 13	sheep serum	sheep serum
C	Zika 2	Zika 2	Zika 10	Zika 10	Zika 18	Zika 18	Dengue 6	Dengue 6	Dengue 14	Dengue 14	no sample	no sample
D	Zika 3	Zika 3	Zika 11	Zika 11	Zika 19	Zika 19	Dengue 7	Dengue 7	Dengue 15	Dengue 15	no sample	no sample
E	Zika 4	Zika 4	Zika 12	Zika 12	Zika 20	Zika 20	Dengue 8	Dengue 8	Dengue 16	Dengue 16	no sample	no sample
F	Zika 5	Zika 5	Zika 13	Zika 13	Dengue 1	Dengue 1	Dengue 9	Dengue 9	Dengue 17	Dengue 17	no sample	no sample
G	Zika 6	Zika 6	Zika 14	Zika 14	Dengue 2	Dengue 2	Dengue 10	Dengue 10	Dengue 18	Dengue 18	no sample	no sample
H	Zika 7	Zika 7	Zika 15	Zika 15	Dengue 3	Dengue 3	Dengue 11	Dengue 11	Dengue 19	Dengue 19	no sample	no sample

Figure 4. 8 ELISA plate layout.

Following the serum incubation, the plate was washed 4 times with PBS-T (0.1%) buffer at a volume of 100µl, pat dried and secondary antibody (anti-human IgG AP) was diluted in Superblock™ buffer at 1:10,000 dilution and added at 50µl/well volume to all wells. This was left to incubate for an hour at room temperature.

The plate was then washed 4 times with 100µl wash buffer per well and pat dried. pNPP substrate was added at 50µl volume to each well and the plate was read at an absorbance of 405nm at 15 minutes, 25 minutes and final reading was taken at 30 minutes. The visible change was observed within 5 minutes in the wells which had Zika IgG samples.

4.4 Results

4.4.1 PCR cloning of pEAQ-HT-ZIKV-NS1-His

ZIKV RNA (Genbank: KX197192.1) was extracted from cell culture supernatant, followed by reverse transcription PCR for amplification. Primers were designed to construct a C-terminally histidine-tagged ZIKV NS1 with the ability to be inserted into the expression vector pEAQ-HT, i.e. containing the compatible restriction site *AgeI* and *XhoI* in its N-terminus and C-terminus respectively. Adding features including a 6-histidine tag, a stop codon and an *XhoI* restriction site simultaneously would have inevitably made the reverse primer much longer (≥ 60bp) than the forward primer, hence affecting the annealing temperature and the binding of the primers. To overcome that, two sets of primers were designed in which the first set of the forward primer and reverse primer 1 would just add

a 4-histidine tag to the C-terminus of ZIKV NS1 and the second set of the forward primer and reverse primer 2 would add the remaining features. Gradient PCRs were performed to discover the best annealing temperature. From the first gradient PCR, it was found that the best annealing temperature was at 70°C which did not show any primer-dimer in the gel electrophoresis analysis (see Figure 4. 9). PCR products from the first gradient PCR were used as templates in the second gradient PCR. Gel electrophoresis images from both gradient PCRs showed that the end products had a size of approximately 1 Kb, which was as expected. The optimal temperature for the second gradient PCR was around 80°C (see Figure 4. 10). Bands in the agarose gel from the second gradient PCR were cut and purified. Subsequently, the histidine-tagged ZIKV NS1 was restriction digested, purified and ligated to the vector pEAQ-HT.

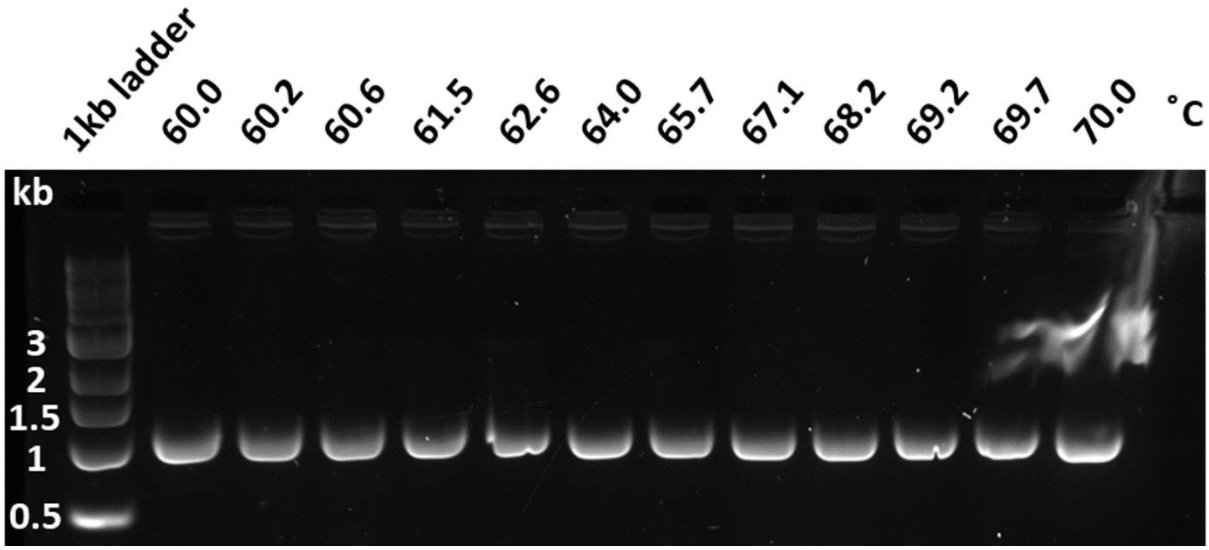


Figure 4. 9 Gradient PCR using ZIKV NS1 forward primer and 'His tag Rev 1' reverse primer for adding the first four histidine tags to C-terminus of ZIKV NS1 sequence

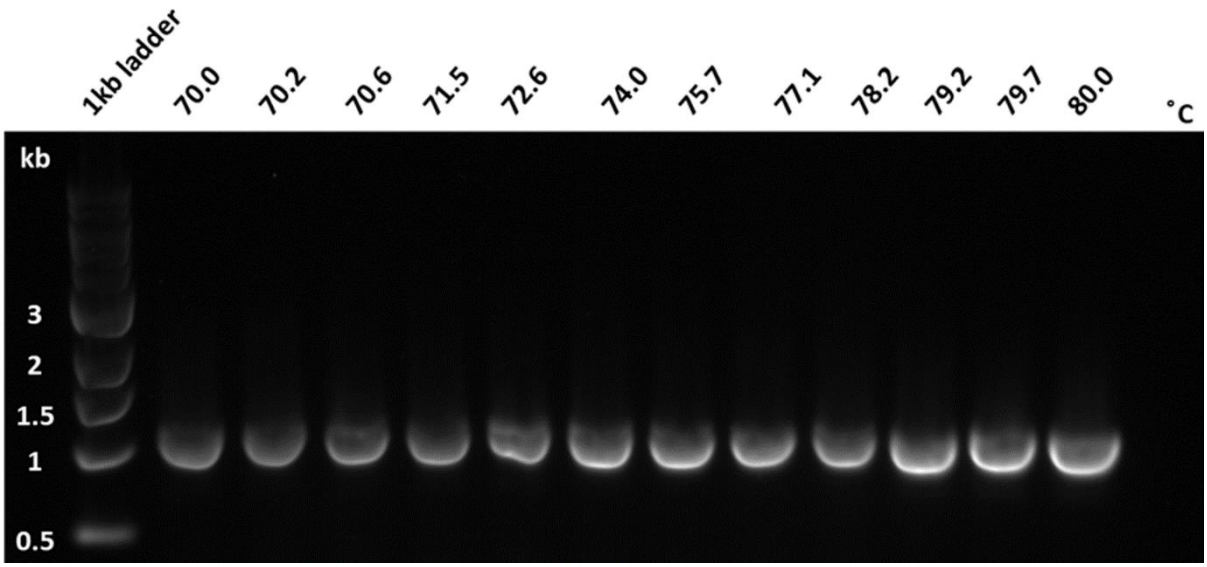


Figure 4. 10 Gradient PCR using ZIKV NS1 forward primer and 'His tag Rev 2' reverse primer for adding the remaining two histidine tags, a stop codon and restriction site XhoI to the C-terminus of ZIKV NS1 sequence. Templates used in this gradient PCR were PCR products from previous gradient PCR.

The ligated plasmids were transformed into DH5α competent cells. Colonies after antibiotic selection were picked, boiled and subjected to colony PCR screening. Two sets of forward and reverse primers were used. Results showed that all colonies contained ZIKV NS1, and the ligation was successful (see Figure 4. 11). The constructed pEAQ-HT-ZIKV-NS1-His plasmids were Sanger sequenced and sent to John Innes Centre (Norwich) to be transformed into Agrobacterium LBA4404 by Dr Keith Sanders.

The production, extraction and purification of ZIKV NS1 were carried out in parallel with Schmallenberg virus (SBV) nucleocapsid (N) protein as a positive control. SBV N protein has previously successfully expressed by *N.benthamiana*. SDS gel electrophoresis results showed that the ZIKV NS1 protein had not been expressed by the plants when compared with SBV N results in which case a single band with the correct size (~26 kDa) were observed in each elution sample 2—5 (see Figure 4. 12).

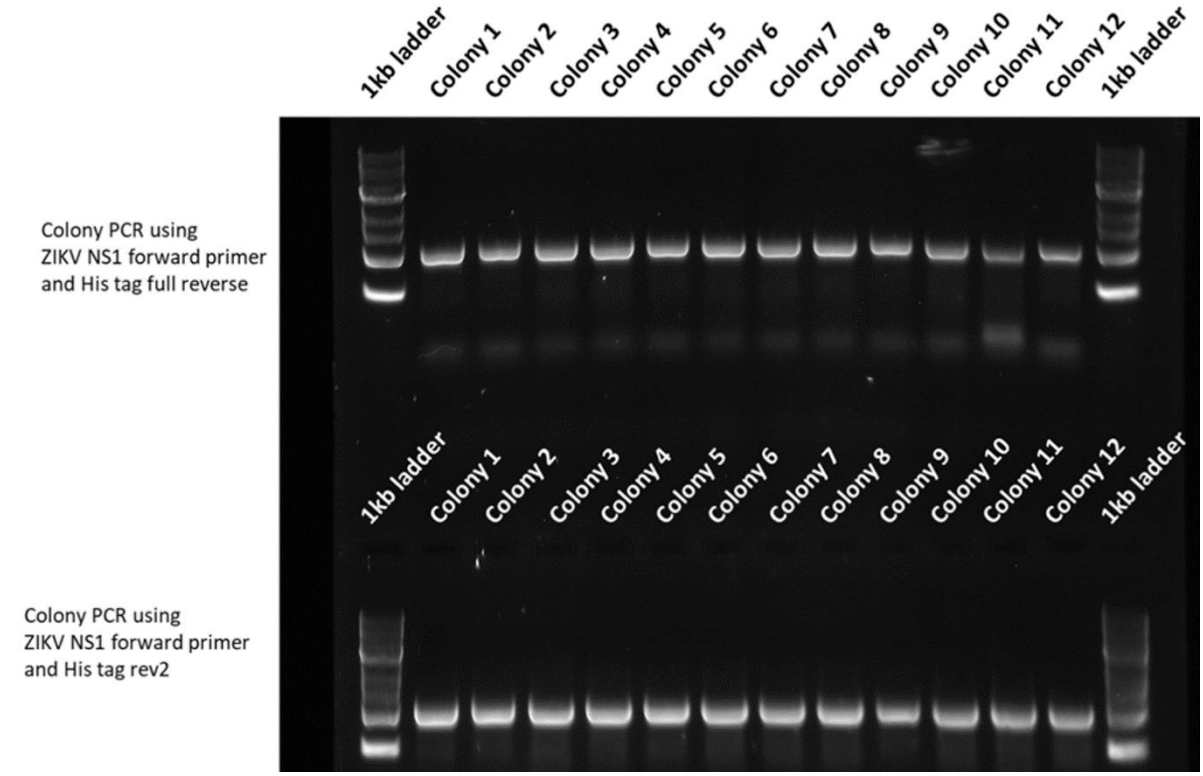


Figure 4. 11 Colony PCR using two sets of primers both confirmed the successful ligation of the vector pEAQ-HT and the insert ZIKV NS1.

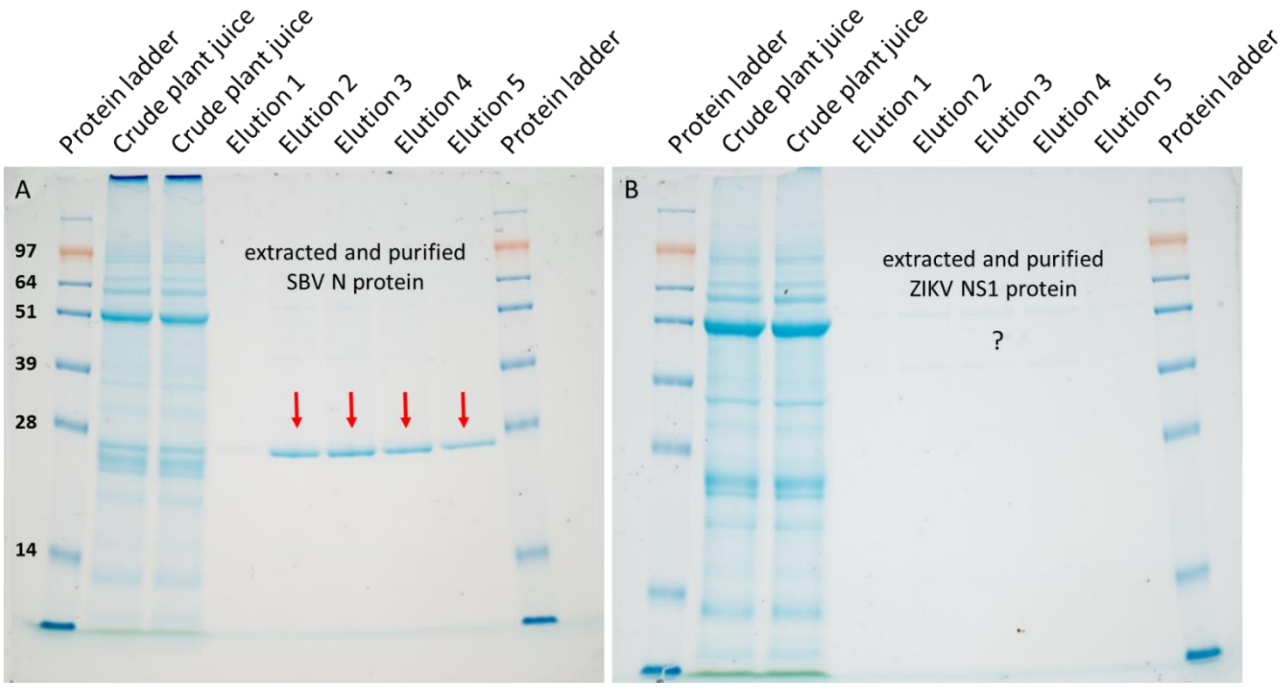


Figure 4. 12 SDS gel electrophoresis confirmed that there were no ZIKV NS1 expressed by the plants N.benthamiana.

4.4.2 Gibson Assembly cloning of pEAQ-HT-ZIKV-NS1-His

Gradient PCR using 'MyInsert F1' and 'MyInsert R1' primers not only amplified ZIKV NS1 but also added pEAQ-HT overlapping regions to ZIKV NS1 in its N and C-terminus. Because pEAQ-HT plasmid already had features including an *AgeI* restriction site, a start codon, two consecutive 6-his tags, a stop codon and *XhoI* restriction site in its multiple cloning site, it is exceptionally convenient to insert ZIKV NS1 into the vector using this method. Figure 4. 13 showed the optimal annealing temperature for using 'MyInsert F1' and 'MyInsert R1' primers was at 80°C. After gel purification, ZIKV NS1 was ready for Gibson Assembly.

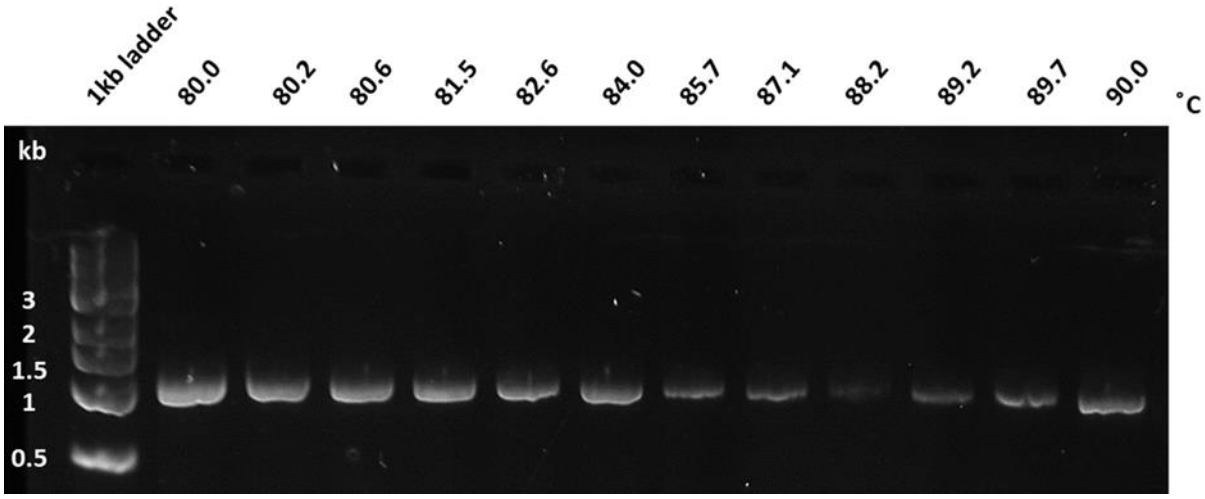


Figure 4. 13 Gradient PCR for amplification of ZIKV NS1 for Gibson Assembly cloning using specifically design ed primers 'MyInsert F1' and 'MyInsert R1'.

The success of Gibson Assembly was confirmed by colony PCR (see Figure 4. 14). Size of bands showing up in the gel electrophoresis was around 1000—1200 bp which was as expected. The final product was sent for Sanger sequencing. Sequencing results were then subject to protein translation using a translate tool (ExPASy, Switzerland) (https://web.expasy.org/translate/) to confirm that ZIKV NS1 sequence was in the open reading frame (see Figure 4. 15).

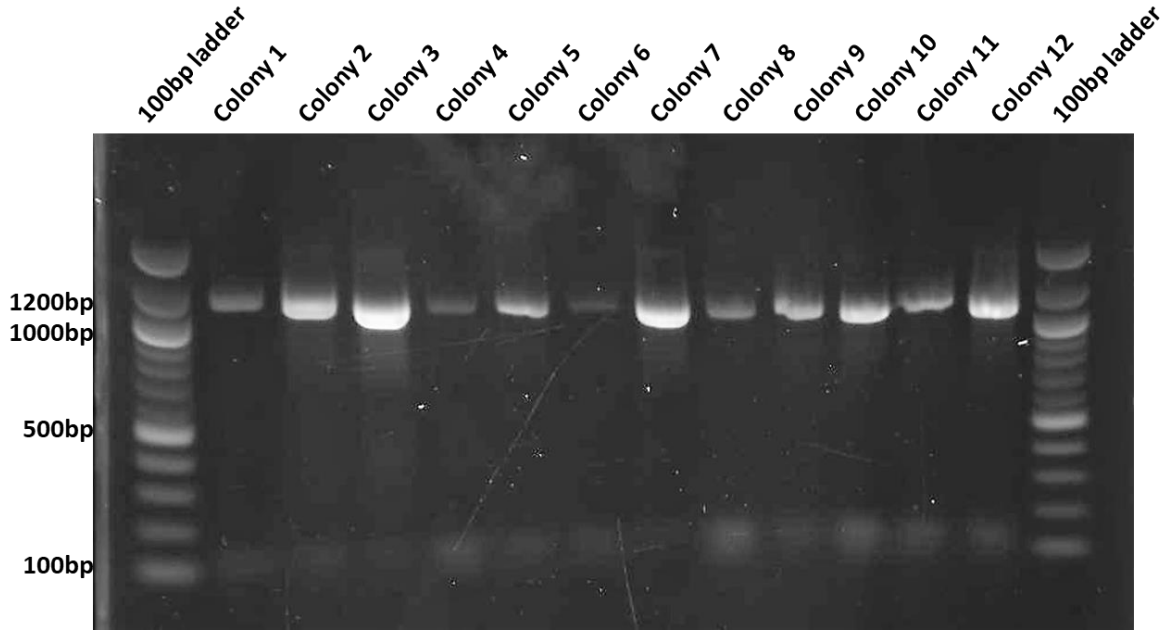


Figure 4. 14 Colony PCR for confirmation of Gibson Assembly. Various brightnesses of the bands may be due to different sizes of the colony when picking, and they were subsequently amplified in different degrees.



Figure 4. 15 Insert check. A. Sanger sequencing results were translated using ExPASy. B. sequences from pEAQ-HT were in Bold. ZIKV NS1 sequence was underlined. Restriction sites AgeI and Xhol were in italic.

Eventually, the constructed pEAQ-HT-ZIKV-NS1-His using Gibson Assembly was sent to John Innes centre for expression in plants. Again, SBV N protein was used as a positive control throughout the expression process. However, gel electrophoresis results were inclusive. There was not a strong band between 39—51 KDa, whereas a clear band was observed in SBV N samples just below 28 KDa (see Figure 4.16).

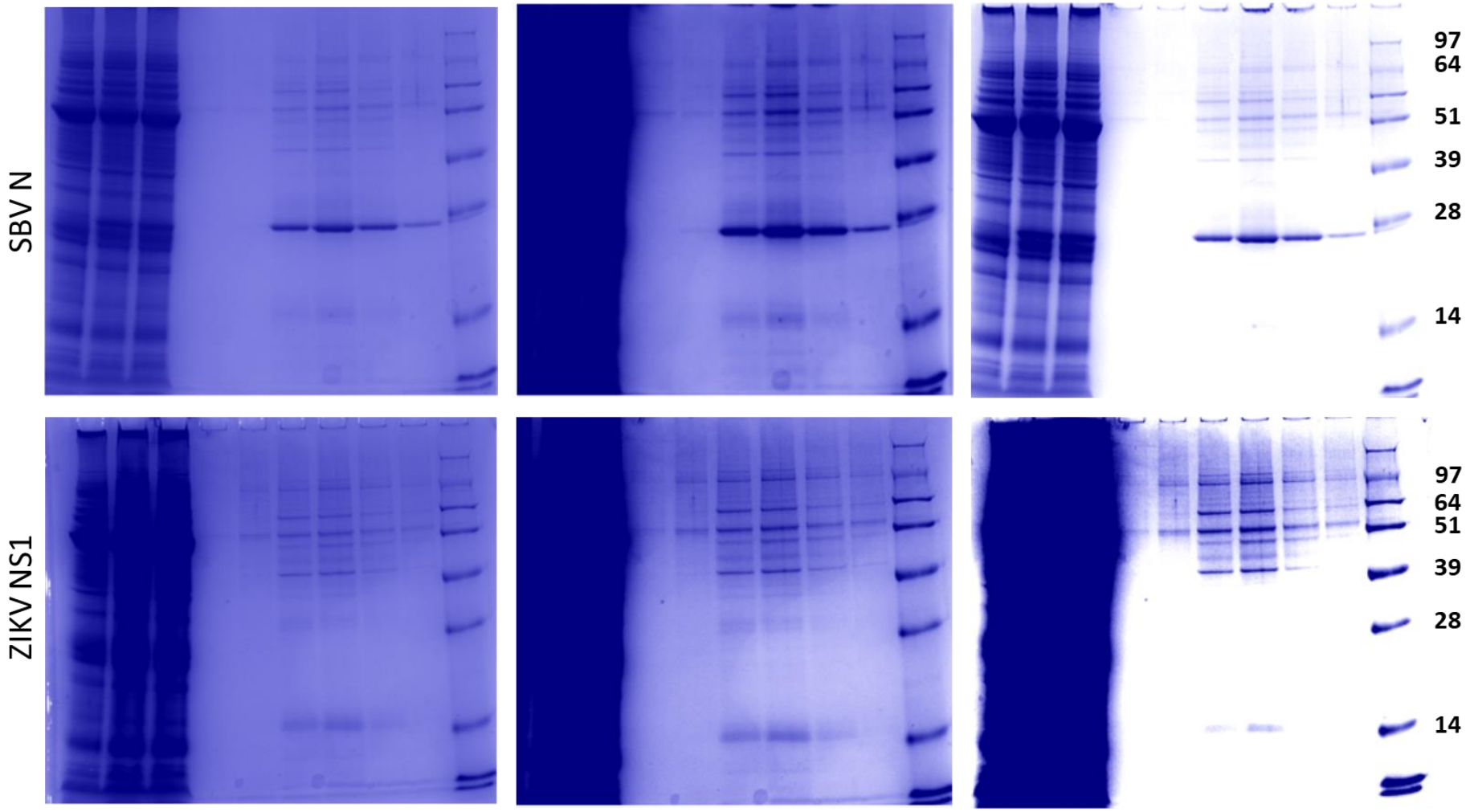


Figure 4. 16 SDS gel electrophoresis performed to check ZIKV NS1 and SBV N proteins expression by plants. A clear band just below 28 KDa was observed in SBV N elution samples after extraction and purification; however, no strong band around the expected size was observed in ZIKV NS1 elution samples.

4.4.3 ZIKV NS1 expression by gene synthesis

Synthesized and optimised ZIKV NS1 was originally in pU57 vector. It was cloned into the pEAQ-HT vector by restriction sites *AgeI* and *XhoI*, and the constructed pEAQ-HT-ZIKV-NS1-C-His was sent for Sanger sequencing prior plant expression. Sanger sequencing results confirmed it was as expected, and the ZIKV NS1 sequence was in the open reading frame for translation (see Figure 4. 17).

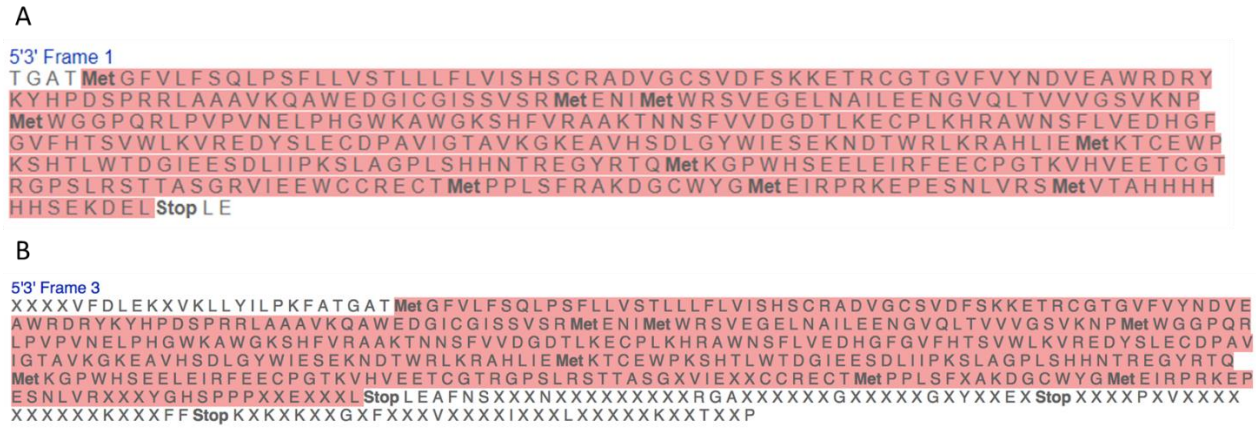


Figure 4. 17 A. Protein translation of synthesised and optimised ZIKV NS1 sequence. B. Protein translation of Sanger sequencing results of pEAQ-HT-ZIKV-NS1-C-His using primers BK79 and BK80.

The plasmid pEAQ-HT-ZIKV-NS1-C-His was transformed into agrobacterium LBA4404 and expressed by plants. Extraction and purification processes of ZIKV NS1 were also the same as the previous two attempts. SDS gel electrophoresis results showed a clear band around 28 KDa for SBV N protein, and a strong band between 38—51 KDa in the ZIKV NS1 gel was also observed this time (see Figure 4. 18), which had never been observed from previous two attempts (see Figure 4. 19). Further western blot experiments are required to confirm the existence of ZIKV NS1.

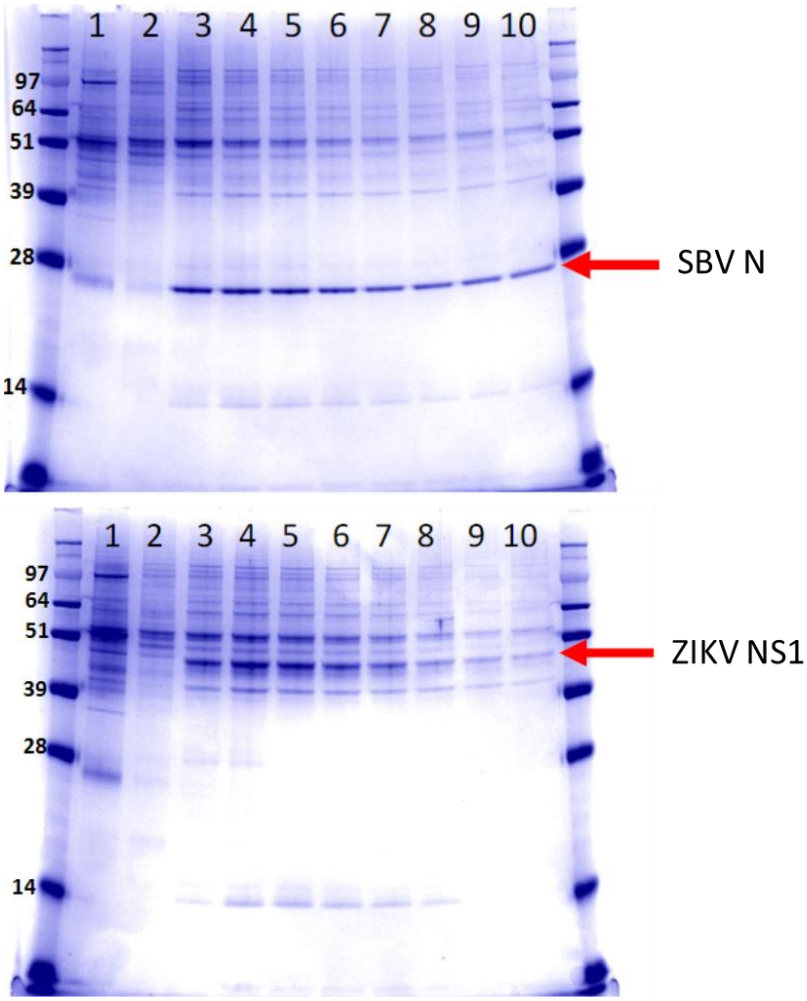


Figure 4. 18 SDS gel electrophoresis performed to check ZIKV NS1 proteins expression by plants. SBV N protein expression was used as positive control. A band just below 28 kDa was seen in the SBV N extraction gel. And a band between 39—51 kDa was seen in the ZIKV NS1 extraction gel.

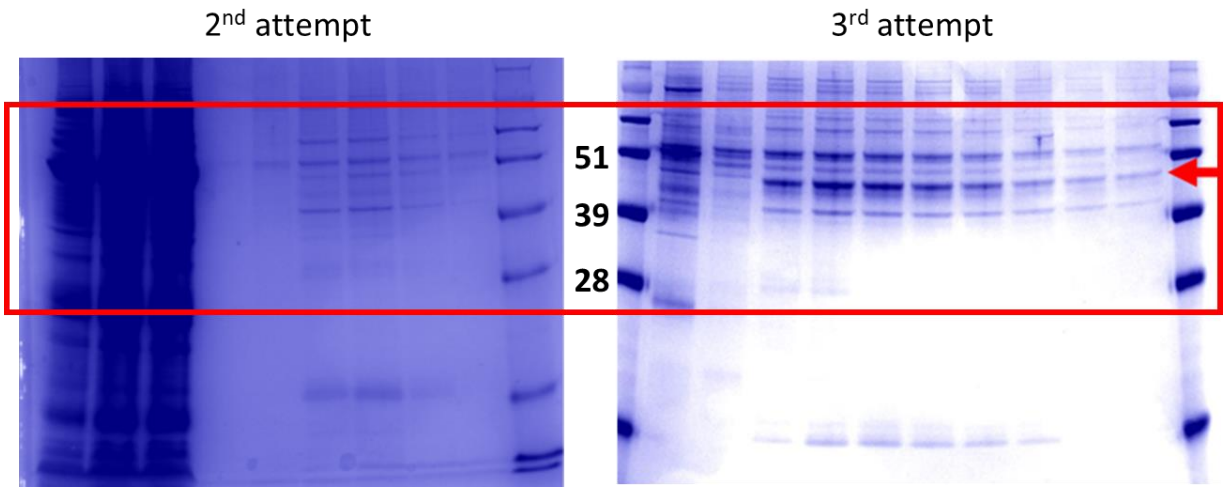


Figure 4. 19 Comparisons of ZIKV NS1 plant expression between second and third attempt. The bands between 39—51 kDa were not seen in the first two attempts.

4.4.4 ZIKV NS1-based ELISA performance

It was determined to use 3X mean OD of negative control as the cut-off value for this ELISA (Lardeux et al., 2016), which was calculated as 0.9. Based on the determined cut-off value and formula (sensitivity=number of true positives/(number of true positives + number of false-negative), specificity=number of true negatives/(number of true negatives + number of false positives)), the sensitivity and specificity of this plant expressed ZIKV-NS1 based ELISA were calculated as 95% (19/20) and 95% (19/20) respectively.

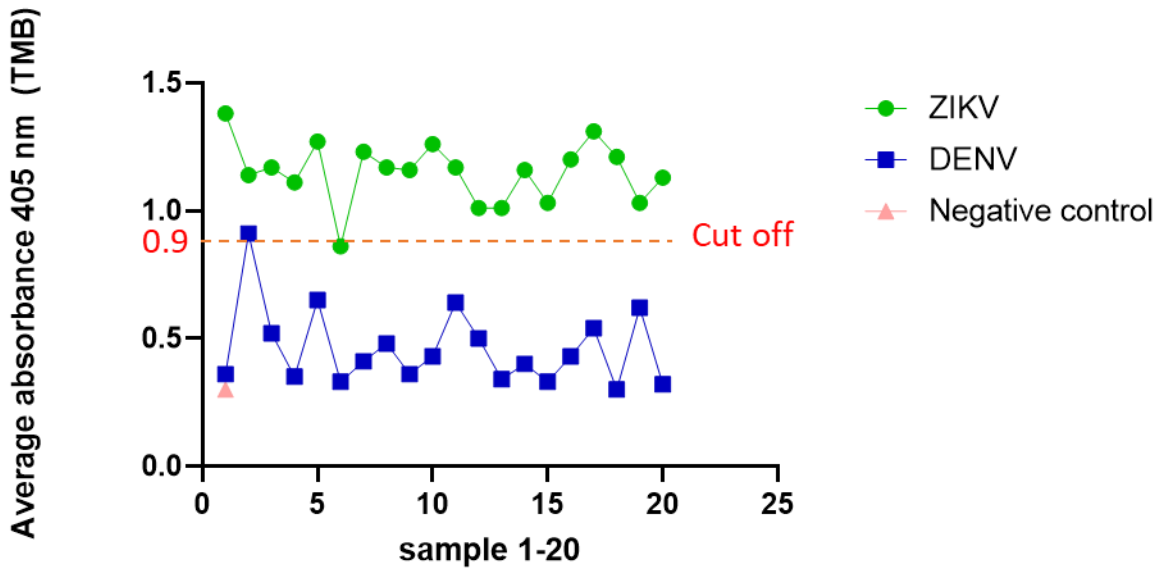


Figure 4. 20 Average absorbance reading at 30 min post substrate addition. Green: ZIKV samples; Blue: Dengue samples; pink: negative controls. Sensitivity (95%) and specificity (95%) of this ELISA were calculated based on a cut-off value of 0.9.

4.5 Discussion

The objective of this project was to express ZIKV NS1 protein in plants using a recently developed plant expression vector pEAQ-HT.

4.5.1 First and second attempt

The first two attempts to clone the ZIKV NS1 sequence into the vector pEAQ-HT were very similar in terms of methods and results. Firstly, they both used wild-type ZIKV NS1 sequence (i.e. not codon-optimised) as the insert. Secondly, they both used traditional PCRs to add required features. In the first attempt, start/stop codons, AgeI/XhoI restriction sites, and 6-his tags were added. In the second attempt, overlapping sequences with the vector were added to the C- and N-terminus of ZIKV NS1 sequence for subsequent cloning. Thirdly, SDS gel electrophoresis results showed that plants clearly did not produce any ZIKV NS1 proteins in the first attempt and gel electrophoresis results from the second attempt were inconclusive where the bands were too weak to be convincing.

After the first attempt clearly failed, a retrospective check by ExPASy found out that the constructed and sequenced pEAQ-HT-ZIKV-NS1-His sequence was not in-frame with an open reading frame (ORF) which meant that the ZIKV NS1 protein could not possibly have been translated and expressed properly. This ORF check should have been done before sending the constructed plasmid to be transformed in LBA4404 and infiltrated into plants for expression. As a lesson learnt, this step was not missed in the second and third attempt. If the second and third attempt were not possible, to make initial amendments based on the first attempt, site-directed mutagenesis could be performed to make nucleotides shift to ensure the ZIKV NS1 sequence was in-frame, although this still may not guarantee the successful expression of ZIKV NS1.

4.5.2 Third attempt

A few more aspects were taken into consideration in the third attempt when making the pEAQ-HT-ZIKV-NS1-C-His expression construct, which were absent in the first two attempts.

4.5.2.1 Codon optimisation

The ZIKV NS1 sequence was codon-optimised for *N. benthamiana*. Nonetheless, whether codon-optimisation plays a vital role in the expression of ZIKB NS1 protein in plants is not entirely known. Successful viral protein expression in plants is reported with and without codon-optimisation. On the one hand, the haemagglutinin (HA) gene of a low pathogenic avian influenza virus of the H7N7 subtype was synthesised, and codon-optimised for Nicotiana tabacum, a close relative of *N. benthamiana*, and its successful expression in *N. benthamiana* was confirmed by SDS-PAGE and western blotting (Kanagarajan et al., 2012).

On the other hand, there are cases of successful plant expression without codon-optimisation for plants. Baculovirus codon-optimized SBV N gene was successfully expressed in *N. benthamiana* (Schellenberg, 2013). Native influenza neuraminidase type1 (NA1) gene sequence was cloned into a pEAQ-HT vector and also successfully expressed in plants (Pua et al., 2017).

4.5.2.2 Kozak sequence

A Kozak (GCCACCATGG) sequence was added upstream of the ZIKV NS1 sequence, which enhances the efficiency of translation initiation (Nakagawa et al., 2008). In addition, Kanagarajan et al. (2012) used the Kozak sequence (GCC ACC) preferred by dicotyledonous plants to express influenza HA protein in plants (Nakagawa et al., 2008).

4.5.2.3 Pathogenesis-related protein 1a (PR 1a)

Ross (1961) reported that by infection with tobacco mosaic virus (TMV) which causes the formation of necrotic lesions, or by treatment with resistance-inducing compounds, e.g. salicylic acid (SA), Nicotiana tabacum acquired resistance to subsequent infection by TMV or many other bacterial and fungal pathogens. This phenomenon was termed systemic acquired resistance (SAR). During the onset of SAR, nine classes of the SAR mRNAs were induced at various levels (Uknes et al., 1993). These gene families include the pathogenesis-related proteins PR-1 (PR-1a, PR-1b, and PR-1c), PR-2 (PR-2a, PR-2b, and PR-2c), PR-3 (PR-3a and PR-3b), PR-4 (PR-4a and PR-4b), and PR-5 (PR-5a and PR-5b), as well as the basic form of PR-1, the acidic and basic forms of class III chitinase, and extracellular β-1,3-glucanase, PR-Q' (Ward et al., 1991). PR-1 consists of a family of three extremely homologous 14-KDa proteins which are acid-soluble, resistant to protease and secreted extracellularly (Uknes et al., 1993). They are among the most produced proteins in response to TMV infection which have been reported to make up approximately 2% of the total leaf protein in infected tobacco (Breen et al., 2017). The plant signalling pathways governing PR-1 gene regulation during SAR are well studied (Rivière et al., 2008).

It was previously shown that a plant ER signal peptide from the soybean gene vspA (VSPαS) or an ER retention signal (KDEL) affected hepatitis B surface antigen (HBsAg) accumulation in transgenic potato (Richter et al., 2000). Moreover, the haemagglutinin (HA) of an HPAI H5N1 was expressed in *N. benthamiana* with the incorporation of PR-1a signal peptide sequence at the N-terminus, and the addition of ER retention signal peptide (KDEL) at the C-terminus of the HA gene (Pua et al., 2017). In addition, it was evident in other systems that the host signal peptide works more efficiently than a transgene's native signal peptide (Tessier et al., 1991). Considering the membrane-associated homodimer form and secreted hexamer form of ZIKV NS1, it was therefore decided to use the signal peptide of PR-1a instead of the original peptide signal of ZIKV NS1 to maximise its accumulation in the ER/expression in plants.

4.5.2.4 SEKDEL sequence

Proteins containing an ER retention signal (H/KDEL) at the C-terminus are retrieved to the ER via KDEL receptor (KDELR) which constitutively cycle between the ER and the Golgi complex (Cole et al., 1998). SEKDEL has been shown to be a hexapeptide ER retention signal (Richter et al., 2000). In Sojikul et al. (2003)'s study, the peptide signal from soybean VSPαS indeed enhanced HBsAg accumulation in transgenic plant system (NT-1 cells), however, they also showed that the addition of SEKDEL to HBsAg had no enhancing effects on HBsAg accumulation in NT-1 cells which was inconsistent with their previous findings. Previous results from the same group showed SEKDEL enhanced the accumulation of HBsAg in potato plants. This inconsistency may be due to the differences in the cellular sorting machinery in potato leaf and NT-1 cells. Although ZIKV NS1 was expressed in *N. benthamiana*, in this study, the functional importance of SEKDEL can not be proven due to the co-existence of other factors such as PR-1a.

4.5.3 Validation of an ELISA assay

Despite the expression of ZIKV NS1 in plants and performing an analytical test with 40 patient sera, the fitness of this plant-based NS1 ELISA has not entirely been determined. According to the World Organisation for Animal Health (OIE, 2019), a validated assay has to have completed three stages: 1) analytical performance characteristics; 2) diagnostic performance; 3) reproducibility and augmented repeatability estimates. In the future, there is still much work to do in terms of validating this plant-based NS1 ELISA, starting from optimising and standardising the assay. Also, at least three laboratories should test the same group of samples comprising no less than 20 samples, with the same aliquots going to each laboratory (OIE, 2019).

Chapter 5 Identification of clade-specific antibodies against Equine Influenza Virus (EIV) using Next Generation Phage Display (NGPD)

5.1 Introduction

5.1.1 Equine Influenza Virus (EIV)

Equine influenza (EI) is a leading cause of respiratory diseases in the horse. Equine influenza virus (EIV) is highly contagious and is transmitted by direct contact and inhalation of aerosols. Historically, outbreaks of EIV have occurred worldwide affecting many countries and brought a substantial adverse impact on the global economy (Sack. A., 2019). Being a re-emergent virus, an outbreak of EIV started in January 2019 in the west midlands of UK. At the time of writing (June 2019), a total of 133 EI cases have been reported (Animal Health Trust, 2019). Clinical manifestations of EI include fever, loss of appetite, weakness, dry cough, muscle soreness and enlarged lymph nodes. EIV can be transmitted across different species; other susceptible species include dogs (Daly et al., 2008), pigs (Tu et al., 2009) and humans (Xie et al., 2016). Although EIV has not been successfully isolated from human specimens (only serological evidence exists of human infection with equine influenza), it remains a potential risk to people with a high level of exposure to EIV (Xie et al., 2016).

EIV belongs to the family of *Orthomyxoviridae* and genus *Influenzavirus A*, which is a group of viruses with negative-sense, single-stranded, and segmented RNA genomes (Bryant et al., 2011). Influenza A virus has 8 separate RNA segments encoding at least 10 proteins: PB2 (polymerase basic 2); PB1 (polymerase basic 1) encoding PB1, PA (polymerase acid); HA (haemagglutinin); NP (nucleoprotein); NA (neuraminidase); M encoding M1 (the matrix proteins) and M2 (ion channel proteins); and NS encoding NS1 (nonstructural protein 1) and NEP/NS2 (nuclear export protein/ nonstructural protein 2). HA, NA and M2 are envelope glycoproteins situated in the host-cell-derived lipid envelope.

M1 lies beneath the envelope, and the core of the virus particle is composed of the ribonucleoprotein (RNP) complex which consists of the viral RNA segments, PB1, PB2, PA and NP, in which the viral RNA is coated with NPs and PB1, PB2 and PA form a polymerase complex (see Figure 5. 1) (Shaw and Palese, 2013).

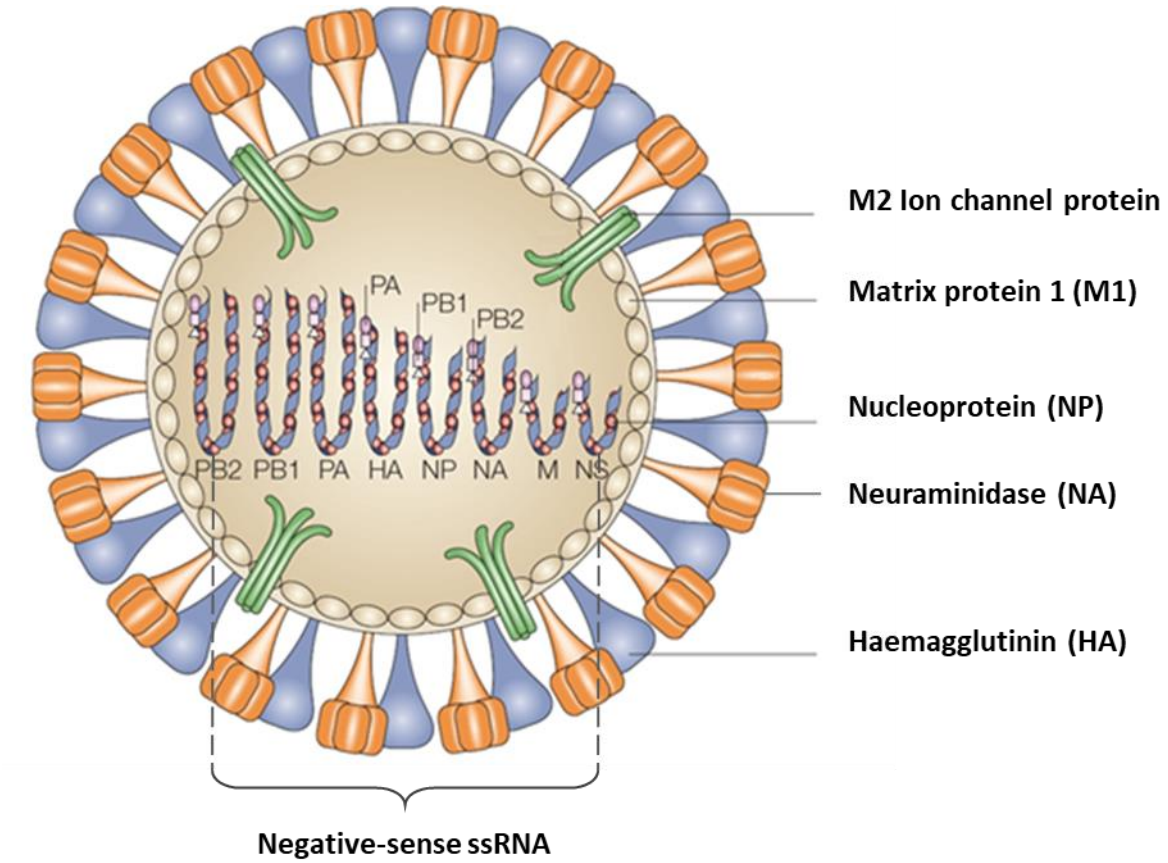


Figure 5. 1 Structure of influenza A virus (Adapted from (Clancy, 2008)). Influenza A virus has 8 RNA segments: PB2, PB1, PA, HA, NP, NA, M and NS.

EIV has two main subtypes: H7N7 (subtype 1) and H3N8 (subtype 2). H7N7 was first recovered in Europe in 1956. However, it has not been isolated from horses since 1979. H3N8 was first isolated in the USA in 1963; it has continued to circulate in equines to this day. Due to antigenic drift, H3N8 evolved into two lineages, Eurasian and American. Subsequently, American lineage emerged into three sub-lineages: Argentinian, Kentucky, and Florida. Furthermore, the evolution of the Florida sub-lineage has resulted in the emergence of two groups of viruses with divergent HA sequences: Florida sub-lineage clades 1 and clade 2 viruses. Right now, Clade 1 and Clade 2 lineage viruses have been

circulating across the globe and causing outbreaks. Clade 1 viruses have been circulating more in the American continent while Clade 2 viruses have been responsible for most of the outbreaks in Europe and Asia (see Figure 5.2).

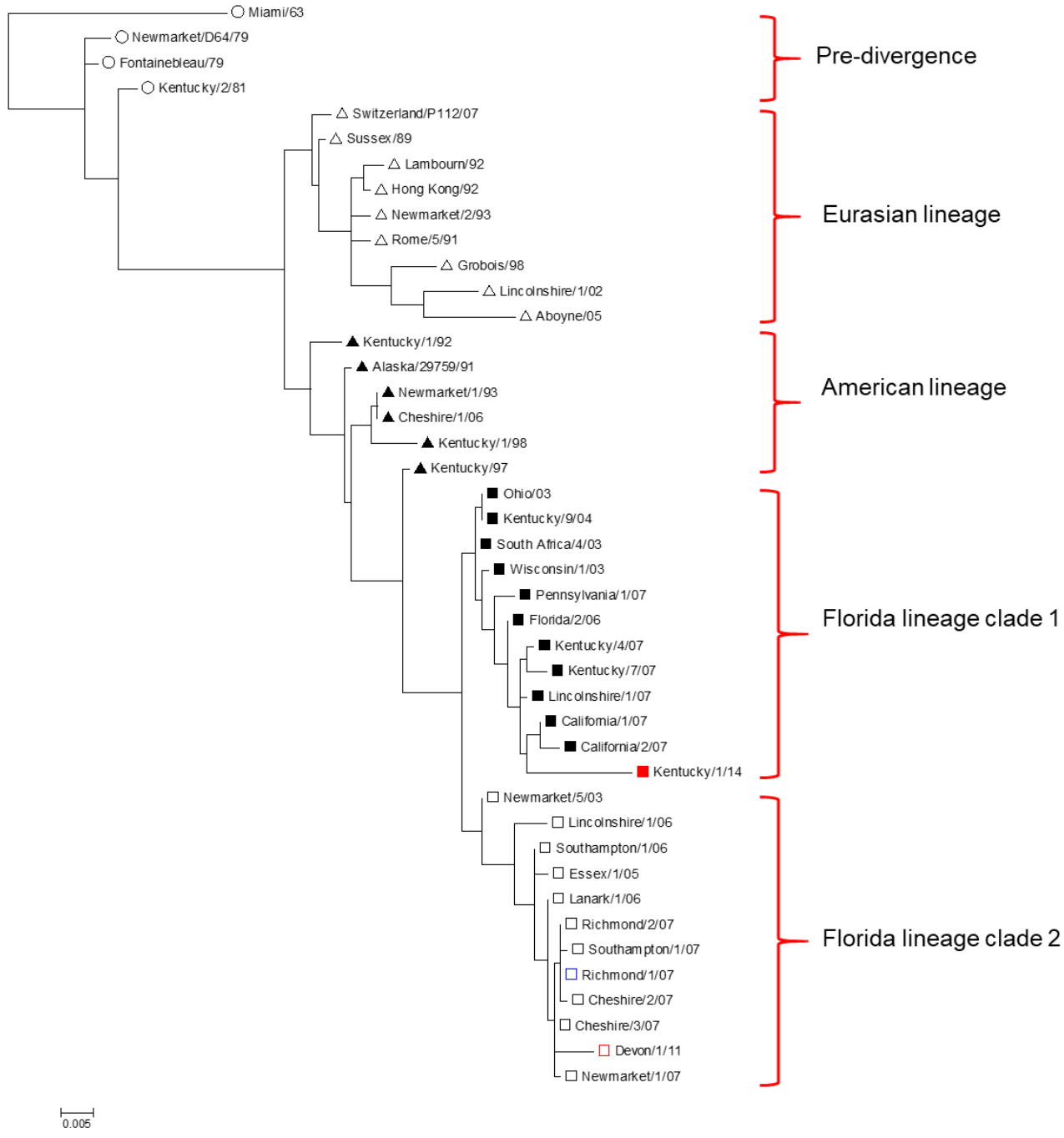


Figure 5. 2 Molecular Phylogenetic analysis by Maximum Likelihood method. The analysis involved 43 nucleotide sequences. Evolutionary analyses were conducted in MEGA7. Kentucky/1/14 is used as a representative of Florida lineage clade 1 EIV in this study, Devon/1/11 represents Florida lineage clade 2 EIV and Richmond/1/07 is used as the backbone of the recombinant EIVs (see Figure 5. 11)

Furthermore, serological tests have remained an essential tool in EI diagnosis and surveillance. Paired-samples collected 10 to 21 days apart must be tested to obtain acute and convalescent titres. Seroconversion, which is defined by at least 4-fold increase in antibody titres between the acute and convalescent sample, must be present to confirm acute infection. Commonly used assays include haemagglutination inhibition (HI), single radial haemolysis (SRH) and ELISA. HI can also be used to characterise different virus isolates using specific antisera (Landolt, 2014). Antigenic matching, a process which compares the antigenic similarity between a given stain, e.g. a vaccine strain, and a circulating strain, is typically performed by raising antisera in animal models, such as ferrets and chicken, and subsequently comparing antibody-antigen reactivity titres of the given strain and the circulating field virus. HI has been regarded as the gold standard for measuring variations among human seasonal influenza virus for many decades (Thi Nguyen et al., 2018). Phage display technology, capable of producing binders, provides an opportunity to produce strain-specific affinity reagents more rapidly and avoid the need to immunise animals.

5.1.2 Phage display

5.1.2.1 Filamentous phage

Filamentous phage are a family of bacteria viruses that infect various Gram-negative bacteria including *Escherichia coli*, *Pseudomonas* and *Salmonella*. They are best characterised by a circular, single-strand DNA encased in a long, slender and flexible tube made up of thousands of copies of a single major coat protein and a few minor proteins at both tips (see Figure 5. 3) (Clackson and Lowman, 2004).

The Ff class of viruses, including M13, fd, and f1, are most studied and used for phage display. They are named after their host cell entry method, which is via the tip of the F conjugative pilus on the surface of male *E. coli*. Ff phages share over 98% genome identity, and their gene products are interchangeable, hence are often referred to collectively.

Furthermore, the production and secretion of Ff phage from infected bacteria do not cause cell lysis. Instead, infected bacteria will keep growing and dividing but at a significantly reduced rate (30—50% of uninfected cells). And the parasitic phage will be produced approximately 200—2000 progeny per cell per doubling time (Sidhu and Geyer, 2015).

The Ff phage genome encodes 11 proteins in total, five of which are structural proteins: pIII, pVI, pVII, pVIII and pIX (see Figure 5. 3). All of the structural proteins are inserted into the inner host cell membrane prior to assembly. pIII and pVIII are synthesized with N-terminal signal sequences that are removed after their insertion into the host cell membrane, whereas, pVI, pVII and pIX are synthesized without signal sequences. Three non-structural proteins pI, pXI and pIV, are morphogenetic proteins required for viral assembly. pII and pX are required in the phage DNA replication processes. pV is an ssDNA binding protein which has the function of sequestering the intercellular ssDNA viral genome and modulating the translation of gene II mRNA.

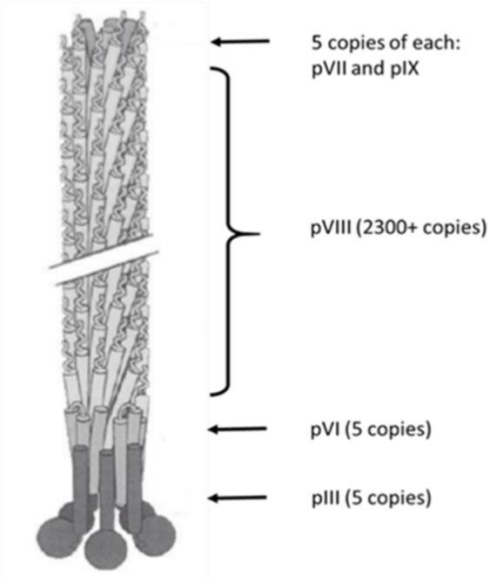


Figure 5. 3 Ff phage structure (Adapted from (Sidhu and Geyer, 2015)).

Viral assembly starts at the distal end (top of the diagram) of the particle and infection starts at the proximal end (bottom of the diagram) of the particle by 5 copies of pIII.

Although all five coat proteins have been used in displaying proteins or peptides to various degrees, the minor coat protein pIII and the major coat protein pVIII are by far the most commonly used for phage display. The typical location to display a 'guest' peptide using pVIII is at the N-terminal end between the signal sequence and the beginning of the mature protein-coding sequence. However, only short sequences can be displayed on every copy of pVIII because larger sizes prevent the phage packaging.

pIII is more tolerant than pVIII to large insertions, however, the infectivity of the resulting phage can be reduced dramatically. As with pVIII, this can be overcome by using phagemid constructs, resulting in the production of hybrid virions that can also bear wild-type pIII. Since such virions no longer rely on the infectivity of the pIII fusion protein, proteins can instead be fused to truncated pIIIs designed with the structure of the protein in mind. These can confer more efficient display, by reducing or eliminating proteolysis of the fusion protein, as well as reducing the size of the phagemid vector (Clackson and Lowman, 2004).

Mature pIII consists of three domains D1, D2, and D3, linked by glycine-rich tetrapeptide and pentapeptide repeats L1 and L2, as well as the C-terminal membrane-anchoring hydrophobic segment which spans the bacterial inner membrane during phage assembly (see Figure 5. 4). pIII, present in five copies at the end tip of the virion, is where the initiation of infection begins when the middle domain D2 binds to the tip of a pilus. Then the D1 domain is released from its normal interaction with D2, and hypothetically the pilus retracts and draws the bound phage to the cellular envelope, allowing D1 to interact with periplasmic protein TolA, the coreceptor. The other two integral cytoplasmic membrane Tol proteins (Q and R) are also essential for phage infection (Sidhu and Geyer, 2015)(see Figure 5. 4).

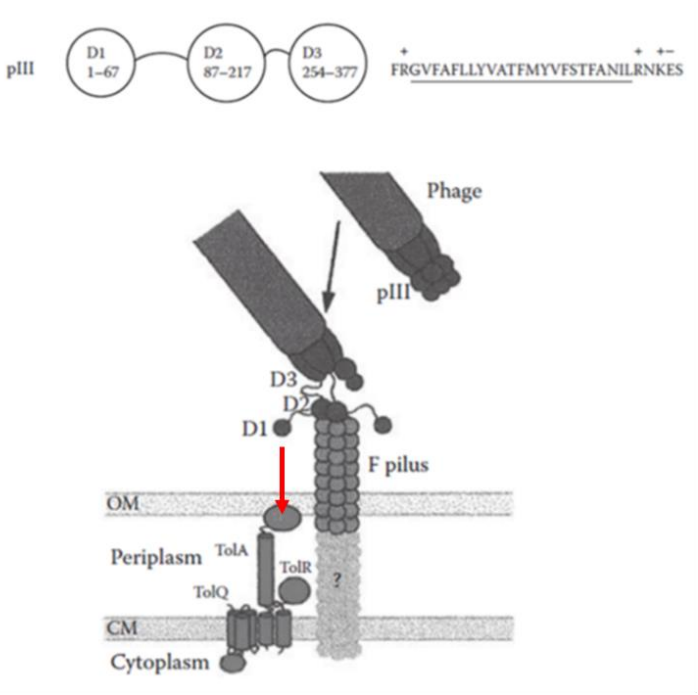


*Figure 5. 4 pIII domain structure and initiation of Ff phage infection (Adapted from (Sidhu and Geyer, 2015))***.** *pIII has three domains and infection initiates from the binding of D2 to the tip of F pilus, followed by the release of D1 and interaction of D1 with co-receptor TolA.*

5.1.2.2 Display formats

Proteins can be displayed by a phage vector when the heterologous protein sequence is inserted directly into the coat protein sequence of natural Ff phage, or by phagemid, a plasmid-based vector, which only contains the fusion protein gene and no other phage genes (Clackson and Lowman, 2004). The phage vector systems rely on the large and genetically unstable phage genomes, whereas the phagemid system is more genetically stable (Loset and Sandlie, 2012).

There are different formats of display that can be used to suit different applications. For example, libraries can be constructed so that all five copies of the pIII fusion protein contain the peptide insert or alternatively only a fraction of the structural proteins contain the insert. The latter can be constructed by the inclusion of a second non-fusion gene either in the same viral genome or through the dual vector system involving a fusion gene encoded on a phagemid and a non-fusion gene supplied by a helper phage. To distinguish

these three formats of display, they were named as "3", "33" and "3+3", respectively (see Figure 5. 5). The same nomenclature also applies to pVIII based display formats, i.e., "8", "88" and "8+8", respectively (Wang and Yu, 2004).

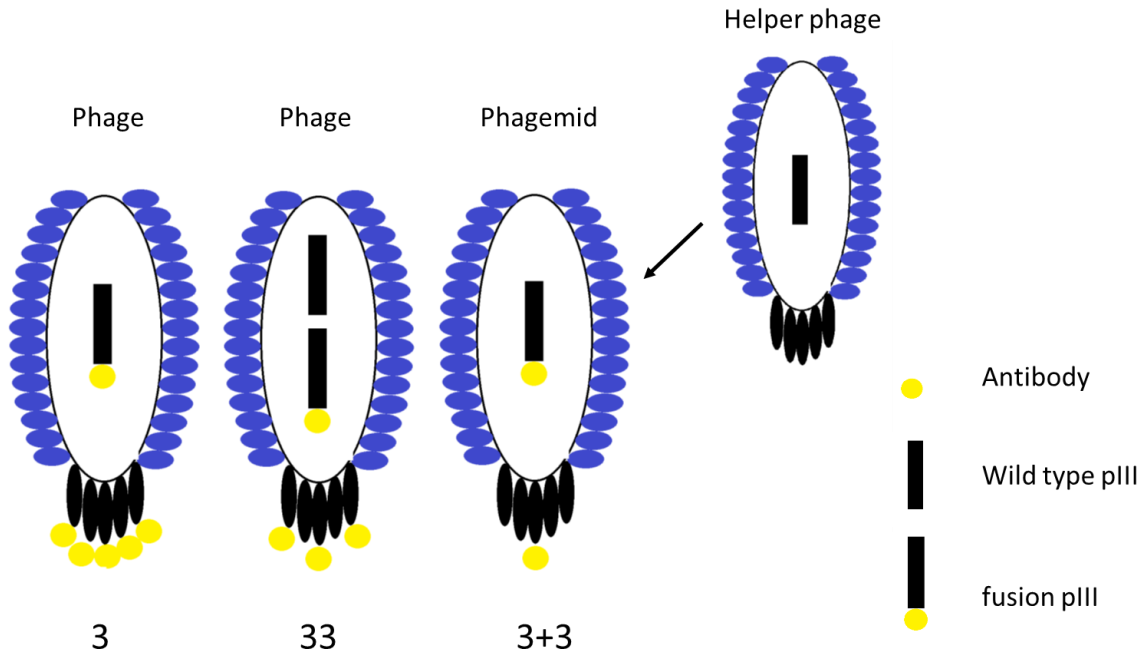


Figure 5. 5 Different formats of phage display (Adapted from (Wang and Yu, 2004)). The '3' system uses a phage vector that has a modified pIII which is fused to the peptide of interest, i.e. antibody. The '33' system uses a phage vector that has both a wild type pIII and a fusion pIII. The '3+3' system uses a phagemid vector in combination with a helper phage. The pIII gene is from two sources. The '3' system can only express one type of pIII; however, the '33' and '3+3' system produce mosaics.

5.1.2.3 Phagemid

Phagemid has an ampicillin resistance gene and two origins of replication, one of which is a plasmid replication origin that allows it to replicate to an extremely high copy number in an *E. coli* host. The other one is a filamentous phage replication origin, which is only active when the phagemid-infected cell is also infected with a filamentous phage acting as a "helper". Without the superinfection of helper phage, phagemid-infected bacterial host cells will not produce phagemid virions. However, when infected by both phagemid and helper phage, phage-encoded proteins from helper phage produced by bacteria cells act

at the phagemid's phage origin of replication and make the single-stranded phagemid DNA, which subsequently is packaged into virion particles efficiently.

In this study, a '3+3' display format was adopted, using a phagemid vector pSD3 (Li et al., 2000) and truncated pIII protein, which lacks the D1 and part of the D2 domain, to display a naïve VHH library which is of high diversity (~$1x10^9$ repertoire) and unbiased and can identify binders for any potential antigen. VHH, the variable domain of the heavy chain, is the antigen-binding site of the naturally-occurring heavy-chain-only antibodies (HCAbs) in *Camelidae* (Sabir et al., 2014) (see Figure 5. 6).

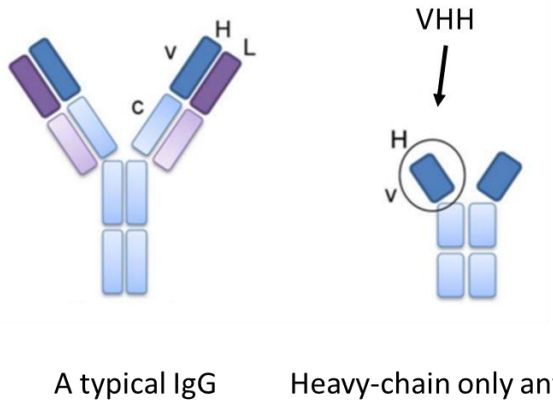


Figure 5. 6 A typical IgG antibody and a VHH (Doshi et al., 2014).

5.1.2.5 Helper Phage

One example of commonly used helper phage is M13K07. It is a modified M13 phage with the mutant gene II of M13mp1, a phage origin of replication, an origin of replication from plasmid p15A and a kanamycin resistance gene. As domain B of the phage origin of replication of M13K07 is disrupted, it is less active than the wild-type origin on the phagemid. As a result, phagemid DNA is preferentially packaged into new virions. A kanamycin resistance gene allows the specific selection of helper-infected bacteria cells. The mutant gene II of M13mp1 allows M13K07 to propagate well enough in the absence

of phagemid and the p15A origin of replication allows helper phage to replicate phage proteins independently (Sidhu and Geyer, 2015).

Helper phage used in this study, termed Ex-phage, was developed by Baek et al. (2002). Ex-phage was genetically engineered based on M13K07 helper phage. Two amber codons were introduced at the 5' region of pIII of M13K07 helper phage by site-directed mutagenesis. As a result, ex-phage has a mutant pIII gene which produces low levels of a functional wild-type pIII in suppressing *E. coli* strains such as XL-1 Blue cells or TG1 cells. Therefore, using ex-phage for packaging phagemids encoding antibody-pIII fusion in suppressing *E. coli* strains produces much higher display level than packaging with MK13K07 (Baek et al., 2002).

5.1.3 Next-generation phage display

A standard antibody phage display experiment consists of three main steps: (1) generation and display of an antibody library, such as the VHH library, (2) enrichment of antigen-binding antibodies by multiple rounds of binding selection (panning) and amplification; (3) recovery of antigen-specific antibodies from phage selection pools. Sanger sequencing is commonly used at each of these steps to decode sequences of antibody fragments recovered from phage pools. It requires the isolation of individual phagemids from phage pools and is practically limited to sequencing a few hundred clones routinely. Since each selection round in phage display gives an output of up to $\sim 10^6$ sequences, the use of next-generation sequencing (NGS) becomes necessary if one must capture and interrogate the entire sequence diversity present in phage selection outputs. With NGS, entire phage pools can be subjected to sequencing (isolation of individual phagemid is not required) and $\sim 10^6$—10^9 sequences can be readily obtained (Barreto et al., 2019).

Ion torrent sequencing of diversified complementarity-determining regions (CDRs) from the VHH library was accomplished in three main steps: PCR amplification of CDRs,

emulsion PCR on Ion sphere particles (ISPs) and sequencing enriched ISPs on an Ion semiconductor chip. To PCR amplify CDRs from phage pools, specifically designed primers were used which hybridize to the fixed framework regions of the phagemid that flank the CDR region. Primers contained barcodes for multiplexing purposes and adaptor sequences to facilitate emulsion PCR (Barreto et al., 2019).

5.2 Aim

This project aimed to identify antibodies that are specific to clade 2 Equine Influenza Viruses (EIV) compared with clade 1 EIV using Next Generation Phage Display (NGPD) analyses and using a VHH library.

5.3 Experiment design and panning strategy

Three experiments were conducted. In experiment 1A, the constructed VHH phage library was panned against A/equine/Richmond/1/07 (H3N8) 7:1 Devon reassortant (hereafter referred to as 'Devon') which represents clade 2 EIV (see Figure 5. 7) In experiment 1B, A/equine/Richmond/1/07 (H3N8) 7:1 Kentucky reassortant (hereafter referred to as 'Kentucky'), representing clade 1 EIV, was used as the target antigen (see Figure 5. 8). In experiment 2, Devon was used as the target antigen, and a subtraction step was included during panning where the VHH library was incubated with Kentucky antigen prior panning against Devon so that in theory most Kentucky-specific binders could be removed (see Figure 5. 9).

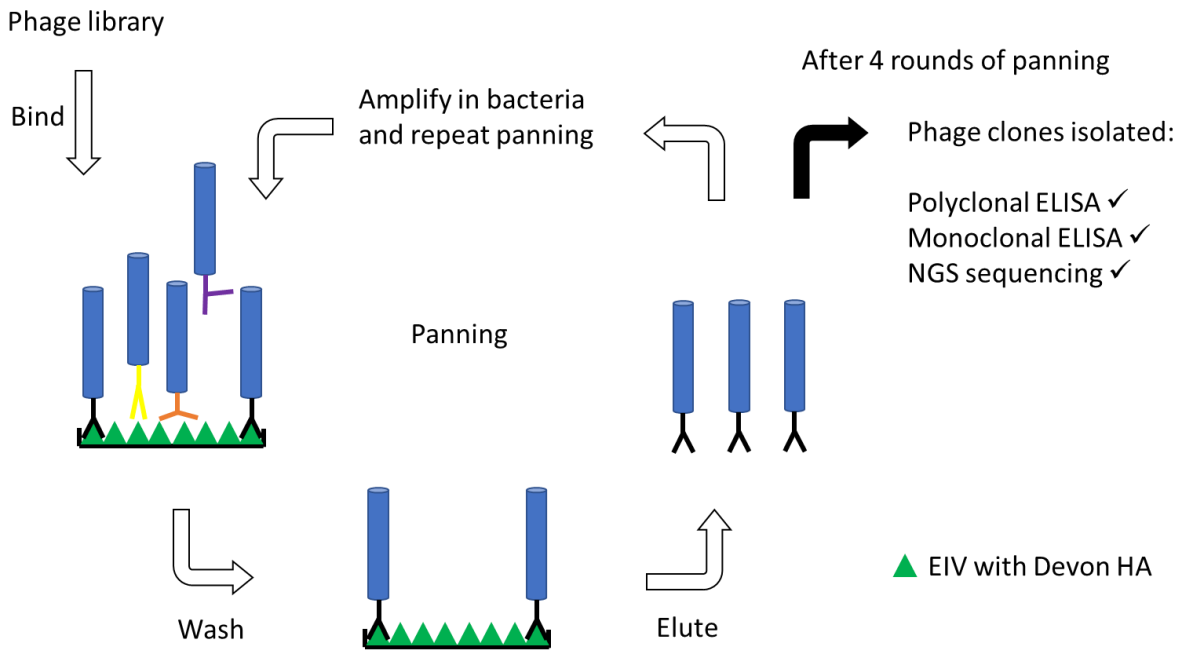


Figure 5. 7 Experiment 1A procedure. The VHH library was directedly incubated with Devon, after four rounds of panning, the eluted phage pool is subjected to polyclonal phage ELISA, monoclonal phage ELISA and next-generation sequencing.

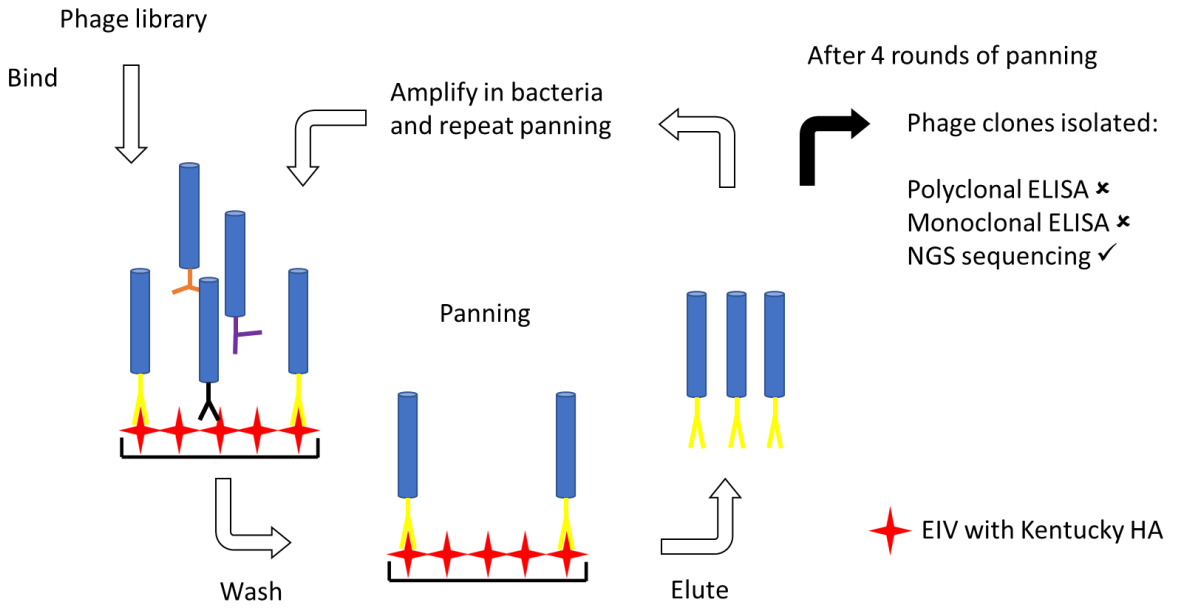


Figure 5. 8 Experiment 1B procedure, same as experiment 1A but phage ELISAs were omitted. And experiment 1B was conducted at the same time as experiment 1A

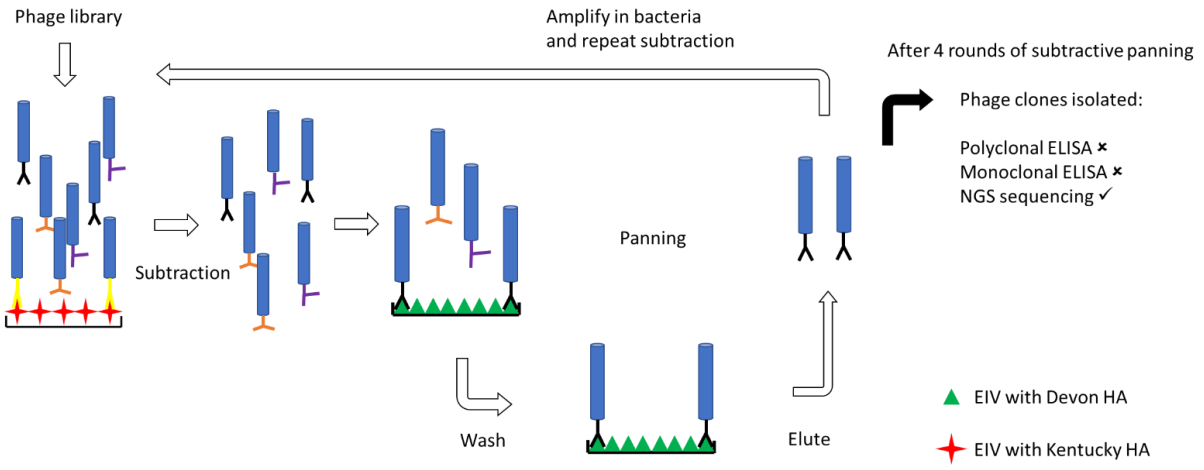


Figure 5. 9 Experiment 2 procedure. A subtraction step was included where phage library was incubated with Kentucky to subtract potential binders before panning against Devon. Subsequently, eluted phage pool was sent for NGS sequencing.

5.4 Materials and methods

5.4.1 General materials

Exphage glycerol stock was kindly provided by Dr Kevin Gough's group, originally given by Baek et al. (2002). Phagemid VHH display vector was constructed and supplied by Dr Alison Gray (see Figure 5. 10).

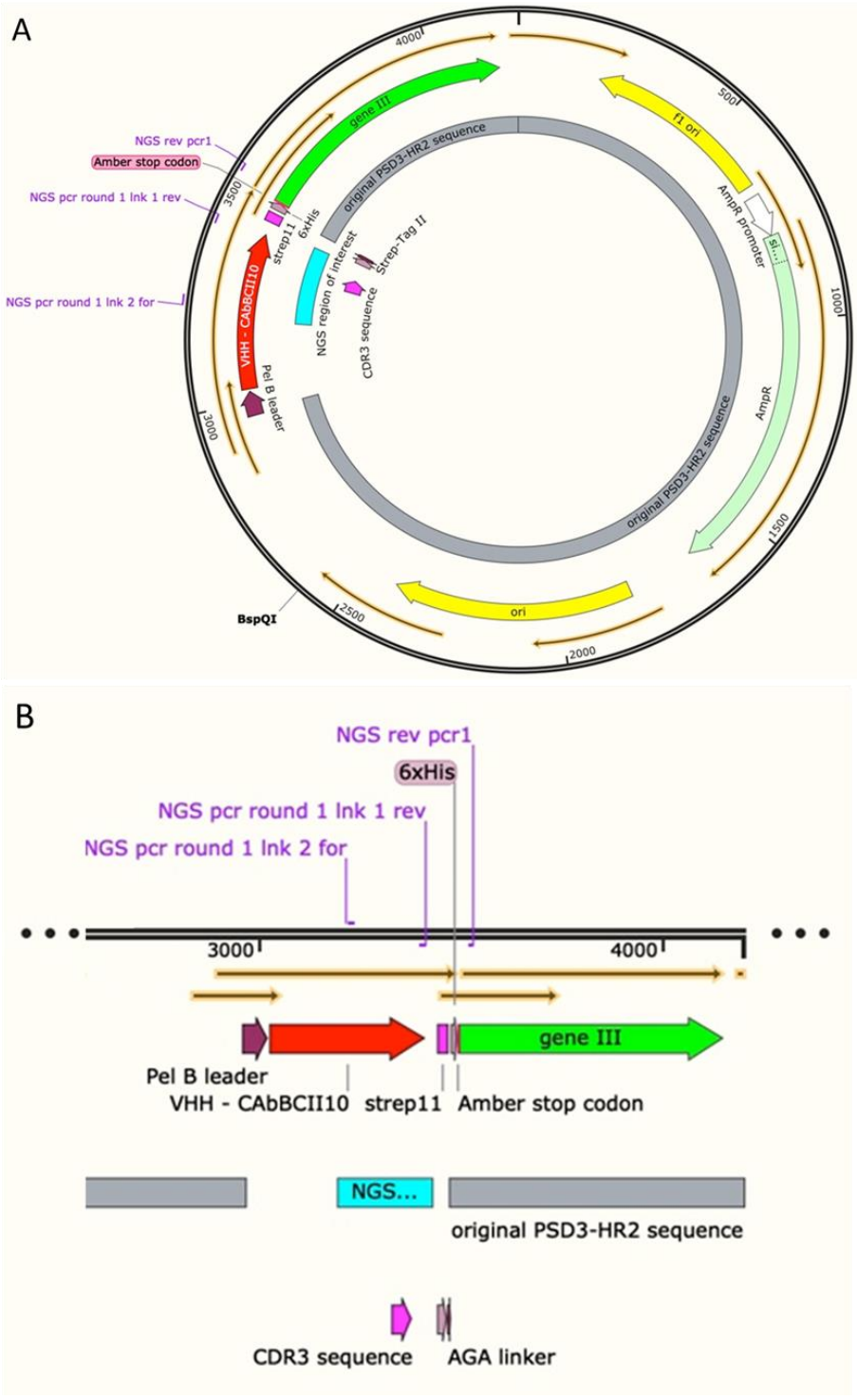


Figure 5. 10 Phagemid construct –pSD3-VHH generated by Dr Alison Gray, not published.

The VHH library (in red) was constructed in the phagemid vector pSD3, with a synthetically randomised CDR3; 12, 16 or 21 amino acid in length. The vector has an ampicillin-resistant gene. VHH gene was downstream of the pelB leader signalling sequence followed by a Strep-tag II and 6xHis-tag (for purification and identification purposes), an amber stop codon (TAG) and a truncated version of phage minor coat protein pIII (in green).

Phage Display Competent Cells: TG1 Electrocompetent Cells were commercially available (Lucigen). The amber suppressor strain TG1 was used because it allowed the pIII protein to be synthesised along with the VHH as a fusion protein, the stop codon before pIII is substituted with a Q. Equine influenza virus stocks (A/equine/Richmond/1/07 (H3N8) 7:1 Devon and Kentucky reassortants)(see Figure 5.11) were kindly given by Dr Debra Delton (Animal Health Trust) and propagated in embryonated hens' eggs by Dr Janet Daly.

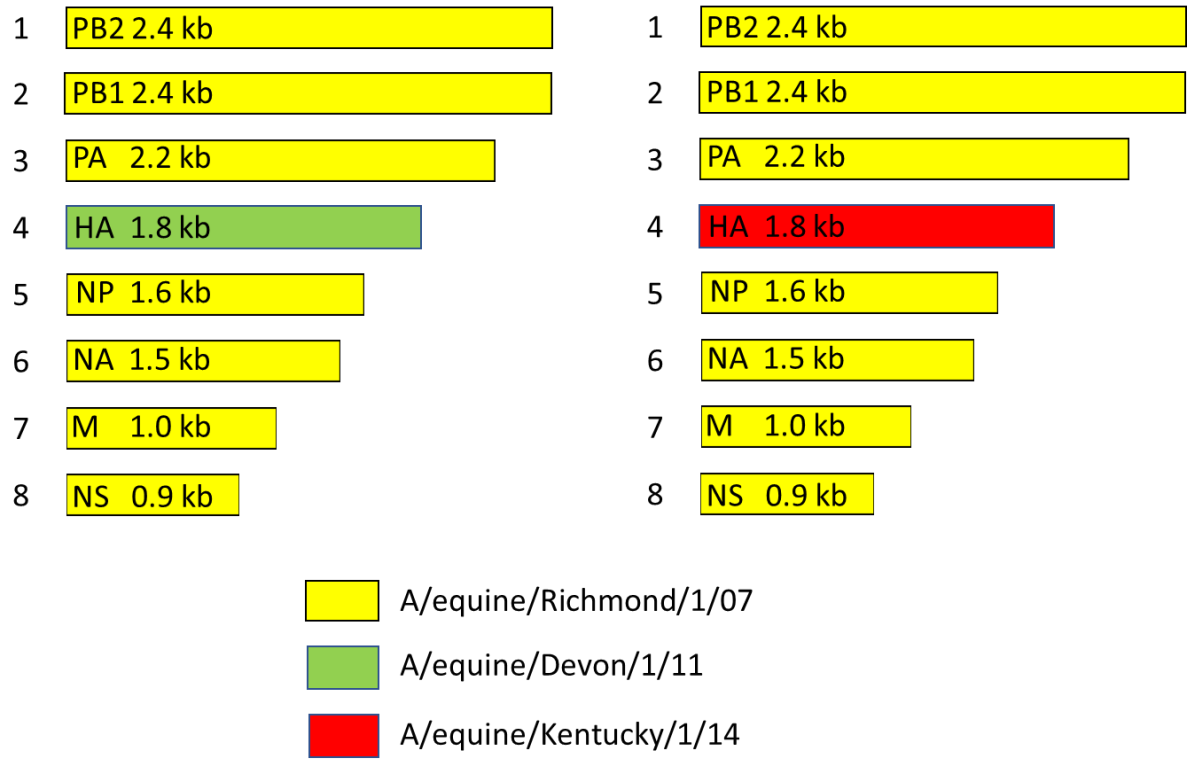


Figure 5. 11 Equine influenza virus reassortants. One stock of virus contains all gene segments from A/equine/Richmond/1/07 except for segment 4, which is from A/equine/Kentucky/1/14. The other stock contains all gene segments from A/equine/Richmond/1/07 but segment 4, which is from A/equine/ Devon/1/11.

5.4.2 Protein assay

Concentrations of target antigens were determined by Bradford protein assay (Thermo Scientific Pierce) according to the manufacturer's instructions.

5.4.3 Helper phage (Ex-phage) production

One litre of 2YT media (Appendix 1) was inoculated with 10ml TG1 that had been grown overnight at 180 rpm and 37°C. TG1 cells in 1L of 2YT were kept growing at 180 rpm and 37°C until they reached OD 0.4. Ex-phage was added to the culture at an MOI of 10 and left for 30 min static at 37°C, then 30 min shaking at 220 rpm, 37°C. One litre of fresh 2YT media was added to the TG1/ex-phage culture to make its total volume to 2L, and it was then split between two 2L flasks. Kanamycin at a final concentration of 50 µg/ml was added to each of the flasks containing 1L of TG1/ex-phage culture, which was continuously kept growing overnight shaking at 220rpm and 30°C. Subsequently, 2L of culture supernatant was collected by centrifugation at 3000 *g* for 20 min.

Ex-phage was then polyethylene glycol (PEG) precipitated by adding 250ml of 20% (w/v) PEG-8000/2.5M NaCl to every litre of culture supernatant. The culture was left on ice for 1 hour. After that, the culture supernatant was centrifuged at 8000 *g* for 20 min. The supernatant was discarded, and a further two rounds of centrifugation at 8000 *g* for 1 min was carried out to ensure all residual PEG/NaCl was removed. The ex-phage pellet was resuspended by adding 30 ml of PBS per litre of initial supernatant. PBS was allowed to soak into the precipitated pellet for 10 min. Finally, ex-phage was titrated using kanamycin 2YT agar plates and stored in 15% glycerol in 500 µl aliquots at -80°C until use.

5.4.4 Helper phage (Ex-phage) titration

One colony of TG1 competent cells was picked from a minimal agar (Appendix 1) plate and grown in 10 ml of 2YT media at 210 rpm and 37°C until they reached OD 0.4–0.6. 2YT agar plates with 50 µg/ml kanamycin were prepared. Five 100-fold serial dilutions of ex-phage were also prepared. The first serial dilution was performed by adding 1 µl of ex-phage to 99 µl of PBS. Nine hundred microlitres of TG1 (OD 0.4–0.6) was added to each of the serial dilutions of ex-phage, 100 µl of which was plated onto 2YT agar plates prepared previously. One negative control plate was included which had no ex-phage in

the TG1 suspension. Furthermore, one 2YT agar with no kanamycin was used as a positive control. Agar plates were incubated at 37°C overnight and colonies were counted to determine the colony-forming unit (CFU)/ml.

5.4.5 TG1 stock production

A colony of TG1 competent cells was picked from a minimal agar plate and grown in 10 ml 2YT media overnight at 210 rpm and 37°C. The bacterial culture was centrifuged at 3000 *g* for 10 min, the supernatant was discarded, and bacterial pellet was resuspended with sterile 25% glycerol. Finally, TG1 stocks were stored in 1 ml aliquots at -80°C.

5.4.6 Experiment 1A and 1B:

5.4.6.1 Round 1 panning

Two Maxisorp microtitre plates were pre-coated with target antigens and incubated at room temperature overnight (see Figure 5. 12). In each plate, 10 wells were coated with 100 µl of antigen at 20 µg/ml, diluted in sodium carbonate buffer pH9.6. The next morning, a colony of TG1 competent cells was picked from a minimal agar plate and grown in 30 ml 2YT media at 210 rpm and 37°C until they reached OD 0.4–0.6 for output phage titration and amplification.

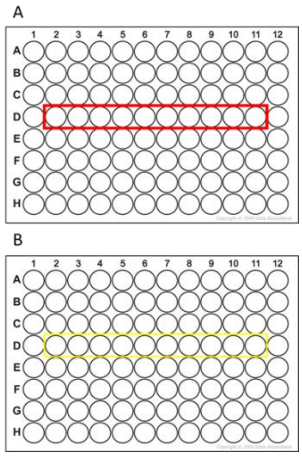


Figure 5. 12 Plate A was coated with Kentucky and plate B was coated with Devon. From D2-D11, 10 wells per plate were pre-coated with 100 µl of each antigen at 20 µg/ml, diluted in sodium carbonate buffer.

The pre-coated Maxisorp microtitre plates were washed with 1X PBS and blocked with 3% (w/v) milk in 1X PBS for 1hours at room temperature. A 2 ml pool was made by pooling 666.6 µl of each VHH sub-library (12-, 16- and 21-mer) phage and blocked with 400 µl of 18% milk in 6X PBS for 1 hour at room temperature. After blocking, the Maxisorp microtitre plates were washed with 1X PBS 3 times, and 100 µl of pre-blocked phage library were added to each of the 10 wells as shown in Figure 5. 12 and incubated at room temperature for 1 hour. After incubation, the plates were washed 10 times with 1X PBST (Appendix 1) followed by 10 times with 1X PBS. For elution, 100 µl of 0.1M glycine pH2 was added to each well and incubated for 10 min. Subsequently, 100 µl of 1M Tris pH7.4 was added to each well to neutralise the phage. For each target antigen, approximately 2 ml of round 1 output phage was pooled from 10 wells, 10 µl of which was used for titration, 1500 µl was used for amplification by infecting bacteria and plating out on bioassay plates, and the rest was stored in 25% (v/v) glycerol at -80°C until further use.

5.4.6.2 Titration for round 1 output phage

One colony of TG1 competent cells was picked from the minimal agar plate and grown in 10 ml 2YT media at 210 rpm and 37°C until they reached OD 0.4–0.6. 2YT agar plates with 1% (w/v) glucose and 150 µg/ml ampicillin were prepared. Four 100-fold serial dilutions of output phage were also prepared. The first serial dilution was performed by adding 10 µl of output phage to 90 µl of PBS. Nine hundred microlitres of TG1 (OD 0.4–0.6) was added to each of the serial dilutions of output phage, 100 µl of which was plated onto 2YT agars prepared previously. One negative control plate was included which had no output phage in the TG1 suspension. Furthermore, one 2YT agar with no ampicillin was used as a positive control. Agar plates were incubated at 37°C overnight and colonies were counted to determine the colony-forming unit (CFU)/ml.

5.4.6.3 Amplification of round 1 output phage for further panning rounds

Two bioassay plates were prepared using 2YT agar, 1% (w/v) glucose and 150µl/ml ampicillin. For each target antigen, 1.5 ml of round 1 output phage was added to 10 ml

of TG1 cells that had been growing to OD 0.4–0.6, and incubated at 37°C static for 30 min. The TG1/output phage mixtures were then centrifuged at 3000 *g* for 10 min. Supernatants were discarded, and cell pellets were resuspended in 1 ml 2YT and plated out on bioassay plates prepared in advance which were then incubated at 37°C overnight. For each antigen, all colonies formed in the bioassay plate were scraped in 5 ml storage media (Appendix 1), 500 µl of which were used for round 2 input phage preparation. The rest were stored at -80°C.

5.4.6.4 Preparation for round 2 input phage

For each antigen, 500µl of round 1 output phage amplified in TG1 was added to 500ml 2YT containing 1% (w/v) glucose, 150 µg/ml ampicillin in a 2L flask and grown to OD 0.4–0.6 at 37°C, 220 rpm in a shaking incubator. Ex-phage was then added to the growing TG1 library at MOI 10 and incubated statically at 37°C for 30 min followed by a further incubation in shaking condition at 37 °C, 220 rpm. After ex-phage infection, TG1 culture was centrifuged at 3000 *g* for 10 min at room temperature. Supernatants were discarded, and the second centrifugation was performed to remove all traces of glucose. TG1 pellets were rinsed once with 20ml 2YT, resuspended in 500ml 2YT with 150 µg/ml ampicillin and 50 µg/ml kanamycin, and incubated in a shaking incubator at 30°C, 200 rpm overnight for the ejection of phage into the supernatant. After that, supernatants were centrifuged at 3000 *g* for 10 min; phage acid precipitated by lowering its pH to 4.2 using HCl/NaOH and finally placed on ice for 60 min. The phage supernatants were then centrifuged at 8000 *g* for 30 min at 4°C. After centrifugation, most of the supernatant was discarded, and around 50 ml was left in the 250 ml bottle. Phage pellets were then resuspended in that 50ml supernatant which had been left and transferred to 50 ml falcon tubes and re-pelleted at 8000 *g* for 10 min. The final supernatants were discarded, and pellets were resuspended with 20 ml PBS and adjusted to pH 7–7.4. Phage suspensions were agitated for 10 min or stored at room temperature overnight, after which they were centrifuged at 12000 *g* for 10 min to remove bacterial debri. Phage supernatants were collected and filtered with a 0.45 µM filter unit. Finally, round 2 input phage was titrated using 2YT agar

plates with 1% (w/v) glucose and 150 µg/ml ampicillin and the remaining phage stored in the same way as ex-phage.

5.4.6.5 Round 2—4 panning

Round 2—4 panning in experiment 1A and 1B were carried out the same way as for round 1 using output phage from the previous rounds. Round 2 and round 4 output phage were screened against both Devon and Kentucky in an additional round, termed round 3 and round 5 screening.

5.4.6.6 Polyclonal ELISA for round 1-5 phage library

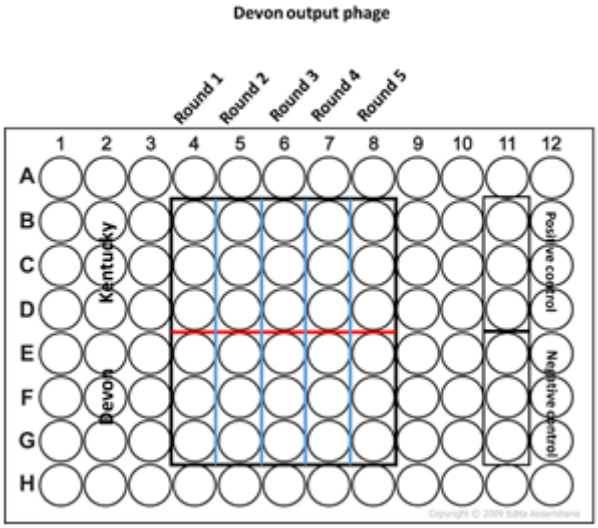


Figure 5. 13 Maxisorb 96 well plate layout for polyclonal ELISA.

Maxisorp ELISA plates were coated with both Devon and Kentucky viruses in triplicates (see Figure 5.13) at a concentration of 20 µg/ml each well and incubated at room temperature overnight. Bovine serum albumin (detected with known anti-BSA scFV-phage) was used as a positive control and ELISA coating buffer pH 9.6 as a negative control. The next morning, ELISA plates were washed with 1XPBS once and blocked with 3% (w/v) milk in 1X PBS for 1 hour at room temperature. Round 1—5 output phage libraries were blocked with 18% (w/v) milk in 6X PBS at room temperature for one hour. After blocking, ELISA plates were washed once with PBS and pre-blocked round 1—5

output phage were added to relevant wells in triplicates for 1-hour room temperature incubation. The anti-M13 antibody (Anti-M13-HRP, GE Healthcare) was also diluted 1:5000 and blocked in 3% (w/v) milk for 1 hour at room temperature. After incubation, ELISA plate was washed with PBST 5 times followed by PBS 5 times, 100 µl of pre-blocked anti-M13 antibody was added to each well including positive and negative control wells and incubated at room temperature for 1 hour. After the final incubation, the ELISA plate was washed with PBST 5 times and another 5 times with PBS; 100 µl of TMB substrate was added to all relevant wells and incubated for 10—15 mins for colourimetric development, after which the enzyme activity was stopped by adding 100 µl of 2N sulphuric acid to each well. Lastly, the ELISA plate was measured using a Labtech LT-4000 Plate Reader for reading at 450 nm.

5.4.14 Monoclonal ELISA

A total of 120 colonies were picked for monoclonal ELISA, 30 colonies from round 2 panning, 30 from round 3 panning, 30 from round 4 panning, and 30 from round 5 screening. TG1 glycerol stocks of round 2—5 phage were spread onto individual Petri dishes and incubated at 37°C until colonies were big enough to be picked. A 96-deep-well plate was prepared by adding 400 µl 2YT media, 150 µg/ml ampicillin and 1% (w/v) of glucose into each deep well. One colony was picked and placed in an individual deep well and allowed for growing overnight at 30°C to produce a master plate. The master plate was then sub-cultured in a new deep well plate by taking 10 µl bacterial culture from each well into 390 µl 2YT media, 150 µg/ml ampicillin and 1% (w/v) glucose in the corresponding well in the new deep well plate. The master plate was subsequently centrifuged at 800 *g*; the pellets were re-suspended in 400 µl 2YT 15% (v/v) glycerol and stored at -80°C. Culture in the new deep well plate was allowed to grow for 2 hours and infected with ex-phage. The ex-phage-infected culture was incubated statically at 37°C for 30 min and in a shaking platform at 220 rpm for further 30 min. The new deep well plate was then centrifuged at 800 *g*; pellets were re-suspended in 400 µl 2YT media, 150 µg/ml ampicillin, and 50 µg/ml kanamycin. The culture was let to grow overnight at 30°C.

The next morning the deep well plate was centrifuged at 800 *g,* and the supernatant from each well was transferred to a new plate. The rest of the ELISA procedure was the same as for the polyclonal ELISA.

5.4.7 Experiment 2

5.4.7.1 Round 1 panning

Round 1 panning in experiment 2 was carried out the same as for round 1 panning in experiment 1A and 1B.

5.4.7.2 Round 2 panning with subtraction

Round 2 input phage was prepared the same way as described before. The pre-coated Maxisorp microtitre plates were washed with 1X PBS and blocked with 3% (w/v) milk in 1X PBS for 1 hour at room temperature. Five hundred microlitres of round 2 input phage were blocked with 100 µl 18% (w/v) milk in 6XPBS for 1 hour at room temperature. After blocking, the first row of 5 wells (B4–B8) (see Figure 5. 14) from the blocked Maxisorp microtitre plates were washed with 1X PBS 3 times, and 100 µl of pre-blocked round 2 input phage were added to each of the 5 wells and incubated at room temperature or 37˚C for 15 min. As soon as the first round of incubation finished, blocking buffer from the next row of 5 wells (C4–C8) was discarded, and wells were washed with 1X PBS 3 times. Round 2 input phage incubated in the first row were directly transferred to the second row using a multichannel pipette and incubated for another 15 min. The same processes were repeated until round 2 input phage reached the last row. After the final 15-min incubation on the subtraction plate, round 2 input phage was added to wells (D4–D8) in the target plate, which had already been blocked and washed, and incubated at room temperature for 60 min. After incubation, the target plate was washed with 1X PBST 10 times followed by 1X PBS 10 times. For elution, 100 µl of 0.1M glycine pH2 was added to each well and incubated for 10 min, after which the eluted phage from each well was transferred to 5 Eppendorf tubes each containing 100µl of 1M Tris pH7.4 for neutralisation. As a result,

there were 5 tubes of 200 µl eluted and neutralised phage that had been through 6 rounds of subtraction and potentially had bound to the target protein. One hundred microlitres of phage were pooled from each tube for subsequent rounds of panning, and the rest were stored in 25% (v/v) glycerol at -80°C.

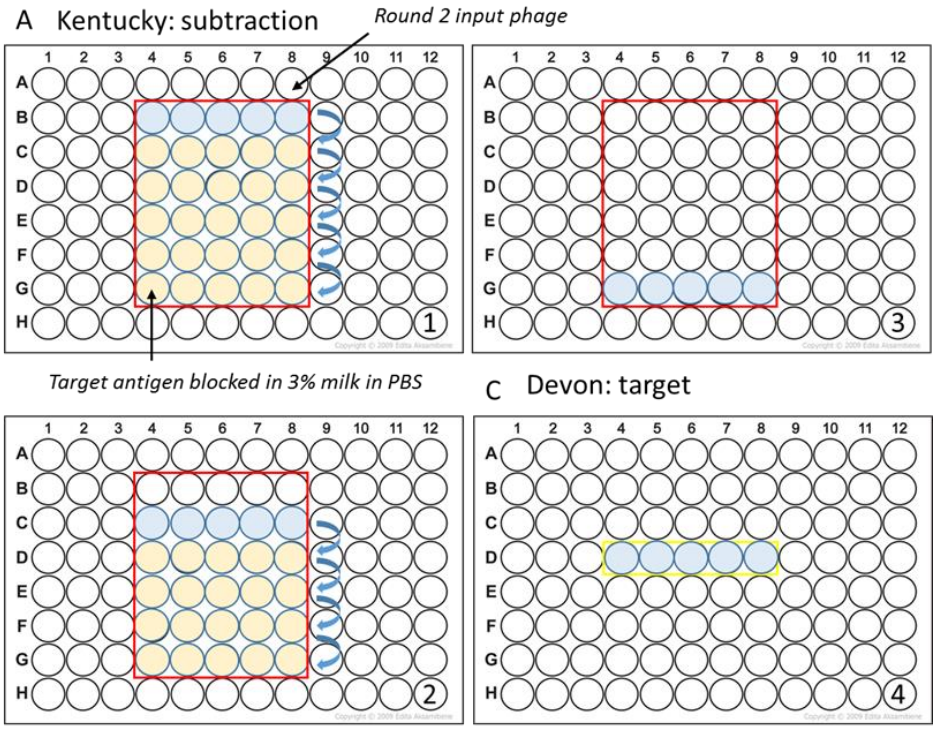


Figure 5. 14 Illustration of round 2 panning against Devon HA with subtraction.

Round 2 input phage was subjected to 6 subtraction rounds in plate A which was pre-coated with Kentucky HA. Before adding input phage to each row, wells were blocked with 3% milk in PBS for at least 1 hour and washed with 1X PBS three times.

5.4.7.3 Round 3—4 panning

Round 3—4 panning in experiment 2 were carried out the same way as for round 2 with subtraction in each panning.

5.4.8 Round 3 and round 5 screening

In experiment 1A and experiment 2, where Devon was the target antigen, round 2 output phage and round 4 output phage were amplified and screened against both Devon and Kentucky antigen as for round 1 panning. Round 4 output phage from experiment 1B were screened against both Devon and Kentucky. This is termed as round 3 and round 5 screening (see Figure 5. 15). The eluted phage were amplified in TG1 and PCR-prepared for NGS.

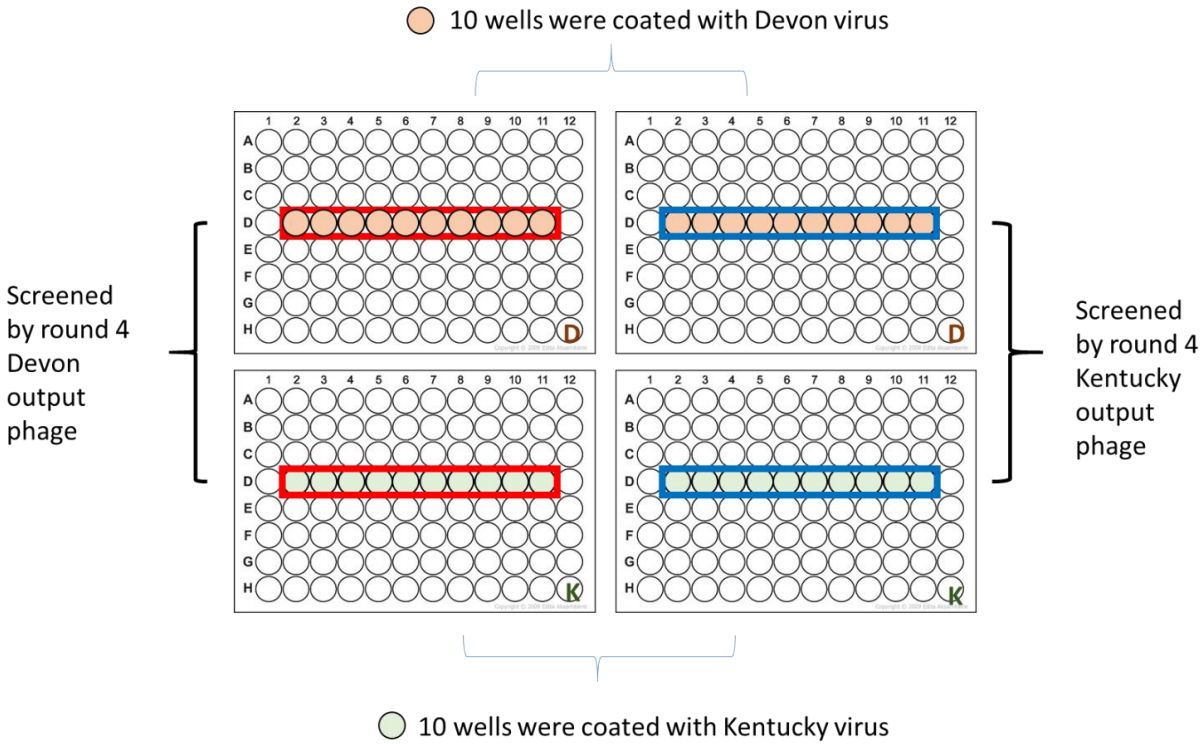


Figure 5. 15 Maxisorb 96 well plate layout for round 3 and 5 screening.

Ten wells in two plates (top left and right) were coated with Devon virus, and 10 wells in other two plates (bottom left and right) were coated with Kentucky virus. Round 4 Devon output phage was screened against both Devon and Kentucky virus coated plates (circled in red); round 4 Kentucky output phage was screened against both Devon and Kentucky virus coated plates as well (circled in blue).

5.4.15 NGS sample preparation— PCR amplification of CDRs

The first step of NGS, which is PCR amplification of CDRs, is completed by the author and the rest of the Ion torrent sequencing is completed by University of Pennsylvania commercial service. Ninety-five screened phage samples were selected for next-generation sequencing, 37 of them were from experiment 1A, 20 from experiment 1B and 38 from experiment 2 (see Figure 5. 16)

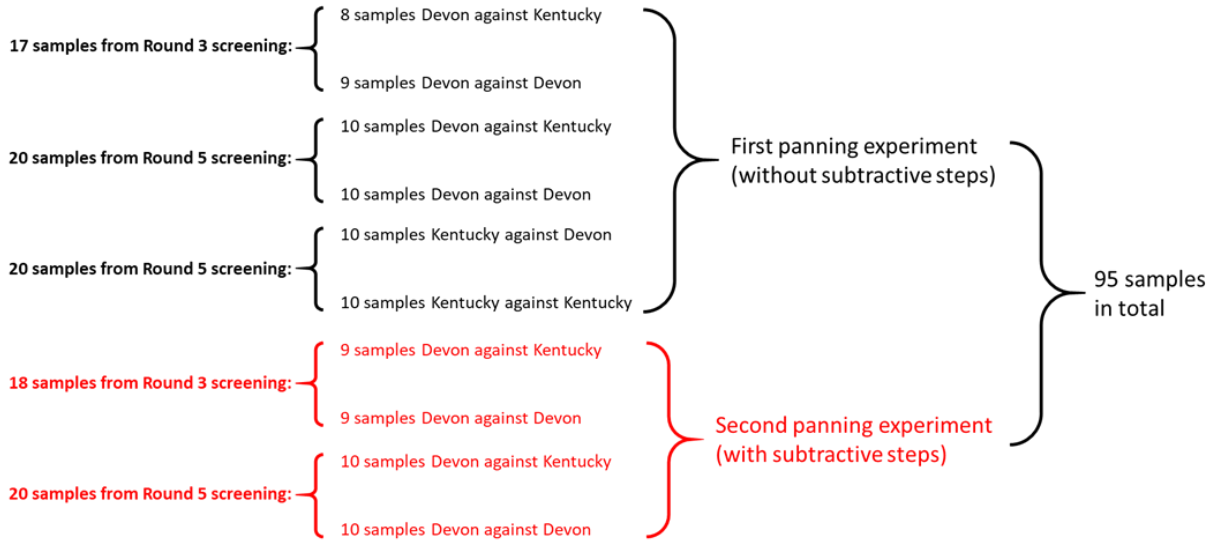


Figure 5. 16 Ninety-five phage samples from two different panning experiments were selected for next-generation sequencing.

Phage was grown out from round 2 and round 4 TG1 glycerol stocks from experiment 1A, 1B and 2 in 50 ml 2YT media, 150 µg/ml ampicillin and 25% (w/v) of glucose. They were grown to OD=0.5 and superinfected with ex-phage as previously described. TG1 culture was centrifuged at 6000 *g*; pellets were re-suspended in fresh 2YT media, 150 µg/ml ampicillin and 50 µg/ml kanamycin. Superinfected, phage/TG1 culture, was incubated overnight at 30°C in a shaking incubator at 150 rpm. Next, 10 ELISA plates (Nunc) were coated with EIV, 5 plates each strain and 10 wells per plate. Antigen-coated ELISA plates were incubated at RT overnight. The next day, ELISA plates were washed with PBS once and blocked with 3% milk in 1XPBS for 1 hour at RT. Phage/TG1 culture was centrifuged at 6000 *g* to harvest the phage supernatant, which was then blocked with 18% milk in 6XPBS for 1 hour at RT (200µl 18% (w/v) milk per 1ml phage). After incubation, the ELISA

plates were washed 1XPBS 3 times, and 100µl of blocked phage were added to the plates in appropriate wells and incubated for 1 hour at RT. Later, all 10 ELISA plates were washed with 1XPBST 10 times and 1XPBS 10 times. For phage elution, 100µl of glycine pH2.0 was added to each well and incubated for 10 min, after 10 min, 100µl of Tris was added to each well for neutralisation, and finally, 200µl of each sample was moved to a 1.5ml Eppendorf tube. Ninety-five phage samples in total were harvested totally.

TG1 were grown in 100ml 2YT to OD=0.5 and aliquoted to 95 1.5ml Eppendorf tubes, 1ml each. Two hundred microlitres of eluted phage from screening were added to each tube and incubated at 37°C static for 1 hour for infection. Each content from the Eppendorf tube was transferred to a fresh and labelled universal tube with 3ml 2YT, 150 µg/ml ampicillin and 25% glucose inside and incubated in a shaking incubator overnight at 30°C, 150 rpm.

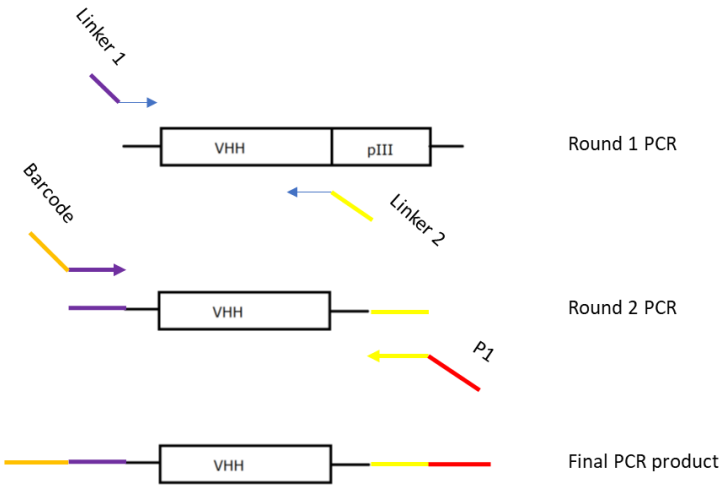


Figure 5. 17 Amplification of CDR3 of VHH library for NGS in two rounds of PCR.

In round 1 PCR, linker 1 and linker 2 were added by . In round 2 PCR 95 barcodes and P1 primer were added to 95 samples.

The next day, 1.5ml bacterial culture from each universal tube was transferred to a 1.5ml Eppendorf tube. All 95 samples were miniprepped and nanodropped. The DNA concentration of each sample was diluted to 10ng/µl. All 95 diluted DNA samples were subjected to round 1 PCR using forward primer VHH PCR link2 f (CTAGAACATTTCACTTAgattcggtaaagggccgc) and reverse primer VHH PCR link2 r (GTAATCCTTGTGGTATCGctagaggaaactgtcacctg)(linker sequences were indicated by upper cases; overlapping sequences with the VHH library were indicated in lower cases)(see Figure 5. 17). PCR products were cleaned up by Machery-Nagel Nucleospin Gel and PCR purification kit. Ninety-five purified PCR products were subjected to round 2 PCR using a universal P1 primer and barcoded reverse primers (barcodes 1-96, except barcode 42) which introduce sites compatible with Ion Torrent platform. The concentration of round 2 PCR products was tested using Qubit (Invitrogen). A pool of a total of 3000 ng DNA comprising all 95 samples (in equal amounts) was made and purified using AMPure XP kit (Beckman Coulter). The concentration of purified DNA pool was then measured and 50µl of 4ng/µl was sent for Next-Generation Sequencing (University of Pennsylvania commercial service).

5.4.16 NGS data analysis

NGS data was decompressed, demultiplexed based on barcodes, reverse-complemented and translated from step 1 to step 4 (see Figure 5. 18). In step 5, three reading frame files for each barcode were combined into one. In step 6, VHH library's flanking motifs surrounding the CDR3 were searched to identify the CDR3 sequence within the NGS data. The flanking sequences used in this study were 5 amino acids long and the left flanking sequence is 'YYCAA' and the right flanking sequence is 'WGQGT'. Only sequences flanked by both YYCAA and WGQGT were used in the next step. Next in step 7 and 8, barcodes representing positive samples were individually compared against the pool of negative control samples barcodes to identify enriched antibodies against the panning target. And the total number of reads (frequency) were calculated by the scripts as well as the ratio

(number of reads in the positive sample vs the number of reads in the negative pool). In step 9 to 11, scripts were used to run a Z test to calculate a Z score upon which each CDR3 sequence could be ranked. The Z score ranking system count on the total frequency of each CDR3 and its presence in the experimental and control replicates, thus rank each candidate based on its likely specificity to the target antigen. The Z score thresholds implied a strong likelihood that the candidate had become enriched against the target due to a binding event and therefore was not simply enriched by chance. Z score thresholds of ≥2, ≥5 or ≥10 were all applied initially, however, a Z score threshold ≥10 was decided based on the huge number of identified binders.

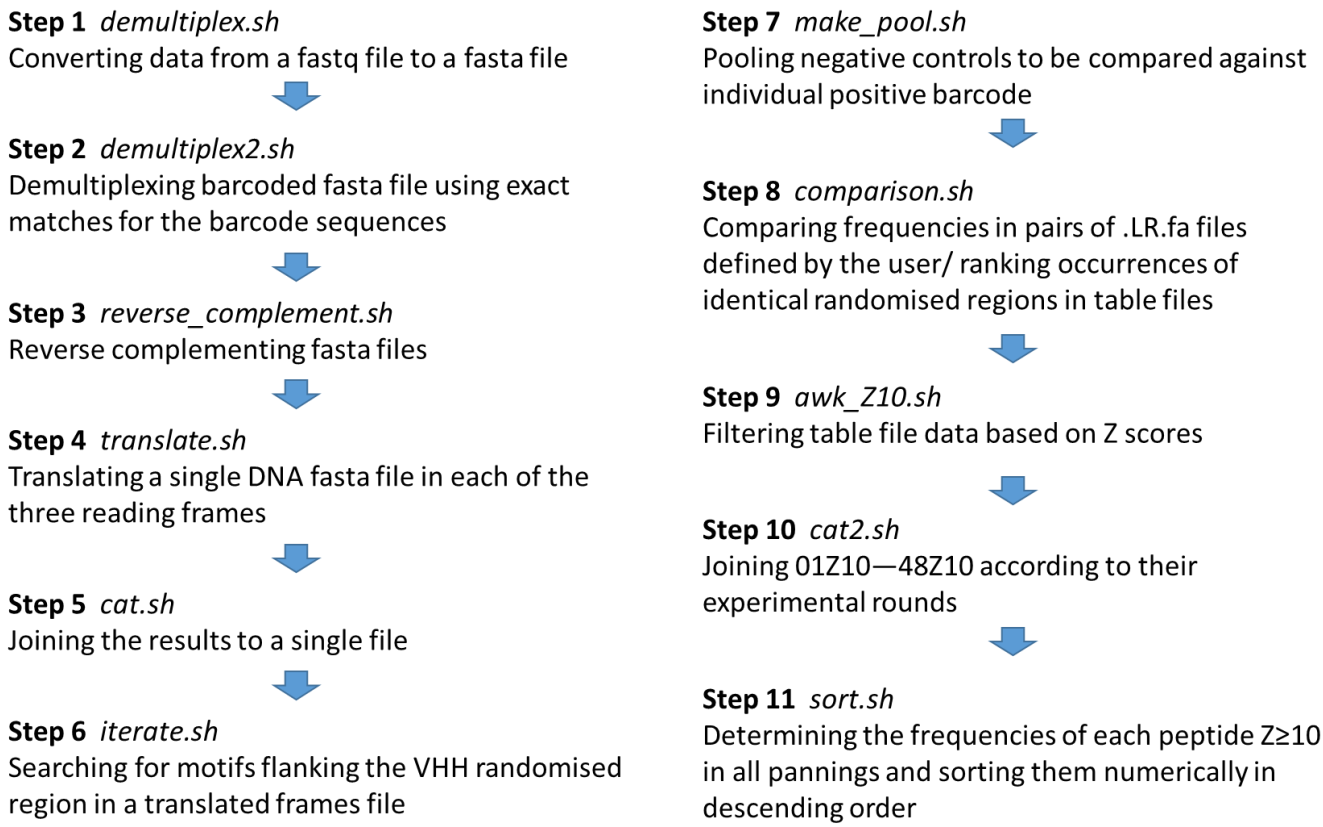


Figure 5. 18 Step by step flowchart of NGS data analysis using Ubuntu, a Linux operating system. Scripts used to analyse the data were written by Dr Jon Owen. Each step and its function was included in Appendix 2.

5.5 Results

5.5.1 Experiment 1A — targeting Devon, no subtraction

5.5.1.1 phage ELSIA —polyclonal phage

Polyclonal ELISAs used phage from the experiment 1A panned against Devon. It was performed twice. In the first time, results showed that the overall absorbance is very low. It could be because the TMB substrate (Thermo Fisher) was out of date. Although there is a difference in wells coated with Devon antigen and wells coated with Kentucky antigen, signals were not increased throughout 5 rounds, indicating the phage were not enriched successfully (see Figure 5. 19).

In a second attempt, an increasing trend in signals through round 1 to round 5, was observed, demonstrating that peptides with certain specificity were enriched through 5 panning rounds. When using a new TMB substrate, the overall absorbance is greatly increased, peaked in round 4 for both Devon and Kentucky. However, the signal difference between two strains becomes very small, indicating that the dominant enriched peptides in each panning round are not specific against one strain or another.

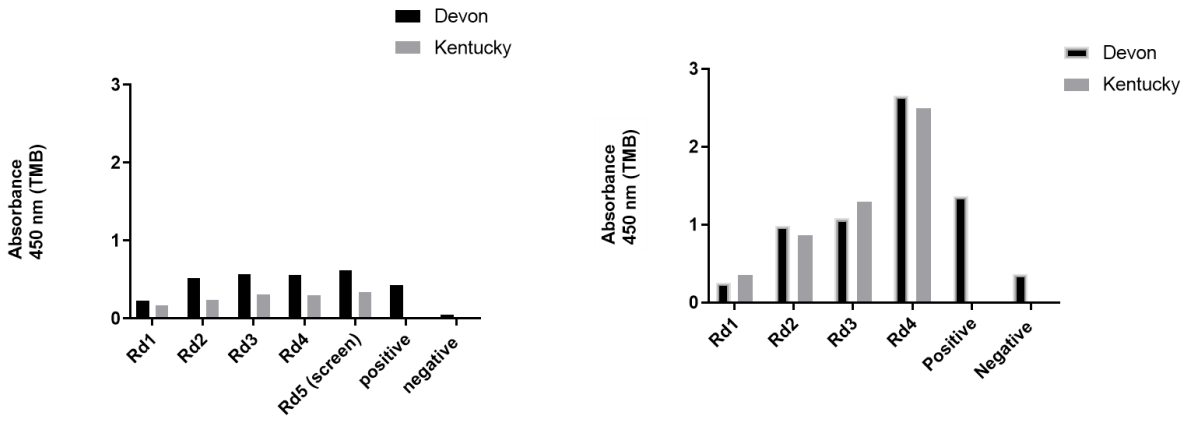


Figure 5. 19 Polyclonal ELISAs for first panning experiment. Results from the first attempt (left figure) show overall signals were very low and not increased throughout panning rounds. In the second polyclonal ELISA, although signals have been increased, indicating successful enrichment, the enriched phage could not differentiate the two targets.

5.5.1.2 phage ELISA —monoclonal phage

No negative control was used in the monoclonal ELISA, therefore an arbitrary background of 0.2 was used to determine the number of positive samples. Thirty colonies were picked from each round, 5 positive samples were identified from round 2, 19 positive samples were from round 3, all samples from round 4 and round 5 were positive (see Figure 5. 21). The increasing number of positive samples through round 2 to round 5 screening correlates with the second polyclonal ELISA data in which showed the binders were enriched, however, the specificities of the binders still could not be determined.

5.5.1.3 NGS sample preparation

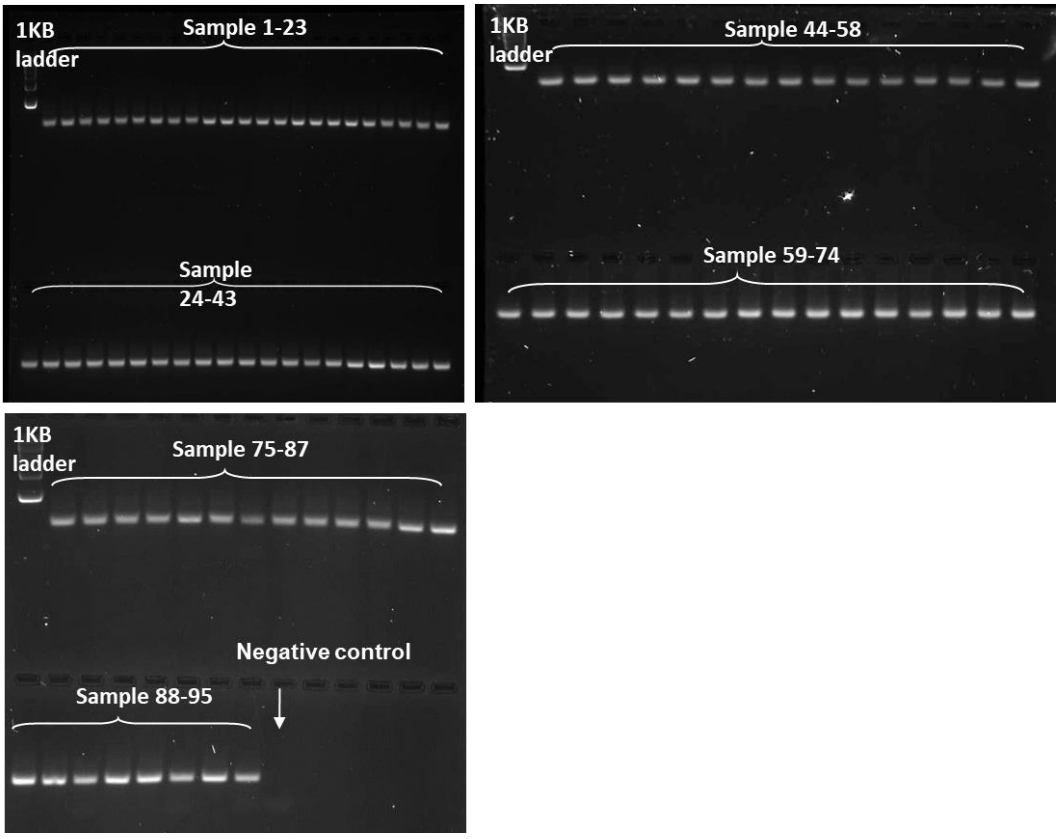


Figure 5. 20 Round 1 PCR results as an example of NGS sample preparation. All 95 samples were amplified successfully and negative control was not contaminated.

VHH library was prepared for NGS in two rounds of PCR with appropriate primers (see Figure 5. 20). Although an inappropriate DNA ladder was used, the size of round 1 PCR should be ~300bp and round 2 PCR product should be around 350bp.

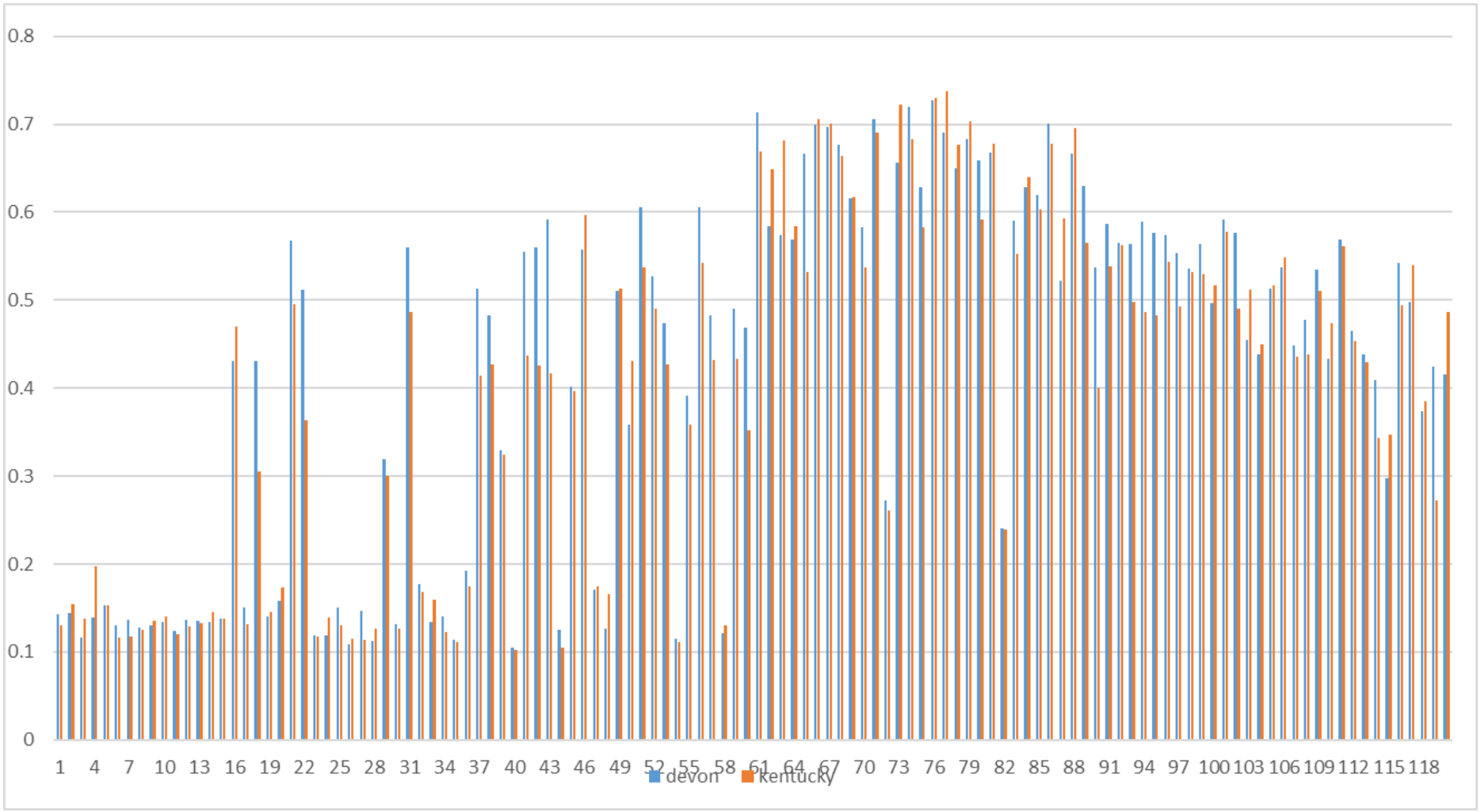


Figure 5. 21 Monoclonal ELISA. 1-30 colonies are from round 2, 31-60 colonies are from round 3, 61-90 colonies are from round 4, 91-120 colonies are from round 5 screening. Earlier rounds had less binders but more diversity; later rounds had more binders but less diversity, as same binder being amplified throughout multiple rounds.

5.5.1.4 NGS data analysis

For experiment 1A, a pool of negative samples, e.g. panned against Devon screened against Kentucky, was made for each round of screening, 8 negative samples from round 3 screening, and 10 negative samples from round 5 screening, respectively. In a screening round, each positive sample, e.g. panned against Devon and screened against Devon, was individually compared with its negative pool. Sequences were then ranked and sorted based on the Z score comparison of matching sequences seen in both positive samples and the negative pool. Z-score cut-offs of 2.0, 5.0, 10.0 and 20.0 were used and finally a cut-off of 10.0 was used to define very high specific enrichment. The most enriched peptide in experiment 1A was 'EFqLDRLRTLTLRNRK' with a percentage frequency of 2.65 (see Table 5. 1). This peptide was also identified at the same percentage frequency in round 5 screening, which means it has been enriched throughout panning rounds.

Round	Peptide sequence[a]	*In silico* assessment[b]	Frequency[c]	Total clone no.[d]	Percentage frequency[e]
Round 3	EFqLDRLRTLTLRNRK	9/9	749652	28247674	2.65
	qPISAqAEPNNLMPVR	9/9	285650	28247674	1.01
	qLSPPYSRSFTPYFGP	9/9	92324	28247674	0.33
	PGPPKITNIRARTTTR	9/9	82446	28247674	0.29
	YqPGHLNSHRTVHRNL	9/9	28964	28247674	0.10
	STYDPLAPENTISIHq	9/9	28462	28247674	0.10
	LPTCWADLVNTKTqPG	9/9	24226	28247674	0.09
	NTDqDAVRTVITVTANCMPPq	9/9	22732	28247674	0.08
	NqPTMTWRQWTLGRMR	9/9	17314	28247674	0.06
	TPARKPLSAAqDTALL	9/9	17218	28247674	0.06
	CPYLqYVWRRPS	9/9	15772	28247674	0.06
	qRCRYLLPQSSLQTAK	9/9	14718	28247674	0.05
	KqTDGTALKRHH	9/9	14640	28247674	0.05
	GPAGqRIDSPRNLRTV	9/9	12454	28247674	0.04
	SLLARPKDNDLPQqSA	9/9	11990	28247674	0.04
	NAqRERQ	9/9	11522	28247674	0.04
	HNSMTSRQRqLHqLLL	9/9	11420	28247674	0.04
	qRPRLLLNPGKDYGPQ	9/9	11034	28247674	0.04
	SATSSTYRTLKPTqSH	9/9	10530	28247674	0.04
	DYqNTVLVTLEV	9/9	10388	28247674	0.04
Round 5	EFqLDRLRTLTLRNRK	10/10	749652	28247674	2.65

Table 5. 1 Candidate peptides identified by NGPD in experiment 1A*. a) Residues coded for by a stop codon were replaced by a lower case q. b) number of samples that the peptide was very highly*

enriched / total number of samples: very high enrichment was defined using a Z-score cut-off ≥10. c) Frequency is the number of times this clone was sequenced. d) A total number of clones sequenced.

5.5.2 Experiment 1B — targeting Kentucky, no subtraction

Round	Peptide sequence[a]	*In silico* assessment [b]	Frequency[c]	Total clone no.[d]	Percentage frequency[e]
Round 5	PYSRFYDKPYVTRWKH	10/10	3099182	28247674	10.97
	YKqHPWWPKPWRRPRT	9/10	3133726	28247674	11.09

Table 5. 2 Candidate peptides identified by NGPD in experiment 1B. *a) Residues coded for by a stop codon were replaced by a lower case q. b) number of samples that the peptide was very highly enriched / total number of samples: very high enrichment was defined using a Z-score cut-off ≥10. c) Frequency is the number of times this clone was sequenced. d) A total number of clones sequenced*.

There was only one screening round in experiment 1B. A negative pool, i.e. panned against Kentucky screened against Devon, was made, comprising 10 negative samples. Each of the 10 positive samples i.e. panned against Kentucky screen against Kentucky, was compared with the negative pool. From the Z score analysis (≥10), two highly enriched peptide sequences were identified: 'PYSRFYDKPYVTRWKH' with a percentage frequency of 10.97 and 'YKqHPWWPKPWRRPRT' with a percentage frequency of 11.09 (see Table 5. 2).

5.5.3 Experiment 2 — targeting Devon, with subtraction

Round	Peptide sequence[a]	*In silico* assessment [b]	Frequency[c]	Total clone no.[d]	Percentage frequency[e]
Round 3	RRTLLGFSKPGPRKRK	9/9	8532199	17912665	47.63
	RRSLLRWTVGRMTRRP	9/9	43784	17912665	0.24
	NqPTMTWRQWTLGRMR	9/9	13302	17912665	0.07
	RRTLWVSKPGPRKRK	8/9	420428	17912665	2.35
Round 5	RRTLLGFSKPGPRKRK	6/10	8532199	17912665	47.63
	qTCKYHKPVLPIMRLR	6/10	26762	17912665	0.15
	SqGRRRWPFRARFRTV	5/10	5237076	17912665	29.24
	qRqKSKYLWMWRIRSH	5/10	23484	17912665	0.13

Table 5. 3 Candidate peptides identified by NGPD in experiment 2. *a) Residues coded for by a stop codon were replaced by a lower case q. b) number of samples that the peptide was very highly enriched / total number of samples: very high enrichment was defined using a Z-score cut-off ≥10. c) Frequency is the number of times this clone was sequenced. d) A total number of clones sequenced*.

As observed, with the subtractive step, the diversity of peptides in experiment 2 was smaller than that in experiment 1A. And for both experiments, earlier panning rounds had higher diversity than later rounds. One peptide 'RRTLLGFSKPGPRKRK' (see Table 5.3) was highly enriched in both round 3 and round 5 with a percentage frequency of ~48%. Another peptide 'SqGRRRWPFRARFRTV' was not seen in round 3 but was enriched in round 5 at a percentage frequency of 29%.

5.6 Discussion

There are many underpinning factors contributing to the huge success of phage display technology. The insertion of a foreign sequence (genotype) at the phage coat protein leads to the display of that sequence (phenotype) on the phage surface. One of the most important factors being the link between the phenotype and the genotype, which makes it possible to select a specific peptide which can be amplified subsequently by re-infecting host *E. coli*. Phage display technology has been applied to almost all disciplines of biological research since its first development (Wang and Yu, 2004).

5.6.1 Replacement of animal use

The present study intended to use phage display technology combined with NGS to identify antibody peptides from a randomised VHH library against two closely related recombinant EIVs for antigenic clade differentiation. Conventionally, a haemagglutination inhibition (HI) test is used to characterise field circulating EIVs and ferret antisera is commonly used in this test. To compare, the ferret antisera are produced by inoculating healthy male ferrets under one year of age intranasally with live virus followed by a subcutaneous injection boost 14 days post-inoculation (Thi Nguyen et al., 2018). However, antibodies produced by phage display are without the need to sacrifice animals. Utilising the same biological mechanisms that are employed by the *in vivo* adaptive immune system antibodies produced by phage display are developmentally, functionally, and structurally identical to those produced *in vivo* (Gray et al., 2016). Moreover, there have been increasing numbers of different animal-friendly affinity reagents (AFAs) (typically recombinant antibodies) developed or commercialised, which are produced without any living immune systems and are available to replace animal immunisation techniques for a wide range of applications. Furthermore, genetic materials from antibodies acquired from immunised human or animal donors produce a non-renewable library which is inadequate for the selection of multiple antibodies to unrelated targets (Gray et al., 2016).

5.6.3 Phage ELISA

After cyclic panning, the resultant polyclonal phage pools from each round are traditionally tested by phage ELISA, in which the phage pool is incubated on an antigen-coated plate and after being washed, developed with an enzyme-conjugated anti-phage antibody against the major capsid protein and a chromogenic substrate specific for the enzyme chosen (Hammers and Stanley, 2014). An increasing trend of signals throughout early to later rounds was observed in the ELISA using polyclonal phage pools in experiment 1A targeting Devon HA. However, the results also showed there was no preferential binding of the polyclonal phage pools to Devon HA or to Kentucky HA. This is probably the outcome

of the enrichment of 'false positive' binders, which are peptides binding to the contaminating proteins in the virus stock, considering the virus stock was produced in embryonated eggs without sufficient purification steps, to blocking reagents, to the plastic matrix used as the solid phase, but not to the mimotopes of the antigen. To overcome this problem, it is paramount to ensure that the purity of the selector molecule is at the highest level possible. Additionally, a few other factors could be considered: 1) using a different solid matrix for different rounds of panning; 2) using alternative blocking agents; 3) using different elution strategies, and 4) using different infection methods for phage amplification (Wang and Yu, 2004).

Traditionally, to further explore specific binders, monoclonal ELISA was used. *E. coli* infected with polyclonal phage is plated out and over a hundred individual colonies are randomly picked and expanded for monoclonal production. These are each tested again by phage ELISA to confirm antigen binding. One hundred and twenty colonies were picked from experiment 1A, 30 colonies from each round 2, 3, 4 and 5. In terms of the number of positive binders, only 5 colonies were from round 2; 19 from round 3; 28 from round 4; and 30 from round 5. This is as expected and supported by previous studies. As with naïve libraries, enrichment is usually not observed during the first two rounds of selection; usually, in the third round, the enrichment ratio (the ratio of clones eluted from a target-coated well to clones eluted from a blank well) is greater than 10 and can be as high as 1000 or more in later rounds (Sidhu and Geyer, 2015), although this cannot be observed from the monoclonal ELISA conducted in the present study due to practicality issue.

Phage pool	Round 1	Round 2	Round 3	Round 4
Starting phage library diversity	1×10^{9}	5×10^{5}	1×10^{6}	1×10^{7}
Phage input	1×10^{11}			
Target eluted phage	1×10^{5}	5×10^{5}	1×10^{6}	1×10^{7}

Non-target eluted phage	1×10^5	1×10^5	1×10^5	1×10^5
Enrichment	1×	5×	10×	100×
Amplified phage pool	1×10^{14}			

Table 5. 4 Phage colony forming units (cfu) in a typical panning experiment (Sidhu and Geyer, 2015)

Phage ELISAs were omitted in experiment 2 because both polyclonal and monoclonal ELISAs for experiment 1A were inconclusive and not providing useful information for specific Devon HA binders. This is consistent with the NGS findings that none of the peptide sequences in experiment 1A have high percentage frequency compared to peptide sequences identified in two other experiments.

5.6.5 Future work

A few strategies could be used to recover candidate VHH clones identified based on CDR3 sequences, such as fragment assembly, rolling-circle amplification and hybridization using biotin probes (Barreto et al., 2019). Furthermore, a rescue strategy was developed using the inverse polymerase chain reaction (PCR) and ligation to isolate VHH clones. The HCDR3 sequences are allowed to be synthesised into any expression vector already containing the VHH scaffold from the same library. In addition, the VHH HCDR3 nucleotide sequences were converted to the optimal codons for expression in *E. coli*. After synthesis of the specific Devon HA or Kentucky HA binders, they will be used to develop ELISAs for testing a panel of EIVs from both clade 1 and clade 2 to see if the binders are not only virus-specific but also clade-specific. Diagnostic assays with the ability to differentiate EIVs from clade 1 to clade 2 could be used to ensure that the horses are vaccinated effectively and with sufficient immunity against currently circulating viruses. They can also help tracking the antigenic evolution of ever-changing influenza viruses, allowing a rapid response if any dramatic changes are detected.

In addition, the percentage frequency of the two peptide sequences identified in experiment 1B are almost four times of the highest one in experiment 1A, which indicates it is probably promising to look for Kentucky HA specific binders and further panning with subtraction steps could be done in this direction.

Chapter 6 Conclusions

This study aimed to develop novel diagnostic assays for emergent/re-emergent viruses using various techniques including pseudotyping, plant expression and next-generation phage display. The first two experimental chapters focused on the Zika virus, whereas the last experimental chapter brought attention to the equine influenza virus.

Zika virus belongs to the flavivirus family, among which there are many other notorious members such as YFV, WNV, JEV and DENV. One of the reasons that ZIKV was chosen as the study model is because it can be handled in biocontainment level 2 laboratories. Successfully pseudotyped ZIKV can be compared with wild type ZIKV head-to-head in diagnostic assays such as virus neutralisation test. Although this study was unsuccessful in pseudotyping ZIKV with VSV backbone, one possible explanation was proposed: virus budding sites were different. VSV buds from the plasma membrane, whereas the replication and assembly of flaviviruses occur on the ER membrane (Lyles, 2007, Barrows et al., 2018). As a result, not enough flavivirus envelope proteins were translocated to the plasma membrane for the VSV virion to incorporate into the pseudotyped virus. Studies on YFV revealed that the prME heterodimer contains at least three ER-retention signals, two in the transmembrane region of prM and at least one in the transmembrane region of E (Ciczora et al., 2010).

Consequently, suggestions for future experiments were provided based on the findings above. A chimeric ZIKV E could be constructed including the C-terminal ZIKV signal sequence, prME heterodimer where all three transmembrane domain mutated to remove ER-retention signal property by adding a stretch of hydrophobic residues composed of alanines and leucines (ALALAL) in the middle of all transmembrane domains of the prME.

Finally, last but not least, the stem, transmembrane domain and cytoplasmic tail of VSV-G which contains an export signal.

With efficient translocation of flavivirus envelope proteins to the plasma membrane, generating pseudotyped ZIKV still may not be achieved, considering flaviviruses undergo a maturation pathway where the prM protein is cleaved by host furin proteases. Subsequently, the immature, spiky and non-infectious virus particle is converted to mature, smooth and infectious virus (Sirohi and Kuhn, 2017). The pseudotyped ZIKV may be non-infectious due to the lack of prM cleavage. There are two potential methods to incorporate furin in the pseudotyping process. Firstly, a plasmid encoding furin could be co-transfected in the producer cells during pseudotyping with heterologous envelope proteins. Secondly, a cell line that ectopically expresses high levels of human furin (Vero-furin) (Mukherjee et al., 2016) could be used as producer cells for the production of more homogenous mature pseudotyped flaviviruses.

In the second experimental chapter, ZIKV NS1 protein was successfully expressed in the plant *Nicotiana benthamiana* using the expression vector pEAQ-HT. A series of optimisations was made during the process, such as performing codon optimisation, including a Kozak sequence that is preferentially used by plants, using PR1a (a protein abundantly produced by the plants during an infection) signal peptide instead of original ZIKV signal peptide, and adding an ER-retention signal SEKDEL. ZIKV NS1, instead of ZIKV E, was chosen to be expressed as the antigen for an ELISA because it does not elicit flavivirus cross-reactive neutralisation antibodies, which is vital during diagnosis when the patient had previous flavivirus exposure. However, using the same method, ZIKV E can be expressed in plants for vaccine development in the future. Moreover, adenoviral vectors used to deliver ZIKV prME were shown to have higher neutralising antibody titres and T-cell immunity than purified, inactivated whole virus vaccine (PIV), DNA and protein subunit

vaccines. The plant-based vaccine has advantages in the ease of production and is easily scalable in epidemic situations. Plant-based vaccines can also overcome the limitations of the vector-based vaccine which can induce toxic inflammatory responses and the potential for pre-existing immunity to the viral vector which can occur due to cross-reactivity with naturally occurring human adenoviruses, leading to accelerated clearance and dampened immunogenicity (Wilder-Smith et al., 2019). Other benefits of the plant-based vaccine include low-cost for production, distribution and delivery, high biosynthetic capacity, no human and animal cells or pathogens involved, therefore minimal risk of contamination with exogenous pathogens (Rosales-Mendoza et al., 2012).

In the last experimental chapter, antibody peptides displayed by bacteriophage that were specific binders to EIV expressing Devon HA and not Kentucky HA (or vice versa) were identified using next-generation sequencing and data analysis. The high-throughput NGS provided a vast amount of data on the presence and frequency of antibody fragments for a single round of panning. By combing through the resulting data, enriched sequences were identified; the Z score was used to distinguish non-specific enrichment and target-specific enrichment. The identified Devon HA binders are readily for rescue by an inverse PCR. Further functional analysis can be performed in an ELISA to test their specificity against other EIV from two different clades. If the specificity is proven, the antibody fragments can also be expressed in plants for the development of diagnostic tests.

Furthermore, phage display technology has been widely applied in vaccine development, including the direct use of phage as an immunogen, identification of mimotopes (peptides interact with the paratope in a similar way as the native epitope but with a different sequence), and study of T-cell specificity (Wang and Yu, 2004). A few examples in which phage have been successfully used as an immunogen carrier in immunization studies were mentioned below. Hepatitis B virus surface antigen mimotopes, displayed on pIII and

pVIII, could induce antibody response resembling that induced by the original antigen, and the phage displayed mimotopes proved to be a better immunogen than synthetic mimotopes or the HBV core peptide (Meola et al., 1995). Mimotopes of Hepatitis B and C viruses, displayed on pIII and pVIII, induced immune response by oral administration, which is specifically cross-reactive with the original antigen (Delmastro et al., 1997). Respiratory syncytial virus G protein epitope, displayed on pIII, was able to elicit high level of circulating antibodies and complete protection was achieved as indicated by the lack of virus in the lungs of mice following intranasal challenge with live RSV virus (Bastien et al., 1997). These examples demonstrated that phage displaying epitope or mimotope could be used directly for the development of vaccines or as vaccine-delivery tools (Wang and Yu, 2004). The phage display technique could also be applied to identify disease-specific peptides, for example, peptides specifically recognised after infection with ZIKV or DENV, for use in diagnostic assays.

Appendix 1

LB broth – 1L

13g Nutrient Broth powder

1L H_2O

LB agar – 500ml

14g Nutrient Agar powder

500ml H_2O

Plasmid purification:

solutions I

50 mM glucose,

25 mM Tris-Cl (pH 8.0)

10 mM EDTA (pH 8.0)

De-ionised H_2O

Solution I

0.2 N NaOH

1% (w/v) SDS

De-ionised H_2O

Solution III

5 M potassium acetate

glacial acetic acid

De-ionised H_2O

TE buffer (500ml)

1M Tris pH8 5ml

0.5M EDTA pH8 1ml

De-ionised H_2O 496ml

10XTBE buffer (1L)

108 g of Tris

55 g of boric acid

7.5 g of EDTA

deionised H_2O

Western blot:

Transfer buffer (1L)

25mM Tris

192mM Glycine

20% (v/v) Methanol

3.03g Tris Base

14.4g Glycine

200ml Methanol

Deionised H_2O

Western blot washing buffer TBST (1L)

25mM Tris Base

137mM NaCl

0.1% (w/v) Tween20

100ml 10x TBS stock solution

1ml Tween20

899ml de-ionised H_2O

1X PBST (1L)

8g of NaCl

0.2g of KCl

1.44g of Na_2HPO_4

0.24g of KH_2PO_4

2ml of tween-20

1 L H_2O

5xM9 salts (500ml)

15g Na_2HPO_4

7.5g KH_2PO_4

2.5g NH_4Cl

1.25g NaCl

Add dH_2O to 500ml and autoclave

25% (w/v) glucose

Dissolve 125g glucose powder in 300 ml H_2O and then make up to 500ml

Filter using Corning® Bottle-Top Vacuum Filter Systems (0.45 µm)

Minimal Agar (100ml)

1.5g Agar powder

78ml H_2O

Autoclave and while it is still in liquid, add the following:

25ml 5xM9 salts

1.6ml 25% glucose*

100µl $MgCl_2$ (20%w/v, sterile filtered)*

50µl thiamine hydrochloride (10mg/ml, sterile filtered)*

(*cannot be reheated)

2YT (500ml)

8g tryptone

5g yeast

2.5g NaCl

Add 500ml dH_2O and autoclave

2YT agar (500ml)

8g tryptone

5g yeast

2.5g NaCl

7.5g agar powder

Add 500ml dH_2O and autoclave

20% (w/v) PEG-8000/2.5M NaCl (1L)

200g PEG8000

146.1g NaCl

Add 1L ddH_2O and autoclave

ELISA coating buffer (1L)

(50mM carbonate/bicarbonate buffer at pH9.6)

1.59g Na_2CO_3

2.93g $NaHCO_3$

1L deionised water

Storage media (5ml)

3.35ml 2YT

1.25ml glycerol

8% (w/v) glucose

2% (v/v) ampicillin (50mg/ml)

Buffers for plant expression

Buffer	Reagent/pH
Extraction buffer 500ml	25ml 1M Tris 50ml 5M NaCl 1.24g Na2S2O35H2O (final con. 10mM) 425ml sterile H2O 0.5ml Triton X-100 (final con. 0.1%V/V)
Binding buffer 500ml	25ml 1M Tris 50ml 5M NaCl 0.5ml Triton X-100 425ml sterile H2O
500mM imidazole stock 200ml	6.808g imidazole powder in 200ml sterile H2O
5/10/20/30mM imidazole wash buffer 50ml	Dilute 0.5/1/2/3ml 500mM imidazole stock in 50ml binding buffer
Elution buffer 50ml	2.5ml 1M Tris 5ml 5M NaCl 25ml 500mM imidazole stock 17.5ml sterile H2O
MMA medium 100ml	10ml 0.1M MES pH 5.6 1ml 1M MgCl2 100 µl 0.1M Acetosyringone

	88.9ml H2O

Oligonucleotide primers used for PCR amplification.

Primer	Sequence (5'- 3')	Function
ZIKV NS1 forward primer	TAAGCAaccggtATGGATGTGG GGTGCTCG	Forward primer for amplifying ZIKV NS1
His tag Rev 1	GTGATGGTGATGTGCAGTCAC CA	Reverse primer for amplifying ZIKV NS1 and adding first 4 His-tags
His tag Rev 2	TGCGCCctcgagTTAGTGATGGT GATGGTGATGTGCAGTCAC	Reverse primer for amplifying ZIKV NS1 and adding the remaining 2 His-tags, a stop codon and an XhoI restriction site*
His tag full reverse	TGCGCCctcgagTTAGTGATGGT GATGGTGATGTGCAGTCACCA TTGACCTATCTAAGTTGC	Reverse primer for amplifying ZIKV NS1 and adding hexa his-tag in a single reaction. It was originally intended to be used to check the PCR products produced by His tag Rev 1 and His tag Rev 2
MyInsert F1	TGTTAAGCTTCTGTATATTCTG CCCAAATTCGCGaccggtGATGT GGGGTGCTCGGTGGA	Forward primer for amplifying ZIKV NS1 in Gibson assembly cloning
MyInsert R1	GGTGATGCCCGGGATGATGGT GATGGTGATGCATaccggtTGCA GTCACCATTGACCTTA	Reverse primer for amplifying ZIKV NS1 in Gibson assembly cloning

BK79	GGTTCTATAAGAAATCTAG	Forward primer for insert amplification from pEAQ-HT
BK80	GTGAGCTCCTGTTTAGCAG	Reverse primer for insert amplification from pEAQ-HT

Restriction sites are given in lower cases, and His-tags underlined. Start/Stop codons are highlighted in red.

Medium, reagents and antibodies

Names	**Reagents/special notes/cat. no.**
Serum Free DMEM (SF DMEM)	Dulbecco's Modified Eagle Medium supplemented with 1% (v/v) L-glutamine and 1% (v/v) penicillin-streptomycin 1mg/ml.
2% or 5% complete medium	Dulbecco's Modified Eagle Medium supplemented with 2% or 5% (v/v) heat inactivated fetal bovine serum, 1 % (v/v) L-glutamine and 1% (v/v) 1mg/ml penicillin-streptomycin.
Agar overlay	D-5 containing 0.9% agar (Sigma-Aldrich)
Opti-MEM reduced serum medium	Thermal Fisher Scientific Catalogue number: 31985062
Lipofectamine 2000 transfection reagent	Invitrogen Catalogue number: 11668027
Jetprime transfection reagent	Polyplus-transfection
Primary antibodies	Rabbit serum raised against influenza A/equine/Sussex/89 (H3N8) kindly

	provided by Dr Debra Elton, Animal Health Trust.
Secondary antibodies	Alexa Fluor™ 546 goat anti-human IgG (H+L) (Invitrogen) Alexa Fluor™ 594 goat anti-rabbit IgG (H+L) (Invitrogen)
SteadyGlo	Promega Catalogue number: E2520
FACS buffer	1% BSA and 1% sodium azide in PBS

Appendix 2

	Script name	Function	Script details
Step 1	demultiplex.sh	Converting data from a fastq file to a fasta file	Seqtk seq -a Ge.fastq >Ge fasta
Step 2	demultiplex2.sh	Demultiplexing barcoded fasta file using exact matches for the barcode sequences	cat Ge.fasta | grep -E -B 1 '^.{0,5}CTAAGGTAAC' | grep - -v '--' > split_barcode_BC01.fasta
Step 3	reverse_complement.sh	Reverse complementing fasta files	seqtk seq -r split_barcode_BC01.fasta > split_barcode_BC01.rev.fasta
Step 4	translate.sh	Translating a single DNA fasta file in each of the three reading frames	perl translate.pl -i split_barcode_BC01.rev.fasta -s opq -f 1 >Ge_BC01.frame1 perl translate.pl -i split_barcode_BC01.rev.fasta -s opq -f 2 >Ge_BC01.frame2 perl translate.pl -i split_barcode_BC01.rev.fasta -s opq -f 3 >Ge_BC01.frame3
Step 5	cat.sh	Joining the results to a single file	cat Ge_BC01.frame1.fasta Ge_BC01.frame2.fasta Ge_BC01.frame3.fasta >Ge_BC01.frames.fasta
Step 6	iterate.sh	Searching for motifs flanking the VHH randomised region in a translated frames file	perl iterate_motifs.pl Ge_BC01.frames.fasta 4
Step 7	make_pool.sh	Pooling negative controls to be compared against individual positive barcode	cat Ge_BC49.frames.fasta.LR.fa Ge_BC50.frames.fasta.LR.fa Ge_BC51.frames.fasta.LR.fa Ge_BC52.frames.fasta.LR.fa Ge_BC53.frames.fasta.LR.fa Ge_BC54.frames.fasta.LR.fa Ge_BC55.frames.fasta.LR.fa Ge_BC56.frames.fasta.LR.fa>exp1R3pDsK.pool.LR.fa
Step 8	comparison.sh	Comparing frequencies in pairs of .LR.fa files defined by the	perl compare.collapsed.sequences_2a.Zscore.pl Ge_BC01.frames.fasta.LR.fa exp1R3pDsK>01.table

		user/ ranking occurrences of identical randomised regions in table files	
Step 9	awk_Z10.sh	Filtering table file data based on Z scores	awk ‘ NR>1 && $4>=10 {print $1;}’ 01.table >01Z10
Step 10	cat2.sh	Joining 01Z10—48Z10 according to their experimental rounds	cat 01Z10 02Z10 03Z10 04Z10 05Z10 06Z10 07Z10 08Z10 09Z10 >exp1R3_screen_Z10
Step 11	sort.sh	Determining the frequencies of each peptide Z≥10 in all pannings and sorting them numerically in descending order	cat expR3_screen_Z10 | sort | uniq -c | sort -nr | sed ‘s/^[\t]*//’ >exp1R3_screen_sorted_Z10

References

ANIMAL HEALTH TRUST 2019. Equine influenza outbreaks reported in 2019. Animal Health Trust

APTE-SENGUPTA, S., SIROHI, D. & KUHN, R. J. 2014. Coupling of replication and assembly in flaviviruses. *Curr Opin Virol,* 9**,** 134-42.

ARMELAGOS, G. J., BROWN, P. J. & TURNER, B. 2005. Evolutionary, historical and political economic perspectives on health and disease. *Soc Sci Med,* 61**,** 755-65.

BAEK, H., SUK, K.-H., KIM, Y.-H. & CHA, S. 2002. An improved helper phage system for efficient isolation of specific antibody molecules in phage display. *Nucleic acids research,* 30**,** e18-e18.

BARRETO, K., MARUTHACHALAM, B. V., HILL, W., HOGAN, D., SUTHERLAND, A. R., KUSALIK, A., FONGE, H., DECOTEAU, J. F. & GEYER, C R. 2019. Next-generation sequencing-guided identification and reconstruction of antibody CDR combinations from phage selection outputs. *Nucleic Acids Research,* 47**,** e50-e50.

BARROWS, N. J., CAMPOS, R. K., LIAO, K. C., PRASANTH, K. R., SOTO-ACOSTA, R., YEH, S. C., SCHOTT-LERNER, G., POMPON, J., SESSIONS, O. M., BRADRICK, S. S. & GARCIA-BLANCO, M. A. 2018. Biochemistry and Molecular Biology of Flaviviruses. *Chem Rev,* 118**,** 4448-4482.

BASTIEN, N., TRUDEL, M. & SIMARD, C. 1997. Protective immune responses induced by the immunization of mice with a recombinant bacteriophage displaying an epitope of the human respiratory syncytial virus. *Virology,* 234**,** 118-22.

BONALDO, M. C., GÓMEZ, M. M., DOS SANTOS, A. A., ABREU, F. V. S. D., FERREIRA-DE-BRITO, A., MIRANDA, R. M. D., CASTRO, M. G. D. & LOURENÇO-DE-OLIVEIRA, R. 2017. Genome analysis of yellow fever virus of the ongoing outbreak in Brazil reveals polymorphisms. *Memorias do Instituto Oswaldo Cruz,* 112**,** 447-451.

BREEN, S., WILLIAMS, S., OUTRAM, M., KOBE, B. & SOLOMON, P. 2017. Emerging Insights into the Functions of Pathogenesis-Related Protein 1. *Trends in Plant Science,* 22.

BRYANT, N. A., RASH, A. S., WOODWARD, A. L., MEDCALF, E., HELWEGEN, M., WOHLFENDER, F., CRUZ, F., HERRMANN, C., BORCHERS, K., TIWARI, A., CHAMBERS, T. M., NEWTON, J. R., MUMFORD, J. A. & ELTON, D. M. 2011. Isolation and characterisation of equine influenza viruses (H3N8) from Europe and North America from 2008 to 2009. *Veterinary Microbiology,* 147**,** 19-27.

CALISHER, C. H., KARABATSOS, N., DALRYMPLE, J. M., SHOPE, R. E., PORTERFIELD, J. S., WESTAWAY, E. G. & BRANDT, W. E. 1989. Antigenic Relationships between Flaviviruses as Determined by Cross-neutralization Tests with Polyclonal Antisera. *Journal of General Virology,* 70**,** 37-43.

CANAKOGLU, N., BERBER, E., ERTEK, M., YORUK, M. D., TONBAK, S., BOLAT, Y., AKTAS, M., KALKAN, A. & OZDARENDELI, A. 2013. Pseudo-plaque reduction neutralization test (PPRNT) for the measurement of neutralizing antibodies to Crimean-Congo hemorrhagic fever virus. *Virology journal,* 10**,** 6-6.

CARNELL, G. W., FERRARA, F., GREHAN, K., THOMPSON, C. P. & TEMPERTON, N. J. 2015. Pseudotype-based neutralization assays for influenza: a systematic analysis. *Frontiers in immunology,* 6**,** 161-161.

CICZORA, Y., CALLENS, N., SERON, K., ROUILLE, Y. & DUBUISSON, J. 2010. Identification of a dominant endoplasmic reticulum-retention signal in yellow fever virus pre-membrane protein. *J Gen Virol,* 91**,** 404-14.

CLACKSON, T. & LOWMAN, H. B. 2004. *Phage display : a practical approach / edited by Tim Clackson, Henry B. Lowman,* Oxford, Oxford : Oxford University Press.

CLANCY, S. 2008. Genetics of the influenza virus. *Nature Education,* 1**,** 83.

COHEN, B. J., AUDET, S., ANDREWS, N. & BEELER, J. 2007. Plaque reduction neutralization test for measles antibodies: Description of a standardised laboratory method for use in immunogenicity studies of aerosol vaccination. *Vaccine,* 26**,** 59-66.

COLE, N. B., ELLENBERG, J., SONG, J., DIEULIIS, D. & LIPPINCOTT-SCHWARTZ, J. 1998. Retrograde Transport of Golgi-localized Proteins to the ER. *The Journal of Cell Biology,* 140**,** 1.
DAI, L., SONG, J., LU, X., DENG, Y. Q., MUSYOKI, A. M., CHENG, H., ZHANG, Y., YUAN, Y., SONG, H., HAYWOOD, J., XIAO, H., YAN, J., SHI, Y., QIN, C. F., QI, J. & GAO, G. F. 2016. Structures of the Zika Virus Envelope Protein and Its Complex with a Flavivirus Broadly Protective Antibody. *Cell Host Microbe,* 19**,** 696-704.
DALY, J., & SOLOMON, T. 2010. The Immunological Basis for Immunization Series Module 13: Japanese encephalitis virus. Geneva: World Health Organization.
DALY, J. M., BLUNDEN, A. S., MACRAE, S., MILLER, J., BOWMAN, S. J., KOLODZIEJEK, J., NOWOTNY, N. & SMITH, K. C. 2008. Transmission of equine influenza virus to English foxhounds. *Emerg Infect Dis,* 14**,** 461-4.
DELMASTRO, P., MEOLA, A., MONACI, P., CORTESE, R. & GALFRÈ, G. 1997. Immunogenicity of filamentous phage displaying peptide mimotopes after oral administration. *Vaccine,* 15**,** 1276-1285.
DI GENNARO, A., LORUSSO, A., CASACCIA, C., CONTE, A., MONACO, F. & SAVINI, G. 2014. Serum Neutralization Assay Can Efficiently Replace Plaque Reduction Neutralization Test for Detection and Quantitation of West Nile Virus Antibodies in Human and Animal Serum Samples. *Clinical and Vaccine Immunology,* 21**,** 1460.
DOSHI, R., CHEN, B. R., VIBAT, C. R. T., HUANG, N., LEE, C.-W. & CHANG, G. 2014. In vitro nanobody discovery for integral membrane protein targets. *Scientific reports,* 4**,** 6760-6760.
DUFFY, M. R., CHEN, T.-H., HANCOCK, W. T., POWERS, A. M., KOOL, J. L., LANCIOTTI, R. S., PRETRICK, M., MARFEL, M., HOLZBAUER, S., DUBRAY, C., GUILLAUMOT, L., GRIGGS, A., BEL, M., LAMBERT, A. J., LAVEN, J., KOSOY, O., PANELLA, A., BIGGERSTAFF, B. J., FISCHER, M. & HAYES, E. B. 2009. Zika Virus Outbreak on Yap Island, Federated States of Micronesia. *New England Journal of Medicine,* 360**,** 2536-2543.
FERNANDEZ-GARCIA, M.-D., MAZZON, M., JACOBS, M. & AMARA, A. 2009. Pathogenesis of Flavivirus Infections: Using and Abusing the Host Cell. *Cell Host & Microbe,* 5**,** 318-328.
FLINT, S. J. 2009. *Principles of virology / S.J. Flint ... [et al.],* Washington, D.C., Washington, D.C. : ASM Press.
GRAY, A. C., SIDHU, S. S., CHANDRASEKERA, P. C., HENDRIKSEN, C. F. M. & BORREBAECK, C. A. K. 2016. Animal-Friendly Affinity Reagents: Replacing the Needless in the Haystack. *Trends Biotechnol,* 34**,** 960-969.
GUTSCHE, I., COULIBALY, F., VOSS, J. E., SALMON, J., D'ALAYER, J., ERMONVAL, M., LARQUET, E., CHARNEAU, P., KREY, T., MEGRET, F., GUITTET, E., REY, F. A. & FLAMAND, M. 2011. Secreted dengue virus nonstructural protein NS1 is an atypical barrel-shaped high-density lipoprotein. *Proc Natl Acad Sci U S A,* 108**,** 8003-8.
HAMMERS, C. M. & STANLEY, J. R. 2014. Antibody phage display: technique and applications. *The Journal of investigative dermatology,* 134**,** 1-5.
HANIKA, A., LARISCH, B., STEINMANN, E., SCHWEGMANN-WESSELS, C., HERRLER, G. & ZIMMER, G. 2005. Use of influenza C virus glycoprotein HEF for generation of vesicular stomatitis virus pseudotypes. *J Gen Virol,* 86**,** 1455-65.
HEINZ, F. X. & STIASNY, K. 2017. The Antigenic Structure of Zika Virus and Its Relation to Other Flaviviruses: Implications for Infection and Immunoprophylaxis. *Microbiol Mol Biol Rev,* 81.
HOWARD, C. R. 2012. *Lecture notes on emerging viruses and human health : a guide to zoonotic viruses and their impact / Colin R. Howard,* Singapore
London, Singapore
London : World Scientific.
HOWARD, G. C. & KASER, M. R. 2007. *Making and using antibodies : a practical handbook / edited by Gary C. Howard and Matthew R. Kaser,* Boca Raton
London, Boca Raton
London : CRC Press.

HUHN, G. D., SEJVAR, J. J., MONTGOMERY, S. P. & DWORKIN, M. S. 2003. West Nile virus in the United States: an update on an emerging infectious disease. *Am Fam Physician,* 68**,** 653-60.
KANAGARAJAN, S., TOLF, C., LUNDGREN, A., WALDENSTRÖM, J. & BRODELIUS, P. E. 2012. Transient Expression of Hemagglutinin Antigen from Low Pathogenic Avian Influenza A (H7N7) in Nicotiana benthamiana. *PLOS ONE,* 7**,** e33010.
LANCIOTTI, R. S., KERST, A. J., NASCI, R. S., GODSEY, M. S., MITCHELL, C. J., SAVAGE, H. M., KOMAR, N., PANELLA, N. A., ALLEN, B. C., VOLPE, K. E., DAVIS, B. S. & ROEHRIG, J. T. 2000. Rapid detection of west nile virus from human clinical specimens, field-collected mosquitoes, and avian samples by a TaqMan reverse transcriptase-PCR assay. *Journal of clinical microbiology,* 38**,** 4066-4071.
LANDOLT, G. A. 2014. Equine Influenza Virus. *Veterinary Clinics: Equine Practice,* 30**,** 507-522.
LARDEUX, F., TORRICO, G. & ALIAGA, C. 2016. Calculation of the ELISA's cut-off based on the change-point analysis method for detection of Trypanosoma cruzi infection in Bolivian dogs in the absence of controls. *Memórias do Instituto Oswaldo Cruz,* 111.
LEE, H.-J., MIN, K.-I., PARK, K. H., CHOI, H. J., KIM, M.-K., AHN, C.-Y., HONG, Y.-J. & KIM, Y. B. 2014. Comparison of JEV neutralization assay using pseudotyped JEV with the conventional plaque-reduction neutralization test. *Journal of Microbiology,* 52**,** 435-440.
LEE, H. J., MIN, K.-I., LEE, J., KANG, S.-H., JEON, W., NAM, J. H., JU, Y. R. & KIM, Y. B. 2009. The prM-independent packaging of pseudotyped Japanese encephalitis virus. *Virology journal,* 6**,** 115-115.
LI, Y., COCKBURN, W., KILPATRICK, J. B. & WHITELAM, G. C. 2000. High affinity ScFvs from a single rabbit immunized with multiple haptens. *Biochem Biophys Res Commun,* 268**,** 398-404.
LINDENBACH, B., THIEL, H.J., & RICE, C.M.. 2007. Flaviviridae :The VirusesandTheir Replication. *In:* KNIPE, D. M., HOWLEY, P. M.. (ed.) *Fields Virology.* 5 ed. Philadelphia/London: Lippincott Williams & Wilkins.
LOSET, G. A. & SANDLIE, I. 2012. Next generation phage display by use of pVII and pIX as display scaffolds. *Methods,* 58**,** 40-6.
LUSTIG, Y., SOFER, D., BUCRIS, E. D. & MENDELSON, E. 2018. Surveillance and Diagnosis of West Nile Virus in the Face of Flavivirus Cross-Reactivity. *Frontiers in Microbiology,* 9.
LYLES, D. S., RUPPRECHT, C.E. 2007. *Rhabdoviridae. ,* Philadelphia/London, Lippincott Williams & Wilkins.
MA, J., CHEN, R., HUANG, W., NIE, J., LIU, Q., WANG, Y. & YANG, X. 2019. In vitro and in vivo efficacy of a Rift Valley fever virus vaccine based on pseudovirus. *Hum Vaccin Immunother***,** 1-9.
MACHALABA, C. C., ELWOOD, S. E., FORCELLA, S., SMITH, K. M., HAMILTON, K., JEBARA, K. B., SWAYNE, D. E., WEBBY, R. J., MUMFORD, E., MAZET, J. A. K., GAIDET, N., DASZAK, P. & KARESH, W. B. 2015. Global avian influenza surveillance in wild birds: a strategy to capture viral diversity. *Emerging infectious diseases,* 21**,** e1-e7.
MAEDA, A. & MAEDA, J. 2013. Review of diagnostic plaque reduction neutralization tests for flavivirus infection. *The Veterinary Journal,* 195**,** 33-40.
MAHMOOD, T. & YANG, P. C. 2012. Western blot: technique, theory, and trouble shooting. *N Am J Med Sci,* 4**,** 429-34.
MANSFIELD, K. L., HORTON, D. L., JOHNSON, N., LI, L., BARRETT, A. D. T., SMITH, D. J., GALBRAITH, S. E., SOLOMON, T. & FOOKS, A. R. 2011. Flavivirus-induced antibody cross-reactivity. *Journal of General Virology,* 92**,** 2821-2829.
MANSFIELD, K. L., LA ROCCA, S. A., KHATRI, M., JOHNSON, N., STEINBACH, F. & FOOKS, A. R. 2013. Detection of Schmallenberg virus serum neutralising antibodies. *J Virol Methods,* 188**,** 139-44.
MATSUURA, Y., TANI, H., SUZUKI, K., KIMURA-SOMEYA, T., SUZUKI, R., AIZAKI, H., ISHII, K., MORIISHI, K., ROBISON, C. S., WHITT, M. A. & MIYAMURA, T. 2001.

Characterization of Pseudotype VSV Possessing HCV Envelope Proteins. *Virology,* 286**,** 263-275.
MCNEIL, C. J. & SHETTY, A. K. 2017. Zika Virus: A Serious Global Health Threat. *Journal of Tropical Pediatrics,* 63**,** 242-248.
MEOLA, A., DELMASTRO, P., MONACI, P., LUZZAGO, A., NICOSIA, A., FELICI, F., CORTESE, R. & GALFRÈ, G. 1995. Derivation of vaccines from mimotopes. Immunologic properties of human hepatitis B virus surface antigen mimotopes displayed on filamentous phage. *The Journal of Immunology,* 154**,** 3162.
MUKHERJEE, S., SIROHI, D., DOWD, K. A., CHEN, Z., DIAMOND, M. S., KUHN, R. J. & PIERSON, T. C. 2016. Enhancing dengue virus maturation using a stable furin over-expressing cell line. *Virology,* 497**,** 33-40.
NAKAGAWA, S., NIIMURA, Y., GOJOBORI, T., TANAKA, H. & MIURA, K.-I. 2008. Diversity of preferred nucleotide sequences around the translation initiation codon in eukaryote genomes. *Nucleic acids research,* 36**,** 861-871.
NATHANSON, N. 2007. *Viral pathogenesis and immunity / Neal Nathanson co-authors Rafi Ahmed ... [et al.],* London, London : Academic Press.
NISHIMURA, N. & BALCH, W. E. 1997. A di-acidic signal required for selective export from the endoplasmic reticulum. *Science,* 277**,** 556-8.
OHST, C., SASCHENBRECKER, S., STIBA, K., STEINHAGEN, K., PROBST, C., RADZIMSKI, C., LATTWEIN, E., KOMOROWSKI, L., STÖCKER, W. & SCHLUMBERGER, W. 2018. Reliable Serological Testing for the Diagnosis of Emerging Infectious Diseases. *In:* HILGENFELD, R. & VASUDEVAN, S. G. (eds.) *Dengue and Zika: Control and Antiviral Treatment Strategies.* Singapore: Springer Singapore.
OIE, W. O. F. A. H. 2019. Principles and methods of validation of diagnostic assays for infectious diseases. *Manual of Diagnostic Tests and Vaccines for Terrestrial Animals.* Office International des Epizooties.
PLOURDE, A. R. & BLOCH, E. M. 2016. A Literature Review of Zika Virus. *Emerging infectious diseases,* 22**,** 1185-1192.
PUA, T. L., CHAN, X. Y., LOH, H. S., OMAR, A. R., YUSIBOV, V., MUSIYCHUK, K., HALL, A. C., COFFIN, M. V., SHOJI, Y., CHICHESTER, J. A., BI, H. & STREATFIELD, S. J. 2017. Purification and immunogenicity of hemagglutinin from highly pathogenic avian influenza virus H5N1 expressed in Nicotiana benthamiana. *Hum Vaccin Immunother,* 13**,** 306-313.
RABE, I. B., STAPLES, J. E., VILLANUEVA, J., HUMMEL, K. B., JOHNSON, J. A., ROSE, L., HILLS, S., WASLEY, A., FISCHER, M. & POWERS, A. M. 2016. Interim Guidance for Interpretation of Zika Virus Antibody Test Results. *MMWR Morb Mortal Wkly Rep,* 65**,** 543-6.
RICHTER, L. J., THANAVALA, Y., ARNTZEN, C. J. & MASON, H. S. 2000. Production of hepatitis B surface antigen in transgenic plants for oral immunization. *Nat Biotechnol,* 18**,** 1167-71.
RIVIÈRE, M.-P., MARAIS, A., PONCHET, M., WILLATS, W. & GALIANA, E. 2008. Silencing of acidic pathogenesis-related PR-1 genes increases extracellular β-(1→3)-glucanase activity at the onset of tobacco defence reactions. *Journal of Experimental Botany,* 59**,** 1225-1239.
ROSALES-MENDOZA, S., RUBIO-INFANTE, N., GOVEA-ALONSO, D. O. & MORENO-FIERROS, L. 2012. Current status and perspectives of plant-based candidate vaccines against the human immunodeficiency virus (HIV). *Plant Cell Rep,* 31**,** 495-511.
ROSS, A. F. 1961. Systemic acquired resistance induced by localized virus infections in plants. *Virology,* 14**,** 340-358.
SABIR, J. S. M., ATEF, A., EL-DOMYATI, F. M., EDRIS, S., HAJRAH, N., ALZOHAIRY, A. M. & BAHIELDIN, A. 2014. Construction of naïve camelids VHH repertoire in phage display-based library. *Comptes Rendus Biologies,* 337**,** 244-249.
SACK. A., C. A., DARAMRAGCHAA. U., CHULUUNBAATAR. M., GONCHIGOO. B., GRAY. G.C.. 2019 Equine influenza virus—a neglected, reemergent disease threat. *Emerg Infect Dis.,* Volume 25, Number 6.

SAINSBURY, F., THUENEMANN, E. C. & LOMONOSSOFF, G. P. 2009. pEAQ: versatile expression vectors for easy and quick transient expression of heterologous proteins in plants. *Plant Biotechnol J,* 7**,** 682-93.
SCHELLENBERG, L. 2013. *Plant-Based Production of RecombinantSubunit Vaccine Candidates and Conjugation to Cowpea Mosaic Virus-Like Particles.* master, RHEINISCH-WESTFÄLISCHE TECHNISCHE HOCHSCHULE AACHEN.
SHAW, M. L. & PALESE, P. 2013. Othomyxoviridae. *In:* KNIPE, D. M., HOWLEY, P. M.. (ed.) *Fields Virology.* 6 ed. Philadelphia/London: Lippincott Williams & Wilkins.
SIDHU, S. S. & GEYER, C. R. 2015. *Phage Display In Biotechnology and Drug Discovery, Second Edition,* Baton Rouge, UNITED STATES, CRC Press.
SIMOES, M., CAMACHO, L. A., YAMAMURA, A. M., MIRANDA, E. H., CAJARAVILLE, A. C. & DA SILVA FREIRE, M. 2012. Evaluation of accuracy and reliability of the plaque reduction neutralization test (micro-PRNT) in detection of yellow fever virus antibodies. *Biologicals,* 40**,** 399-404.
SIROHI, D. & KUHN, R. J. 2017. Zika Virus Structure, Maturation, and Receptors. *J Infect Dis,* 216**,** S935-s944.
SOJIKUL, P., BUEHNER, N. & MASON, H. S. 2003. A plant signal peptide–hepatitis B surface antigen fusion protein with enhanced stability and immunogenicity expressed in plant cells. *Proceedings of the National Academy of Sciences,* 100**,** 2209.
SOLIGNAT, M., GAY, B., HIGGS, S., BRIANT, L. & DEVAUX, C. 2009. Replication cycle of chikungunya: a re-emerging arbovirus. *Virology,* 393**,** 183-97.
SOLOMON, T. 2003. Recent advances in Japanese encephalitis. *J Neurovirol,* 9**,** 274-83.
SONG, H., QI, J., HAYWOOD, J., SHI, Y. & GAO, G. F. 2016. Zika virus NS1 structure reveals diversity of electrostatic surfaces among flaviviruses. *Nature Structural &Amp; Molecular Biology,* 23**,** 456.
STEINHAGEN, K., PROBST, C., RADZIMSKI, C., SCHMIDT-CHANASIT, J., EMMERICH, P., VAN ESBROECK, M., SCHINKEL, J., GROBUSCH, M. P., GOORHUIS, A., WARNECKE, J. M., LATTWEIN, E., KOMOROWSKI, L., DEERBERG, A., SASCHENBRECKER, S., STOCKER, W. & SCHLUMBERGER, W. 2016. Serodiagnosis of Zika virus (ZIKV) infections by a novel NS1-based ELISA devoid of cross-reactivity with dengue virus antibodies: a multicohort study of assay performance, 2015 to 2016. *Euro Surveill,* 21.
STETTLER, K., BELTRAMELLO, M., ESPINOSA, D. A., GRAHAM, V., CASSOTTA, A., BIANCHI, S., VANZETTA, F., MINOLA, A., JACONI, S., MELE, F., FOGLIERINI, M., PEDOTTI, M., SIMONELLI, L., DOWALL, S., ATKINSON, B., PERCIVALLE, E., SIMMONS, C. P., VARANI, L., BLUM, J., BALDANTI, F., CAMERONI, E., HEWSON, R., HARRIS, E., LANZAVECCHIA, A., SALLUSTO, F. & CORTI, D. 2016. Specificity, cross-reactivity, and function of antibodies elicited by Zika virus infection. *Science,* 353**,** 823-6.
TAKIKAWA, S., ISHII, K., AIZAKI, H., SUZUKI, T., ASAKURA, H., MATSUURA, Y. & MIYAMURA, T. 2000. Cell fusion activity of hepatitis C virus envelope proteins. *J Virol,* 74**,** 5066-74.
TANI, H. 2014. Analyses of Entry Mechanisms of Novel Emerging Viruses Using Pseudotype VSV System. *Tropical medicine and health,* 42**,** 71-82.
TANI, H., KOMODA, Y., MATSUO, E., SUZUKI, K., HAMAMOTO, I., YAMASHITA, T., MORIISHI, K., FUJIYAMA, K., KANTO, T., HAYASHI, N., OWSIANKA, A., PATEL, A. H., WHITT, M. A. & MATSUURA, Y. 2007. Replication-Competent Recombinant Vesicular Stomatitis Virus Encoding Hepatitis C Virus Envelope Proteins. *Journal of Virology,* 81**,** 8601.
TESSIER, D. C., THOMAS, D. Y., KHOURI, H. E., LALIBERTE, F. & VERNET, T. 1991. Enhanced secretion from insect cells of a foreign protein fused to the honeybee melittin signal peptide. *Gene,* 98**,** 177-83.
THI NGUYEN, D., SHEPARD, S. S., BURKE, D. F., JONES, J., THOR, S., NGUYEN, L. V., NGUYEN, T. D., BALISH, A., HOANG, D. N., TO, T. L., IQBAL, M., WENTWORTH, D. E., SPACKMAN, E., VAN DOORN, H. R., DAVIS, C. T. & BRYANT, J. E. 2018. Antigenic characterization of highly pathogenic avian influenza A(H5N1) viruses

with chicken and ferret antisera reveals clade-dependent variation in hemagglutination inhibition profiles. *Emerg Microbes Infect,* 7**,** 100.
THOMAS, S. J., NISALAK, A., ANDERSON, K. B., LIBRATY, D. H., KALAYANAROOJ, S., VAUGHN, D. W., PUTNAK, R., GIBBONS, R. V., JARMAN, R. & ENDY, T. P. 2009. Dengue plaque reduction neutralization test (PRNT) in primary and secondary dengue virus infections: How alterations in assay conditions impact performance. *Am J Trop Med Hyg,* 81**,** 825-33.
TU, J., ZHOU, H., JIANG, T., LI, C., ZHANG, A., GUO, X., ZOU, W., CHEN, H. & JIN, M. 2009. Isolation and molecular characterization of equine H3N8 influenza viruses from pigs in China. *Archives of Virology,* 154**,** 887-890.
UKNES, S., DINCHER, S., FRIEDRICH, L., NEGROTTO, D., WILLIAMS, S., THOMPSON-TAYLOR, H., POTTER, S., WARD, E. & RYALS, J. 1993. Regulation of pathogenesis-related protein-1a gene expression in tobacco. *Plant Cell,* 5**,** 159-69.
VAN DEN POL, A. N., MAO, G., CHATTOPADHYAY, A., ROSE, J. K. & DAVIS, J. N. 2017. Chikungunya, Influenza, Nipah, and Semliki Forest Chimeric Viruses with Vesicular Stomatitis Virus: Actions in the Brain. *J Virol,* 91.
WADE, R. D. 1989. ELISA and other solid phase immunoassays: Edited by D M Kemeny and S J Challacombe. pp 367. John Wiley, Chichester, UK. 1988. $47.95 ISBN 0-471-90982-3. *Biochemical Education,* 17**,** 109-109.
WAGNER, E. K. 1999. *Basic virology / Edward K. Wagner, Martinez J. Hewlett,* Malden, Mass.
Oxford, Malden, Mass.
Oxford : Blackwell Science.
WANG, L. F. & YU, M. 2004. Epitope identification and discovery using phage display libraries: applications in vaccine development and diagnostics. *Curr Drug Targets,* 5**,** 1-15.
WARD, E. R., UKNES, S. J., WILLIAMS, S. C., DINCHER, S. S., WIEDERHOLD, D. L., ALEXANDER, D. C., AHL-GOY, P., METRAUX, J. P. & RYALS, J. A. 1991. Coordinate Gene Activity in Response to Agents That Induce Systemic Acquired Resistance. *The Plant cell,* 3**,** 1085-1094.
WHITT, M. A. 2010. Generation of VSV pseudotypes using recombinant ΔG-VSV for studies on virus entry, identification of entry inhibitors, and immune responses to vaccines. *Journal of virological methods,* 169**,** 365-374.
WILDER-SMITH, A., HOMBACH, J., FERGUSON, N., SELGELID, M., O'BRIEN, K., VANNICE, K., BARRETT, A., FERDINAND, E., FLASCHE, S., GUZMAN, M., NOVAES, H. M., NG, L.-C., SMITH, P. G., THARMAPHORNPILAS, P., YOON, I.-K., CRAVIOTO, A., FARRAR, J. & NOLAN, T. M. 2019. Deliberations of the Strategic Advisory Group of Experts on Immunization on the use of CYD-TDV dengue vaccine. *The Lancet Infectious Diseases,* 19**,** e31-e38.
WONG, S. J., FURUYA, A., ZOU, J., XIE, X., DUPUIS, A. P., 2ND, KRAMER, L. D. & SHI, P.-Y. 2017. A Multiplex Microsphere Immunoassay for Zika Virus Diagnosis. *EBioMedicine,* 16**,** 136-140.
XIE, T., ANDERSON, D. B., DARAMRAGCHAA, U., CHULUUNBAATAR, M. & GRAY, C. G. 2016. A Review of Evidence that Equine Influenza Viruses Are Zoonotic. *Pathogens,* 5.
YEH, C. T., HAN, C. M., LO, S. Y., OU, J. H., FAN, K. D., SHEEN, I. S., CHU, C. M. & LIAW, Y. F. 1994. Early detection of anti-HCc antibody in acute hepatitis C virus (HCV) by western blot (immunoblot) using a recombinant HCV core protein fragment. *Journal of clinical microbiology,* 32**,** 2235-2241.